THE HISTOLOGY, MICROBIOLOGY, AND MOLECULAR ECOLOGY OF TISSUE-LOSS DISEASES AFFECTING ACROPORA CERVICORNIS IN THE UPPER FLORIDA KEYS

by

Katheryn W. Patterson
A Dissertation
Submitted to the
Graduate Faculty
of
George Mason University
in Partial Fulfillment of
The Requirements for the Degree
of
Doctor of Philosophy
Environmental Science and Public Policy

Committee:

_____ Dr. Esther C. Peters, Dissertation Director

_____ Dr. Cara Frankenfeld, Committee Member

_____ Dr. Patrick Gillevet, Committee Member

_____ Dr. Robert Jonas, Committee Member

_____ Dr. E.C.M. Parsons, Committee Member

_____ Dr. Albert Torzilli, Graduate Program Director

_____ Dr. Robert Jonas, Department Chairperson

_____ Dr. Donna M. Fox, Associate Dean, Office of Student Affairs & Special Programs, College of Science

_____ Dr. Peggy Agouris, Dean, College of Science

Date: _____ Summer Semester 2015
George Mason University
Fairfax, VA

The Histology, MicrobiOlogy, and Molecular Ecology of Tissue-Loss Diseases Affecting Acropora cervicornis in the Upper Florida Keys

A Dissertation submitted in partial fulfillment of the requirements for the degree of Doctor of Philosophy at George Mason University

by

Katheryn W. Patterson
Master of Science
George Mason University, 2010

Director: Esther C. Peters, Professor
Department of Environmental Science and Public Policy

Summer Semester 2015
George Mason University
Fairfax, VA

DEDICATION

This dissertation is in memory of and dedicated to two professors, mentors, and friends that helped inspire and challenge me to be the person I am today. Thank you for encouraging me to stay on the path to become a marine biologist, Dr. Fr. Gerald Regan, S.J., and thank you for everything you did to help me achieve my dream of going to graduate school, Dr. Shawn B. Allin. I will always hold you both close in my heart.

.

ACKNOWLEDGEMENTS

I would first like to thank my Mom, my brothers—Stephen and Brian—and all of my family members and friends for always supporting, encouraging, and believing in me throughout this entire experience. My dissertation would not have been possible without the expertise, guidance, support, and patience of my committee members: Drs. Peters, Frankenfeld, Gillevet, Jonas, and Parsons. I am forever grateful to all of my committee members for having confidence in me throughout this journey even when I lacked it at times. To my advisor, Dr. Peters, thank you for bringing me into your collaborative network and introducing me to coral disease research in the Florida Keys. I would also like to thank Dr. Peters for welcoming me into her histology lab, volunteering so much of her time to train me in what I now truly appreciate as the art of histology, for her astute reviews of this work, and for her never-ending encouragement. Special thanks are also owed to: Dr. Margaret Miller (NOAA/NMFS Southeast Fisheries Science Center), GMU's MicroBiome Analysis Center (MBAC) and Ken Nedimyer (Coral Restoration Foundation), for their collaboration, logistical support, and in-kind donations. I also thank Dr. Masoumeh Sikaroodi for her endless help and support throughout all steps of my molecular work, from troubleshooting PCRs to all of the time, help, and patience she offered me with my analyses. I am forever grateful for all of the friendships and experiences I gained while conducting this research. Thank you to Dr. David Allen for your support in the field, and thank you to all of my lab mates at GMU's Histology Lab and MBAC for their encouragement, advice, and pizza parties. I am forever thankful to Dr. Lorelei and Andrew Crerar for opening their home to me, and always supporting me through the many adversities life brought me during this process. I would like to give a special thanks to my dear friend Suzanne Hough for always having a vote of confidence in me, and for always finding the silver lining in situations when I needed it most. I am forever grateful to Bryan LeBlanc, Jason O'Bryhim, Lisa Schreffler, and Zach Siders for their unwavering support and encouragement and for always being there for me. I am very thankful for the Pham, Reinecke-Keller, and McAliley families, who welcomed me into their homes, entrusted me to watch their children, and contributed to my financial livelihood, which helped me keep my sanity. Finally, a heartfelt thank you goes to Sharon Bloomquist, Joanne Zimmerman, Roslyn Cress, and Sally Evans for their assistance and support throughout this process. This research would not have been possible without the financial support from the Cosmos Club Foundation, NOAA Coral Reef Conservation Program via the Aquarius Reef Base Program, and GMU's Environmental Science and Policy Department. The study was conducted under Florida Keys National Marine Sanctuary Permit #FKNM-2011-032-A1.

TABLE OF CONTENTS

LIST OF TABLES

LIST OF FIGURES

LIST OF ABBREVIATIONS

Adenosine phosphosulfate ..... APS
Adenosine triphosphate ..... ATP
Apparently healthy ..... AH
Applied Biosystems® ..... ABI
Aquarius Reef ..... AQ
Base pair ..... bp
Basic local alignment search tool ..... BLAST
Black-band disease ..... BBD
Bovine serum albumin ..... BSA
Complementary metal-oxide-semiconductor ..... CMOS
Conch Shallow Reef ..... CS
Coral C
Coral Restoration Foundation ..... CRF
Coral surface microlayer ..... CSM
Coral surface mucopolysaccharide layer ..... SML
Coral-associated Rickettsiales 1 ..... CAR1
Denuded skeleton ..... DS
Deoxynucleotide triphosphate ..... dNTPs
Deoxyribose nucleic acid ..... DNA
Diseased ..... D
Emulsion polymerase chain reaction ..... emPCR
Ethidium bromide ..... EtBr
Ethylenediaminetetraacetic acid ..... EDTA
Florida Keys National Marine Sanctuary ..... FKNMS
French Reef ..... FR
George Mason University ..... GMU
Healthy-on-diseased ..... HD
Healthy-on-diseased section of diseased branch ..... HDD
Hematoxylin and eosin stain ..... HE
Highly deionized Formamide ..... Hi-Di™
Internal Lane Standard-600 ..... ILS-600
International Union for Conservation of Nature ..... IUCN
Ion Personal Genome Machine® ..... PGM™
Key Largo Dry Rocks ..... KLDR
Kruskal-Wallis sum rank test ..... KW
Length-heterogeneity polymerase chain reaction ..... LH-PCR

Linear discrimant analysis ..... LDA
Linear discrimant analysis effect size ..... LEfSe
Little Conch Reef LC
Mann-Whitney-Wilcoxon test ..... MWW
Molasses Reef ..... MO
Movat's modified pentachrome stain ..... MMP
Multitag pyrosequencing ..... MTPS
MultiVariate Statistical Package ..... MVSP
Nearest Alignment Space Termination ..... NAST
Next-generation sequencing ..... NGS
Operational taxonomic unit ..... OTU
pH-sensitive field-effect transistor ..... pHFET
Polymerase chain reaction ..... PCR
Principal coordinate analysis ..... PCO
Pyrophosphate ..... PPi
Python nearest alignment space termination ..... PyNAST
Quantitative insights into microbial ecology ..... Qiime
Rapid tissue loss ..... RTL
Restriction fragment length polymorphism ..... RFLP
Ribosomal Database Project ..... RDP
Rickettsiales-like organisms ..... RLOs
Sediment ..... S
Self-contained underwater breathing apparatus ..... SCUBA
Terminal restriction fragment length polymorphism ..... T-RFLP
The MicroBiome Analysis Center ..... MBAC
Tissue-loss margin ..... TLM
Tris-Acetate-EDTA ..... TAE
U.S. Endangered Species Act ..... ESA
U.S. National Marine Fisheries Service ..... NMFS
U.S. National Oceanic and Atmospheric Administration ..... NOAA
Unique fraction matrix ..... UniFrac
White plague ..... WPL
White plague type I ..... WPL-I
White plague type II ..... WPL-II
White plague type III ..... WPL-III
White pox disease ..... WPD
White syndrome ..... WS
White-band disease ..... WBD
White-band disease type I ..... WBD-I
White-band disease type II ..... WBD-II
Yellow-band disease ..... YBD

ABSTRACT

THE HISTOLOGY, MICROBIOLOGY, AND MOLECULAR ECOLOGY OF TISSUE-LOSS DISEASES AFFECTING ACROPORA CERVICORNIS IN THE UPPER FLORIDA KEYS

Katheryn W. Patterson, Ph.D.

George Mason University, 2015

Dissertation Director: Dr. Esther C. Peters

The combined effects of anthropogenic stressors and threats associated with global climate change, including increased coral disease occurrence and frequency, duration of coral bleaching, and impacts from ocean acidification, put coral reef ecosystems at a high risk of collapse. Tissue-loss diseases (white-band disease and rapid tissue loss) have caused dramatic declines in *Acropora cervicornis* (staghorn coral) populations across the Caribbean and tropical western Atlantic Ocean. As a result, the species is listed as threatened under the United States Endangered Species Act and critically endangered under the International Union for Conservation of Nature's Red List. Bacterial infections have been suggested as causative agents in many coral diseases worldwide, but identifying specific pathogenic microorganisms remains inconclusive. Reef sediment may play a role, as the uncharacteristic upward progression of white-band disease often begins where branches touch sediment. Tissue-loss diseases affecting *A. cervicornis* were

investigated using histopathological examinations and bacterial 16S rDNA next-generation sequencing. The microbiomes of apparently healthy *A. cervicornis*, diseased *A. cervicornis*, and adjacent sediment samples were compared. Taxonomic and phylogenetic analyses found Proteobacteria to be the dominant phylum present in all reef-sediment and coral-tissue samples. Sediment-associated microbial communities were significantly more diverse than those associated with coral tissue, and microbial communities associated with apparently healthy *A. cervicornis* were more diverse than communities associated with diseased coral tissue. This study confirmed the presence of bacteria from families Vibrionaceae and Rickettsiaceae, both of which have been previously associated with coral diseases. Vibrionaceae bacteria were found in both coral and sediment samples while Rickettsiaceae bacteria were limited to coral tissue samples. Linear discriminant analysis revealed that communities associated with the tissue-loss margin of a disease lesion were significantly more enriched with Vibrionaceae bacteria than apparently healthy communities. Histopathological examinations of all coral tissues, even apparently healthy tissues, revealed moderate to severe hypertrophy in epidermal mucocytes, dissociation of mesenterial filaments, necrosis of cnidoglandular bands, and atrophy of the calicodermis. This study provides histological and molecular evidence that *A. cervicornis* health was in decline prior to the presentation of a tissue-loss lesion. More conservative approaches should be adopted when assessing disease prevalence, and the progression of disease needs to be examined molecularly using more specific tissue sampling. This work also supports prior observations that coral tissue-loss diseases are polymicrobial diseases associated with an imbalance of residential bacterial populations

and proposes that the increase in bacteria of family Vibrionaceae is an early biomarker of disease in *A. cervicornis* prior to gross tissue loss.

PREFACE

The biology and ecology of *Acropora cervicornis*

Coral reef ecosystems are mainly found in clear, warm, oceanic waters that lie within the tropical latitudes of 23.4°N to 23.4°S (Goreau et al. 1979; Moberg and Folke 1999). *Acropora cervicornis* (staghorn coral) is a hermatypic stony coral that is classified in the phylum Cnidaria, order Scleractinia, and class Anthozoa (Aronson et al. 2008). This coral produces its exoskeleton by depositing successive layers of calcium carbonate ($CaCO_3$) (Goreau et al. 1979). *A. cervicornis* is described as a branching coral that is comprised of long cylindrical branches that typically grow 2 m in length and are golden in color (Aronson and Precht 2001a, 2001b; Boulon et al. 2005; Aronson et al. 2008). Sub-branches emerge nearly at right angles and form loosely packed or 'open' colonies. *A. cervicornis* has been one of the three most significant contributors to the underlying framework of tropical Atlantic reef ecosystems, providing substrate for colonizing benthic organisms, serving as critical habitats for commercially important invertebrate and fish species, and serving as a source of biogenous carbonate sediment (Adey 1978; Boulon et al. 2005). The rapid calcification rates of *A. cervicornis* have been linked to the symbiotic single-celled dinoflagellate algae, called zooxanthellae, that live in the gastrodermal cells of coral tissues (Goreau et al. 1979). Corals provide excretion products to the algal cells while the zooxanthellae provide nutritional photosynthetic products to the corals in return (Knowlton 2001). Zooxanthellae found in *A. cervicornis* have been identified to be from the genus *Symbiodinium*, and these dinoflagellates provide 90

percent of the coral's energy budget from their phototrophic contribution, enhance coral calcification, and are responsible for giving the coral most of its color (Boulon et al. 2005).

A. cervicornis colonies are found in shallow tropical reefs throughout the Caribbean, southern Gulf of Mexico, and along the east coast of Florida and have been documented as far north as Fort Lauderdale, between Port Everglades (26°05.34′N; 80°06.26′W) and Hillsboro Inlet (26°15.28′N; 80°04.51′W) (Goldberg 1973; Vargas-Ángel et al. 2003). Prior to the mid-1980s, acroporids dominated the fore-reef zones at depths of 5–25 m. *A. cervicornis* is now typically found scattered along the upper to mid-reef slope regions, in lagoon areas that encounter low to moderate wave exposure, and are common in back- and patch-reef habitats at depths ranging from zero to 34 m (Jaap et al. 1989; Boulon et al. 2005; Aronson et al. 2008). These corals grow at a relatively fast rate of 10–20 cm per year in comparison to other Atlantic reef-building coral species. The branches of *A. cervicornis* can easily be broken due to strong wave action and human interaction, as the coral's skeleton is quite porous (Adey 1978; Tunnicliffe 1981; Highsmith 1982; Boulon et al. 2005). Fortunately, the dominant mode of reproduction for this species is asexual fragmentation, which allows the broken branches to grow into new colonies under favorable conditions and reattach to the substrate (Boulon et al. 2005). This reproductive strategy gives *A. cervicornis* a competitive spatial advantage over other coral species, as it is able to locally dominate hard-bottom and coral-reef habitats (Highsmith 1982). Regardless of whether a branch fragment is carried long distances by waves and currents or settles within close proximity of the original colony, favorable

conditions allow for populations to expand and occupy new areas (Shinn 1976; Highsmith 1982; Jaap et al. 1989).

A. cervicornis, like many stony coral species, has the ability to reproduce both asexually and sexually (Highsmith 1982). Some massive coral species are estimated to reach sexual maturity when their colonies grow to be approximately 10 cm in diameter, which typically takes about 8 years, but since *A. cervicornis* is faster growing, this species is likely to reach sexual maturity at a younger age (Szmant 1986). These corals are hermaphroditic broadcasters that release their gametes into the water column during massive spawning events that take place only a few nights during the months of July, August, and/or September (Boulon et al. 2005). Fertilization and larval development both occur externally to the parental colonies. Little is known about larval settlement in this species, but it is believed that their planula larvae live amongst plankton until settlement (Boulon et al. 2005). Thus, the widely dispersing larvae of *A. cervicornis* are thought to provide some protection for the corals against the risk of extinction (Knowlton 2001).

Coral reef ecosystems

Coral reefs are valued as one of the most biologically diverse and productive ecosystems on Earth (Connell 1978; Reaka-Kudla 1997; Moberg and Folke 1999; Spalding et al. 2001; Wilkinson 2002, 2004, 2008; Burke 2004; Carpenter et al. 2008; Waddell and Clarke 2008; Burke et al. 2011). Although coral reefs account for less than 0.1% of benthic oceanic terrain (Reaka-Kudla 1997), these reefs extend over approximately 250,000 km^2 of the ocean and are estimated to be home to 25 percent of all known marine species (McAllister 1995; Spalding et al. 2001). Moreover, it is estimated that there are at least 835 species of hermatypic, or reef-building, corals and these corals are responsible for supporting an overall biodiversity of approximately 1–9

million species (Reaka-Kudla 1997; Knowlton 2001). The high habitat heterogeneity and three-dimensional architecture of coral reef ecosystems facilitate niche diversification, which helps to maintain high biodiversity and allows for the possibility of evolution of new species (Risk 1972; Luckhurst and Luckhurst 1978). Coral reef ecosystems are also interconnected to surrounding ecosystems such as mangrove forests and sea grass beds and it is the interactions between these three ecosystems that function together to help support the high biodiversity of marine organisms in these areas (Green and Short 2003).

Healthy coral reefs provide a diverse array of essential ecosystem services that support the livelihoods of an estimated 850 million people, or one-eighth of the world's population (Burke et al. 2011). The ecological and economic values of coral reefs continue to increase as corals not only provide critical habitat for numerous species, but also provide storm protection to coastal communities, food security to global human populations, medicinal possibilities, benefits from nutrient cycling, and tourism and recreational activities, as well as cultural, social, and aesthetic benefits (Costanza et al. 1997; Moberg and Folke 1999; Cesar et al. 2003; Conservation International 2008; Glaser and Mayer 2009; Burke et al. 2011). Of these services, most value assessments focus on revenue generated from tourism, reef-related fisheries, coastal protection, and biodiversity, as the prices for these services and their associated goods are traceable in markets and are thus relatively easy to calculate (Burke et al. 2011).

Economic assessments have indicated that the potential net benefit of the world's reefs is approximately US $30 billion (Wilkinson 2002; Cesar et al. 2003; Conservation International 2008). Burke et al. (2011), estimated that activities such as tourism and recreation generated approximately US $11.5 billion annually, while reef-related fisheries

accounted for US $6.8 billion and ecological values applied to ecosystem services such as coastal protection and biodiversity were worth an estimated US $10.7 billion and US $5.5 billion, respectively. Additionally, the annual net benefits from reef-related goods and services produced by Caribbean coral reefs specifically, were estimated to be worth approximately US $5.9 billion alone (Burke 2004; Burke et al. 2011). After evaluating all the net benefits, the corresponding global asset value of coral reefs was estimated to be nearly US $800 billion (Cesar et al. 2003).

Coral diseases

Infectious diseases are believed to play a major role in coral reef degradation worldwide and it has been suggested that anthropogenic stressors are contributing to coral diseases (Richardson 1998; Dustan 1999; Rosenberg and Loya 2004; Sutherland et al. 2004; Weil 2006; Lesser et al. 2007; Aronson et al. 2008). Disease is defined as any interruption, cessation, deviation, proliferation, or other malfunction of vital body functions, systems, or organs (Sutherland et al. 2004). This definition also includes any impairment that interferes with or modifies the performance of normal function such as responses to environmental factors or combinations of factors (Galloway et al. 2007). Coral diseases are mostly observed in the field when signs of morbidity/mortality or lesions are found on the coral colony (Work and Aeby 2006). Coral lesions are typically recognized as changes in tissue color, shape, size, and/or texture; however, disease diagnosis can be challenging as many coral disease signs can be similar for two or more diseases (Richardson 1998; Pantos et al. 2003; Pantos and Bythell 2006; Work and Aeby 2006).

The first descriptive reports of scleractinian tissue degradation due to disease appeared in the 1970s (Antonius 1973; Richardson 1998). Between the 1970s and 1990s

only three coral diseases were recorded: black-band disease (BBD), white-band disease (WBD), and white plague (WPL). BBD was first reported by A. Antonius in 1973, while the latter two diseases were first documented in 1977 (Dustan 1977; Gladfelter et al. 1977). Many coral diseases are associated with pathogenic organisms, such as bacteria, cyanobacteria, fungi, and protists. However pathogenic agents have only been identified for a handful of coral diseases (Peters 1997; Sutherland et al. 2004; Galloway et al. 2007, 2009).

During the last three decades, the number of coral diseases that have been identified has increased exponentially, as well as the number of reported disease events or outbreaks, and the number of coral species being affected by disease (Richardson 1998; Harvell et al. 1999; Green and Bruckner 2000; Hughes et al. 2003; Pandolfi et al. 2003; Rosenberg and Loya 2004; Sutherland et al. 2004; Weil 2004; Williams and Miller 2005; Vollmer and Kline 2008). Current estimates indicate that more than 40 reported diseases affect approximately 150 coral species that are found on reefs in 63 countries (Galloway et al. 2009). The wider Caribbean region has been coined the coral disease "hot-spot" since 66 percent of reported disease outbreaks have occurred in this area, despite being home to only 8 percent of the world's total coral-reef area (Green and Bruckner 2000). Furthermore, 82 percent of reef-building scleractinians in the Caribbean have been reported to be affected by at least one disease (Weil 2004; Galloway et al. 2007). Despite various hypothesized explanations, the reason behind this phenomenon is still unknown and no causal mechanism has been established (Pandolfi et al. 2003; Weil 2004; Hoegh-Guldberg et al. 2007).

Elevated levels of coral disease have been linked to a variety of anthropogenic activities and disturbances that alter environmental conditions (Lamb and Willis 2011). In Australia, coral diseases were 15 times more prevalent on reefs that contained tourism platforms than at nearby reefs that lacked such platforms (Lamb and Willis 2011). Specifically, Lamb and Willis (2011) found that acroporid corals had the greatest disease prevalence and exhibited an 18-fold increase in disease prevalence at reefs where tourism platforms were present, which was most likely due to cumulative effects of a number of factors. The introduction of potentially toxic compounds and elevated nutrient concentrations from agricultural runoff and sewage outflows may exacerbate coral diseases (Bruno et al. 2003). Specifically, coral diseases such as white pox disease (WPD) (Sutherland et al. 2010) and WPL have been associated with proximity to sewage outfalls that contain human enteric viruses (Kaczmarsky et al. 2005; Futch et al. 2011). (Sutherland et al. 2011) showed that distinct strains of the human pathogen, *Serratia marcescens*, were responsible for causing disease in *A. palmata*, linking environmental interactions between public health practices and coral reef health and survival.

The ecological effects of disease (and coral bleaching) are expected to be severe as growth rates of corals are typically much slower than the tissue loss and mortality rates associated with a disease (Knowlton 2001; Smith 2013). The loss of hermatypic corals in Belize, specifically acroporids, resulted in an ecological phase shift from coral-dominated to algal-dominated reefs in the country (Hughes 1994; Aronson and Precht 2001b). As a result, coral epizootics and destruction of reef habitats can cause detrimental impacts to the millions of species that rely on these ecosystems (Costanza et al. 1997; Cesar et al. 2003). Despite these impacts, relatively little is understood about the causes of coral

disease outbreaks and transmission of the pathogenic microorganisms causing diseases due to a lack of baseline data and epizootiological information (Richardson 1998; Harvell et al. 1999; Knowlton 2001).

Tissue-loss diseases affecting *Acropora cervicornis*

In the last 30 years, emerging diseases, compounded with climate change and anthropogenic factors, have led to more than an 80 percent population reduction in *A. cervicornis* across the Caribbean and tropical western Atlantic Ocean (Aronson et al. 2008; Carpenter et al. 2008). Before 1980, acroporid corals dominated shallow Caribbean reefs. These corals were reduced to smaller, scattered patches by 1990 due to epizootic events (Knowlton 2001). Most recent estimates show that 80–98 percent of *A. cervicornis* individuals have been lost in the last 30 years and there has been a 97 percent decline in this species specifically in the Florida Keys (Aronson et al. 2008). These declines resulted in the corals being listed as threatened under the United States Endangered Species Act (ESA) and as critically endangered under the International Union for Conservation of Nature's (IUCN) Red List (Aronson et al. 2008).

Coral decline is a growing concern worldwide as the area of live coral-tissue coverage is declining at an estimated rate of 9.2 percent per year (Côté et al. 2005). Although tissue loss in *A. cervicornis* is caused by a variety of factors, the predominant source of tissue loss is caused by disease outbreaks (Miller et al. 2006; Carpenter et al. 2008). Acroporid diseases such as WBD are thought to be the primary cause for the unprecedented region-wide species decline during the 1980s and diseases are an ongoing concern today (Aronson and Precht 2001a, 2001b; Williams and Miller 2005). Furthermore, disease-related tissue loss has caused higher mortality in acroporid corals

than resulting mortalities from hurricanes in the last 20–25 years (Aronson and Precht 2001b).

The three described acroporid tissue-loss diseases are white-band disease type I (WBD-I), white-band disease type II (WBD-II), and rapid tissue loss (RTL). Each of these diseases exhibits different progressive tissue-loss patterns that expose the bare skeleton of the diseased corals when polyps and coenenchyme, or the tissue between polyps, disappear (Sutherland et al. 2004; Williams and Miller 2005). WBD has been affecting acroporid corals since the 1970s, while RTL is a newly described disease, the first documented report followed an epizootic event in the Florida Keys in 2003 (Gladfelter et al. 1977; Williams and Miller 2005). Gladfelter (1982) first described WBD, but now two variations of the disease have been recorded, WBD type I and type II (Ritchie and Smith 1998). Both types of WBD exclusively affect branching acroporid corals. WBD-I affects both *Acropora palmata* and *A. cervicornis* throughout the Caribbean, whereas WBD-II has been reported affecting *A. cervicornis* in the Bahamas (Gladfelter 1982; Ritchie and Smith 1998; Sutherland et al. 2004).

WBD-I progresses rapidly in acroporid corals resulting in tissue loss of up to 2 cm per day (Gladfelter 1982; Peters et al. 1983). The disease is described to originate at the base of a coral colony or branch, although it can begin in the middle of a branch, and then progresses towards the branch tips (Gladfelter 1982; Peters et al. 1983; Pantos and Bythell 2006). As the disease progresses, a white band of denuded skeleton results and creates a sharp boundary between the normally pigmented tissue and skeleton (Gladfelter 1982). Although histological examinations of WBD tissues have revealed the presence of Gram-negative bacterial colonies in both diseased- and apparently healthy-tissue samples

(Peters et al. 1983), no specific causative pathogen could be established because diseased-tissue samples were also found that did not have these bacterial aggregates (Pantos and Bythell 2006). Rickettsiales-like bacteria have also been associated with WBD-I (Casas et al. 2004); however, the results of a study conducted by (Kline and Vollmer 2011) suggested that these microorganisms are not likely involved in causing WBD-I and suggested that the disease is rather caused by Gram-positive infectious bacteria.

WBD-II differs from WBD-I in that the tissue-loss lesion (2 to 20 cm wide) associated with type II includes a section of bleached tissue between the normally pigmented tissue and the tissue-loss margin (Ritchie and Smith 1998). Often, the bleached area will progress faster than the tissue-loss lesion, but bleaching is also known to arrest at times. When bleaching ceases, the tissue-loss margin catches up to the normally pigmented coral tissue, causing WBD-II to closely resemble WBD-I. Since there is no longer an observable bleached section separating the tissue-loss margin and the normally pigmented tissue, the two diseases become indistinguishable in the field by short-term gross observations (Ritchie and Smith 1998). Similar to WBD-I, WBD-II also originates at the base or middle of a coral colony or branch, progressing upward towards the branch tips. WBD-II has also been observed originating at the branch tips and progressing towards the coral colony's base (Ritchie and Smith 1998). Although no causative agent or pathogen has been identified for WBD-II, the disease has been associated with the presence of the bacterium *Vibrio harveyi (carchariae)* in coral mucus samples collected from the bleaching margin. However, efforts to fulfill Koch's

postulates have been unsuccessful and there is currently no defined pathogen for WBD-II (Work and Meteyer 2014).

The third acroporid-specific disease, RTL, was first found in 2003 after an epizootic event at White Bank Dry Rocks, Florida Keys (Williams and Miller 2005). This disease was characterized by multi-focal lesions of rapid tissue loss in irregular patterns along coral branches. Gross observations of RTL lesions were not consistent with either WBD-I or -II (Williams and Miller 2005). Gladfelter (1982) described a proximal gradation of algal colonization on the denuded skeleton after affected acroporid corals lost tissue in WBD. In the case of RTL, uniform degrees of algal colonization were found on exposed skeleton post tissue loss, thus indicating that the entire area lost tissue at approximately the same time (Williams and Miller 2005). Although the etiology of RTL is not understood, experiments have shown that RTL is transmissible by the corallivorous snail, *Coralliophila abbreviata* (Williams and Miller 2005).

An overview of coral disease research

Most described coral diseases only account for the gross phenotypic expression of the disease and little effort has been made to apply standardized biomedical tools to determine cause (Work and Aeby 2006). In many cases, tissue lesions are non-specific and may have multiple causes. However, the default assumption is often that infectious agents—specifically bacteria—are responsible (Work and Aeby 2011). This lack of standardized health assessment tools has limited coral disease investigations (Work and Aeby 2010).

Four standardized biomedical methods have been applied to investigating animal diseases: (1) field investigations, (2) microscopic pathology, (3) laboratory biodetection, and (4) fulfillment of Koch's postulates (Wobeser 2007). In a review of the coral disease

literature, biodetection methods were used the most (43%) for coral disease investigations, 74% of which focused specifically on culture or molecular characterization of bacteria or fungi from corals (Work and Meteyer 2014). Both culture-based and culture-independent methods have shown that corals favor specific mutualistic (Reshef et al. 2006) populations of bacterial associates (Ritchie and Smith 1997, 2004; Rohwer et al. 2002). Furthermore, 16S rDNA sequencing analyses have shown that coral-bacteria communities are host species-specific, and are significantly different than bacterial-associated communities found in the surrounding seawater (Rohwer et al. 2001, 2002; Frias-Lopez et al. 2002; Bourne and Munn 2005). However, species composition from culture-dependent and culture-independent analyses have yielded significantly different results (Fuhrman and Campbell 1998; Rohwer et al. 2001). The coral holobiont, with regards to coral disease, has been studied intensively using biodetection tools (Rosenberg et al. 2007b; Vega Thurber et al. 2009), but despite increasing efforts pathogen identification is still problematic.

Molecular investigations alone are not enough if the true etiology and pathogenesis of tissue-loss diseases are to be understood, because these tools are generally used to identify and propose individual pathogenic organisms. Molecular tools fail to connect tissue pathology with microorganisms and are not capable of defining the cellular host response. Although biodetection methods have found unique bacterial communities in apparently healthy and diseased coral tissues, molecular methods are not capable of inferring whether the identified bacteria were responsible for causing cellular damage (Work and Meteyer 2014). The true meaning of these molecular analyses simply cannot be interpreted in the absence of a more complete diagnostic picture.

While coral-disease investigations have predominately focused on identifying a causative pathogen through laboratory biodetection, histological efforts have decreased over time (Work and Meteyer 2014). Work and Meteyer (2014) found that standard histopathology examinations at the light microscopic level only accounted for 11% of coral disease investigative efforts. Histopathology provides a means to visually analyze susceptibilities to physical injuries, environmental impacts, and mechanisms and repair in target cells and coral tissues (Peters et al. 2005). By examining both apparently healthy and diseased coral tissues, feeding, immune and physical defense mechanisms, growth, and reproduction can be observed (Peters 1984; Galloway et al. 2007). Without histological examinations, pathology cannot be understood and the relationship between the coral, potential causative agents, and marine environment remains incomplete (Work and Meteyer 2014).

Histopathological diagnostic tools are critical for determining cellular changes in the coral tissue due to disease as changes may be occurring well before gross lesions can be observed. Such knowledge is critical in order to gain understanding about the etiology of tissue-loss diseases. Histopathology is an underutilized, culture-independent approach to coral disease diagnostics that provides critical information towards understanding coral disease pathogenesis (Work et al. 2008b). The limited use of multidisciplinary diagnostic tools in coral disease investigations have resulted in a lack of robust etiological characterization (Sutherland et al. 2004; Rogers 2010). (Bourne et al. 2009) emphasized the importance of using multidisciplinary investigations to understand what factors are driving the increase in coral disease outbreaks.

GOALS AND HYPOTHESES

This study used an interdisciplinary methodological approach to fulfill three of four standardized biomedical methods to further our understanding and characterize tissue-loss diseases affecting *A. cervicornis*: (1) field investigations through photographic documentation and lesion description; (2) microscopic pathology using histopathology examinations; and (3) biodetection through molecular analysis. Fulfillment of Koch's postulates was not attempted in this study, which is the fourth standard biomedical approach. This project compared the composition of bacterial communities associated with apparently healthy *A. cervicornis*, diseased *A. cervicornis*, and reef sediment to determine whether bacterial communities play a role in tissue-loss diseases affecting *A. cervicornis*. This research:

1. described the microanatomy of apparently healthy and diseased *A. cervicornis* tissues using histopathological techniques,
2. characterized the microflora of apparently healthy *A. cervicornis* from offshore reefs in the Upper Florida Keys using molecular analyses,
3. compared bacterial communities associated with apparently healthy and diseased *A. cervicornis* from the Upper Florida Keys using molecular analyses,

4. compared bacterial communities associated with apparently healthy and diseased *A. cervicornis* tissue with sediment samples collected from the adjacent environment in the Upper Florida Keys using molecular analyses, and
5. determined if the presence of key taxa (Rickettsiales and Vibrionales) were found in association with apparently healthy and diseased *A. cervicornis* tissue.

Histopathological diagnostic tools are critical for determining cellular changes in the coral tissue due to disease as changes may be occurring well before gross lesions can be observed. Histological examinations described and compared the microanatomy of apparently healthy, healthy-on-diseased, and diseased *A. cervicornis* tissues. This study also characterized diseased *A. cervicornis* tissues on a finer spatial scale by examining the normally pigmented area of the diseased branch (healthy-on-diseased section of the diseased branch, HDD), the tissue-loss margin (TLM), and the denuded skeleton (DS) portions of the diseased samples. Ten histological parameters were also observed between WBD and RTL samples to test for differences between tissue-loss disease types.

$H_0$1: Histopathological parameter scores do not differ between apparently healthy and diseased *A. cervicornis* tissues.

H_A1: Histopathological parameter scores are different between apparently healthy and diseased *A. cervicornis* tissues.

$H_0$2: Histopathological parameter scores do not differ between white-band disease and rapid tissue loss.

H_A2: Histopathological parameter scores are different between white-band disease and rapid tissue loss.

Recognizing disease requires an understanding of what "good health" is by defining a normal range of gross, microscopic, physiological, biochemical, and behavioral attributes or functions in a coral species (Peters 1984). Disease diagnosis and potential mitigation of future outbreaks requires fundamental knowledge of the composition and distribution of the microbial communities associated with both apparently healthy and diseased colonies (Beleneva et al. 2005). Despite efforts, apparently healthy communities remain largely uncharacterized (Bourne and Munn 2005), and little research efforts have examined *A. cervicornis* bacterial communities specifically. Therefore, this study characterized the community composition of apparently healthy *A. cervicornis,* and compared the bacterial-associated communities of apparently healthy and diseased *A. cervicornis* to test the following hypothesis:

$H_0$3: The bacterial communities associated with apparently healthy *A. cervicornis* tissues do not differ from the bacterial communities associated with diseased *A. cervicornis* tissue.

H_A3: The bacterial communities associated with apparently healthy *A. cervicornis* tissues are different from the bacterial communities associated with diseased *A. cervicornis* tissue.

Few studies to date have directly linked reef sediment as a potential environmental driver or abiotic pathogen of coral disease. Coral Restoration Foundation (CRF) nursery manager, Ken Nedimyer, hypothesized that a microorganism(s) in the reef sediment was responsible for triggering the uncharacteristic upward progression of WBD-I (pers. comm. 2011). This phenomenon was observed on *A. cervicornis* branches

that were touching sediment in both the CRF nursery and outplanted colonies on reefs in the Upper Florida Keys during the summer of 2011 and 2012. Therefore, this study compared the microbial communities associated with reef sediment with coral-associated bacterial communities to test this study's fourth hypothesis:

$H_0$4: Bacteria in the surrounding sediment are not a source of potential pathogens.

H_A4: Bacteria in the surrounding sediment are a source of potential pathogens.

There is some debate regarding the association of Rickettsiales-like bacteria and WBD-I. Rickettsiales-like bacteria, particularly in the surface mucopolysaccharide layer (SML), have been associated with WBD-I (Casas et al. 2004). (Casas et al. 2004) found that both apparently healthy and WBD-affected acroporid bacterial communities were dominated by a coral-associated Rickettsiales 1 (CAR1) bacterium using cloning and sequencing methods. However, (Kline and Vollmer 2011) showed that Rickettsiales-like bacteria were not likely involved in causing WBD-I because ampicillin, an ineffective antibiotic against obligate intracellular bacteria such as *Rickettsia*, effectively suppressed disease transmission during their experiments. (Kline and Vollmer 2011) instead suggested that the disease was caused by transmissible Gram-positive infectious bacteria. Despite conflicting findings in the literature, Rickettsiales-like organisms (RLOs) have been observed in *A. cervicornis* tissue histologically. Therefore, this study used more advanced sequencing techniques to examine the relative abundance of Rickettsiales bacteria found in association with apparently healthy and diseased *A. cervicornis* tissue to test the hypothesis:

$H_0$5: Rickettsiales abundance does not differ in apparently healthy and diseased *A. cervicornis* tissue.

H_A5: Rickettsiales abundance is different in apparently healthy and diseased *A. cervicornis* tissue.

(Ritchie and Smith 1998) identified *Vibrio harveyi (carchariae)* as the putative pathogen of WBD-II, but Pantos and Bythell (2006) noted that no vibrios were detected in WBD-I diseased tissue using culture-independent techniques. (Gil-Agudelo et al. 2006) also associated WBD-II with the presence of *V. harveyi (carchariae)* in SML samples collected from the bleaching margin of the disease lesion. Most recently, (Sweet et al. 2014) proposed that a histophagus ciliate, *V. harveyi (carchariae),* and two other candidate bacterial pathogens were potential primary pathogens of WBD. All three of the candidate bacteria have previously been indicated as potential causative agents in similar tissue-loss diseases: white syndrome (Sweet and Bythell 2012), WBD-II (Gil-Agudelo et al. 2006), and WBD in Indonesian acroporids (Hakim et al. 2012). Ultimately, no causative agent or pathogen has yet been identified for WBD-II, because *V. harveyi (carchariae)* could not be reisolated and no definitive identification has been documented. Therefore, this study used more advanced sequencing techniques to examine the relative abundance of Vibrionales found in association with apparently healthy and diseased *A. cervicornis* tissue to test a fourth hypothesis:

$H_0$6: Vibrionales abundance does not differ in apparently healthy and diseased *A. cervicornis* tissue.

H_A6: Vibrionales abundance is different in apparently healthy and diseased *A.* cervicornis tissue.

CHAPTER 1: HISTOLOGICAL DIFFERENCES WERE OBSERVED BETWEEN APPARENTLY HEALTHY AND TISSUE-LOSS AFFECTED *ACROPORA CERVICORNIS*

Introduction

Coral diseases have caused significant declines in coral coverage worldwide since the 1970s (Goreau et al. 1998; Richardson 1998; Harvell et al. 1999; Green and Bruckner 2000; Pandolfi et al. 2003). Once dominating shallow Caribbean reefs, *Acropora cervicornis* (staghorn coral) and *A. palmata* (elkhorn coral) populations have experienced unprecedented declines largely due to these epizootic events (Bruckner 2002). Acroporid populations have declined by 80 percent across the Caribbean and tropical western Atlantic Ocean (Harvell et al. 2002) and by 95 percent in the Florida Keys (Miller et al. 2003). These declines resulted in the listing of these two species as threatened under the United States Endangered Species Act (ESA) (Hogarth 2006). These declines have disrupted the coral community and led to the replacement of acroporid dominant reefs responsible for the ecosystem's architecture with low encrusting agariciids (Aronson et al. 1998; Aronson and Precht 2001b; Graham et al. 2006).

Disease is defined as any interruption, cessation, deviation, proliferation, or other malfunction of vital body functions, systems, or organs (Sutherland et al. 2004). This definition also includes any impairment that interferes with or modifies the performance of normal function such as responses to environmental factors that can be caused by

combinations of abiotic and biotic factors (Galloway et al. 2007). However, many coral diseases have been described solely on the basis of gross observation and disagreements exist as to whether observed changes affecting corals are actually signs of disease (Sutherland et al. 2004; Weil 2004; Galloway et al. 2007; Lesser et al. 2007; Waddell and Clarke 2008).

Coral host responses are limited to growth anomalies, patterns of discoloration, and tissue loss (Work and Aeby 2006), where lesions can have multiple potential etiological agents that fluctuate over time (Work and Aeby 2011; Work et al. 2012). This has led to the naming of at least eight described "white" or tissue-loss diseases in the Caribbean, each characterized by the loss of symbionts and extensive tissue necrosis (Sutherland et al. 2004): white-band disease (WBD) type I (WBD-I) (Gladfelter 1982), WBD type II (WBD-II) (Ritchie and Smith 1998), white plague (WPL) type I (WPL-I) (Dustan 1977), WPL type II (WPL-II) (Richardson et al. 1998), WPL type III (WPL-III) (Richardson et al. 2001), white-pox disease (WPD) (Holden 1996), rapid tissue loss (RTL) (Williams and Miller 2005), and shut-down reaction (Antonius 1977). Moreover, it can be challenging to distinguish tissue-loss damage resulting from coral disease with tissue-loss resulting from predation (Patterson et al. 2002; Sutherland et al. 2004). Because diseases are often described and named based on a single observation, it is often difficult to distinguish differences in tissue loss patterns from coral diseases using short-term field observations (Ritchie and Smith 1998).

With regards to acroporids, three described tissue-loss diseases affect *A. cervicornis*: WBD-I, WBD-II, and RTL. WBD-I was one of the first described coral diseases, and was first documented in 1977 (Gladfelter et al. 1977). Both types of WBD

involve a progressive lesion whose tissue-loss margin is described as a white-band. As the disease progresses, a white band of denuded skeleton results and creates a sharp boundary between the normally pigmented tissue and skeleton (Gladfelter 1982). WBD-II has been distinguished from WBD-I, as WBD-II also includes a section of bleached tissue between the normally pigmented tissue and the tissue-loss margin (Ritchie and Smith 1998). RTL was not defined until 2003 and is characterized by the presence of multi-focal lesions of rapid tissue loss in irregular patterns along branches (Williams and Miller 2005). However, coral diseases are not the only source of tissue loss in this species. Corallivores, such as *Coralliophila abbreviata*, are also a source of tissue loss in acroporids. Further adding to the conundrum of disease identification, recent tissue losses observed in *A. cervicornis* that cannot be attributed to predation are frequently identified as WBD regardless of the rate of tissue loss and lesion pattern observed on the colony (Precht et al. 2002; Williams and Miller 2005). This lack of standardized nomenclature of gross lesions increases the existing ambiguity surrounding coral diseases and has produced gross descriptions subject to interpretation.

Despite more than a decade of dedicated coral disease research, still very little is known about coral diseases and their causes (Pollock et al. 2011). The lack of standardized biomedical tools in coral health assessment greatly limits the thoroughness and effectiveness of coral disease investigations (Work and Aeby 2010). Unlike most animal disease investigations, coral disease studies have been driven towards the identification of presupposed microbial pathogens based on gross observations (Richardson 1998; Sutherland et al. 2004; Polson et al. 2008; Work and Aeby 2011; Work and Meteyer 2014). These assumptions about the microbial etiology have led to a

number of culture-based and culture-independent (mostly using molecular techniques) studies, but microscopic pathology has consistently taken a minor role in coral disease research (Work and Aeby 2011; Work and Meteyer 2014). In fact, Work and Meteyer (2014) showed that histopathological efforts have decreased over time and have only been used as an investigative tool in 11% of the coral disease literature. Conversely, most animal diseases depend heavily on documentation of histopathology and pathogenesis of disease at the tissue and cellular level to fulfill Koch's postulates (Work and Meteyer 2014).

Histopathology is an underutilized, culture-independent approach to coral disease that provides critical information towards understanding coral disease pathogenesis (Work et al. 2008b). Work and Meteyer (2014) hypothesized that the lack of progress in understanding coral disease causation is greatly due to the fact that limited efforts have been made to document what is happening to sick corals at the cellular level. Histopathology is necessary for understanding a coral's response to infection or to one or more abiotic pathogens at the microscopic level, and for understanding the relationship between the host and causative agent (Work and Meteyer 2014). Histopathological diagnostic tools are critical for determining cellular changes in the coral tissue due to disease as changes may be occurring well before gross lesions can be observed. Such knowledge is critical in order to gain understanding about the etiology of tissue-loss diseases.

Routine histological examinations (Peters et al. 2005) of 43 *A. cervicornis* samples were performed in this study to describe the microanatomy of coral sections of apparently healthy, healthy-on-diseased, and diseased *A. cervicornis* tissue. Using

procedures that are similar to those used to diagnose diseases in humans and other organisms, the samples were examined histologically to look for the presence or absence of bacteria or parasites associated with different tissues and to identify any morphological differences that might indicate the presence of functional impairment. Histopathological examinations have mostly been used to compare apparently healthy and diseased coral tissues, and few examine the tissue loss margin. To further our understanding about tissue-loss diseases affecting *A. cervicornis*, this study compared histological observations of diseased *A. cervicornis* on a finer spatial scale. Therefore, the normally pigmented area of the diseased branch (healthy-on-diseased section of the diseased branch, HDD), the tissue-loss margin (TLM), and the denuded skeleton (DS) portions of the diseased samples were further examined to test for differences in tissue condition among the sample types. This study also tested histological differences between WBD and RTL samples.

Methods

Field site

Apparently healthy and diseased *A. cervicornis* colonies were grossly identified during surveys conducted in the Upper Florida Keys during June 2011 and July 2012. Samples were collected from nursery, restored, and naturally recruited *A. cervicornis* colonies, where restored sites contained either outplanted (i.e., from the Coral Restoration Foundation's (CRF) nursery), transplanted (i.e., from nearby naturally recruited populations), or a mixture of both colony types as explained in (Miller et al. 2014) (Table 1). In 2011, samples were collected from the CRF nursery and three restored sites, Key Largo Dry Rocks (KLDR), Molasses Reef (MO), and Aquarius Reef (AQ), using SCUBA. Restored coral colonies at KLDR, Molasses Reef, and some restored Aquarius

Table 1. Characteristics of all field sites in the Upper Florida Keys.

Field Site	Site type	Depth (m)	Latitude (N)	Longitude (W)
CRF Nursery	Nursery	10	24° 58.940	80° 26.153
KLDR	Outplant	6–7	25° 7.280	80° 17.798
Molasses Reef	Outplant	8–9.5	25° 0.599	80° 22.373
Aquarius	Outplant	16	24° 57.000	80° 27.217
French Reef	Outplant	10	25° 2.084	80° 20.891
Conch Shallow	Outplant	5–7	24° 57.083	80° 27.594
Little Conch	Wild	5.5	24° 56.780	80° 28.210

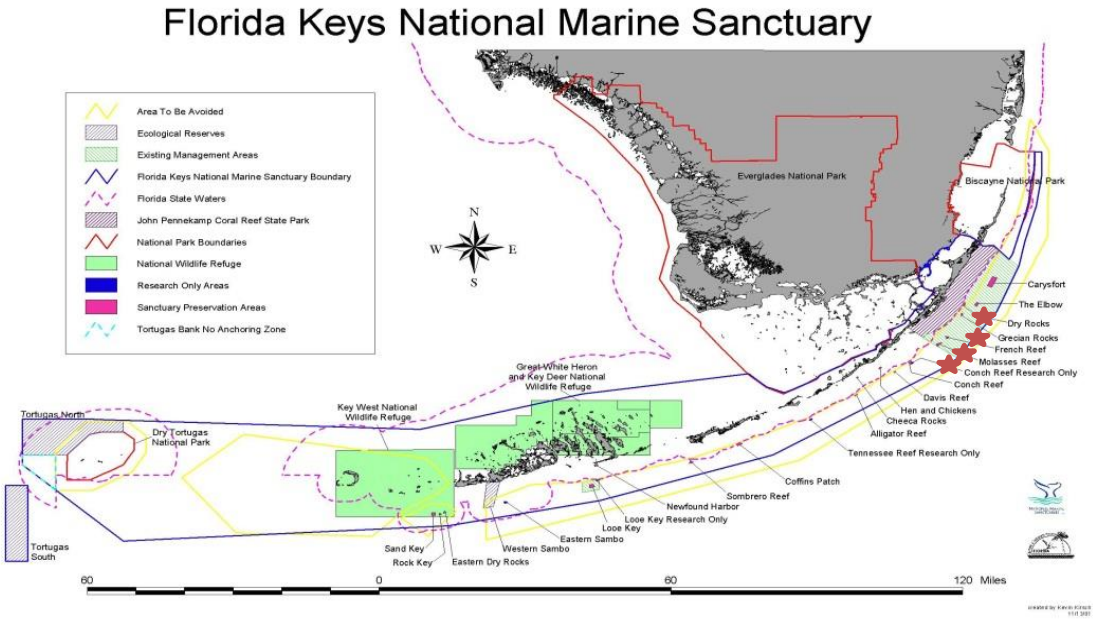

Figure 1. Map of the Florida Keys National Marine Sanctuary, where stars indicate specific field sites where samples were collected (sites not listed include CRF Nursery and Aquarius) (NOAA 2015).

colonies originated from the CRF nursery. All sites except for AQ were found in shallow (5–10 m) fore-reefs, and AQ samples were collected from a deeper fore-reef (16 m) (Figure 1). In 2012, samples were collected from two restored sites, French Reef (FR) (nursery origin) and Conch Shallow (CS) (transplanted), and a naturally recruited site, Little Conch Reef (LC), in addition to KLDR and MO—all shallow fore-reefs found between 6-10 m. Temperature for all sites varied little during the collection period 30–32°C.

Sample collection 2011

A. cervicornis colonies were photographed in situ and 3-cm coral branch fragments were collected using heavy-duty wire clippers. Two coral-tissue sample types were collected from each field site: apparently healthy tissue from a colony exhibiting no disease signs (apparently healthy, AH) (n=8), and normally pigmented tissue from a branch not exhibiting a tissue-loss lesion within a diseased colony and tissue from a branch showing signs of active tissue loss (diseased, D) (n=7). Samples were always collected from apparently healthy colonies first, then diseased, in an attempt to prevent contamination. Nitrile gloves were worn and were changed when moving between colonies.

Each sample was placed into a separate BD Falcon™ tube that had been perforated with holes made by drilling and then the sample-containing tubes were placed into mesh bags. Once on the boat, the tubes containing coral fragments were placed into a cooler filled with seawater for transport back to the laboratory. Collection tools were disinfected in 10% bleach and rinsed in between field sites to further prevent contamination. On return to the laboratory, coral fragments were aseptically subsampled for histology and molecular analysis using large, thick stainless steel disposable

microtome blades. Coral subsamples to be used for histopathological examinations were fixed in a Z-Fix: seawater (1:4) solution (Z-Fix Concentrate, Anatech, Ltd., Battle Creek, MI) (Domart-Coulon et al. 2006), and molecular subsamples were preserved with RNAlater®.

Sample collection 2012

Because *A. cervicornis* colonies have been dramatically reduced in number by tissue-loss diseases in the Florida Keys and continue to be threatened today (Jaap et al. 1989; Aronson and Precht 2001a, 2001b; Porter et al. 2001; Miller et al. 2002; Williams and Miller 2005; Aronson et al. 2008), only one AH tissue sample was collected from three of the five field sites in order to cause minimal disturbance to the reef. In addition to the AH sample, two samples were collected per diseased colony: a normally pigmented fragment from a branch not exhibiting a tissue-loss lesion within a diseased colony (healthy-on-diseased, HD) (n=12), and tissue from a branch showing signs of active tissue loss (diseased, D) (n=13). HD and D coral samples were collected from three different diseased *A. cervicornis* colonies for most field sites. Because three diseased colonies were not always present at every field site, samples were only collected from field sites where at least two colonies showing signs of active disease were present. After AH and D *A. cervicornis* colonies were identified and photographed, samples were collected and transported to the laboratory following the same methodology as the 2011 field season. On return to the lab, the coral fragments were photographed, subsampled, and fixed for histology in Z-Fix: seawater solution in the same manner as in 2011, and molecular subsamples were once again preserved with RNAlater®. Histological samples were transported back to George Mason University's (GMU) Histology Laboratory, Fairfax, VA, while coral-tissue samples for molecular analysis were transported to The

MicroBiome Analysis Center (MBAC), Manassas, VA. All samples were kept at -20°C until processing.

Histopathology

Routine histological and light microscopy techniques were employed to gather baseline information about tissue-loss diseases affecting *A. cervicornis* (Peters et al. 2005). On arrival to GMU's Histology Laboratory, Z-Fix preserved samples (n=26) were grossly photographed using a Nikon COOLPIX P7000 (Nikon, Inc., Melville, NY). All AH and HD samples were first trimmed into approximately 2-cm fragments using a Dremel tool with a diamond-coated tile-cutting blade. Samples were then decalcified in a 10% ethylenediaminetetraacetic acid (EDTA) solution that was adjusted to pH 7 with sodium hydroxide pellets. The solution was changed every 24–48 h until no skeleton remained (*N.B.*: samples were placed oral side down in a megacassette to allow the carbon dioxide produced during decalcification to freely escape without disrupting the coral tissue).

All samples that contained a tissue-loss margin (this included a portion of intact coral tissue, and denuded skeleton), were enrobed in 1.5% (w/v) NuSieve® GTG® agarose (Lonza Rockland, Inc., Rockland, ME) prior to decalcification and trimming to preserve the cellular architecture of the sample and keep necrotic tissues, microbial communities, and adjacent coral tissue sections undisturbed during processing (Bythell et al. 2002). After agarose was added to each tissue mold, the samples were placed into a vacuum oven to remove any air bubbles adhering to the sample to ensure that the agarose successfully filled all interstitial spaces of the sample. Samples were vacuumed for 1 min at 15–22 mm Hg, then pressure was released. Vacuuming was repeated two additional times for 1 min each, and vacuum temperature was held at 60°C. After solidification at

room temperature, excess agarose was trimmed to expose the skeleton on the aboral side of the sample to enhance the infiltration of the EDTA solution during decalcification.

After decalcification, samples were rinsed in running tap water for approximately 30 min and were stored in 70% ethanol. Tissues were trimmed into 2- to 3-mm-thick sections and were placed in plastic cassettes for embedding. Samples were dehydrated through a graded series of ethanol (70–95%, three changes of 100% reagent alcohol), cleared with three changes of Richard-Allan Scientific™ Signature Series Clear-Rite™ 3 (Thermo Fisher Scientific, Inc., Waltham, MA), and infiltrated with three changes of molten Paraplast Plus® (Sigma-Aldrich Co. LLC., St. Louis, MO) using a VENTANA PTP-1530 Renaissance Tissue Processor (Ventana Medical Systems, Inc, Tucson, AZ). Lastly, samples were embedded in Paraplast Xtra® (Sigma-Aldrich Co. LLC., St. Louis, MO) at a Microm AP280 embedding station (MICROM Laborgeräte GmbH, Germany) (Peters et al. 2005).

Embedded tissues were sectioned sagittally at 5 µm using an Olympus CUT 4060 microtome (Olympus America Inc., Center Valley, PA) and were then mounted on glass microscope slides. Multiple sections from each block were stained separately with Harris's hematoxylin and eosin (HE) (Prophet et al. 1992; Carson and Hladik 2009), Giemsa, and Movat's modified pentachrome (MMP) (which shows changes in the pH and mucus composition) (Yevich and Barszcz 1983), coverslipped with Permount™ mounting medium (Thermo Fisher Scientific, Inc., Waltham, MA), and examined using light microscopy.

Ten histopathological parameters were observed and semi-quantitatively scored on a gradient scale of 1 to 5 to determine tissue condition as defined by (Miller et al.

2014): general tissue condition, zooxanthellae presence, epidermal mucocyte condition, mesenterial filament mucocyte condition, severity of degeneration of cnidoglandular bands, severity of dissociation of mesenterial filaments, calicodermis condition, severity of lost costal tissue, abundance of epidermal RLOs, and abundance of filament RLOs. RLOs have been defined as basophilic clusters of large coccoid bacterial cells that are found in the mucocytes of coral tentacles, on polyp oral discs, and in the cnidoglandular bands (free ends) of mesenterial filaments. RLOs were highlighted within coral tissue sections as dark purple clusters by Giemsa.

Histological parameters were compared for apparently healthy and diseased tissues to test for differences in tissue condition. Descriptive statistics for each sample type were calculated and compared using a Mann-Whitney-Wilcoxon (MWW) test known as the Wilcoxon rank-sum test. Parametric approaches, e.g., Student's t-test and ANOVAs, were not appropriate to compare the ordinal histological scores or the mean colony scores as the data would be truncated between the minimum and maximum scores (0-5). MWW was used to test for differences (1) between apparently healthy and diseased histological parameters, (2) among apparently healthy, healthy-on-diseased, and diseased samples, (3) among apparently healthy, healthy on diseased, and three portions of a diseased branch, HDD, TLM, DS, and (4) between WBD and RTL.

Results

Histopathological summary

The cellular architecture of AH *A. cervicornis* tissues was maintained and the tissues were overall in good condition. The mean histopathological scores for each parameter observed in AH *A. cervicornis* tissue ranged from good to very good (1-2), except in the case of mesenterial filament mucocytes (M=2.8, SD=0.8), epidermal RLOs

(M=3.4, SD=0.5), and mesenterial filament RLOs (M=2.7, SD=1.2) (Table 2). Overall, the zooxanthellae abundance was consistently higher in the surface body wall compared to diseased tissues, minimal karyolysis of zooxanthellae was observed, and the mesoglea was thicker in the epidermis of AH tissues compared to diseased tissues. Epidermal mucocytes observed in the 2011 AH samples were numerous and relatively uniform in size. Few epidermal mucocytes were hypertrophied (swollen or enlarged) and few gaps were observed in these samples. Conversely, epidermal mucocytes observed in two of the three AH samples from 2012 were not in as good as condition as what was observed in the 2011. More hypertrophied mucocytes were present in the 2012 AH samples, and there were many areas where mucocytes were either sloughing off from the epidermis or were completely missing in sections of the surface body wall (Figure 2). The condition and severity scores for these two samples in particular were worse than some of the diseased samples examined. Much cellular debris and necrotic cells were present throughout the tissue sections. Furthermore, the cnidoglandular bands of the mesenteries were dissociating, gaps were present between the mesogleal pleats, and cells were missing in the mesenteries.

Epidermal tissue was present and covered more than three-quarters of the costal spaces observed in more than 80 percent of the AH samples. In many cases, the epidermis covering these areas was attenuated (thinned or atrophied) but was still intact. More zooxanthellae were found in the gastrodermis of AH samples than in diseased samples. The cnidoglandular bands of the mesenterial filaments showed little to no vacuolation, few cellular gaps, and few to no mucocytes were hypertrophied. Acidophilic

Table 2. Summary statistics for histopathological observations on all apparently healthy (n=11), healthy-on-diseased (n=12), and diseased (n=20) *A. cervicornis* tissue samples. Condition scores applied were 0 = excellent, 1 = very Good, 2 = good, 3 = fair, 4 = poor, and 5 = very poor; whereas severity scores were categorized as follows 0 = within normal limits, 1 = minimal change, 2 = mild changes, 3 = moderate changes, 4 = marked changes, and 5 = severe tissue changes.

Tissue Health	**Apparently Healthy**			**Healthy-on-Diseased**			**Diseased**		
Parameter	**Mean**	**SD**	**Range**	**Mean**	**SD**	**Range**	**Mean**	**SD**	**Range**
General Condition 10x	1.9	1.0	1–4	3.7	1.1	2.0–5.0	4.4	0.4	3.8–5.0
Zooxanthellae 10x	1.8	1.0	1–4	2.8	0.6	2.0–4.0	3.4	0.5	2.8–4.7
Epidermal Mucocytes Condition	1.9	0.9	1–3.3	3.5	1.1	2.0–5.0	4.2	0.5	3.1–5.0
Mesenterial Filament Mucocytes	2.8	0.8	2–4	3.4	1.4	1.0–5.0	3.8	0.7	2.3–5.0
Degeneration Cnidoglandular Bands	1.5	1.4	0–4	3.7	1.2	2.0–5.0	4.0	0.6	2.9–4.9
Dissociation of Mesenterial Filaments	1.0	1.4	0–4	3.5	1.2	2.0–5.0	3.7	1.0	1.1–4.4
Costal Tissue Loss	1.9	1.1	1–4	3.8	1.2	2.0–5.0	3.9	0.7	2.5–5.0
Calicodermis Condition	0.6	1.0	0–3	3.8	1.2	2.0–5.0	3.8	0.7	2.1–4.7
Epidermal RLOs	3.4	0.5	3–4	3.5	1.0	2.0–5.0	3.3	0.8	2.0–4.8
Filament RLOs	2.7	1.2	0–4	3.6	0.8	2.0–5.0	2.9	1.2	1.0–4.3

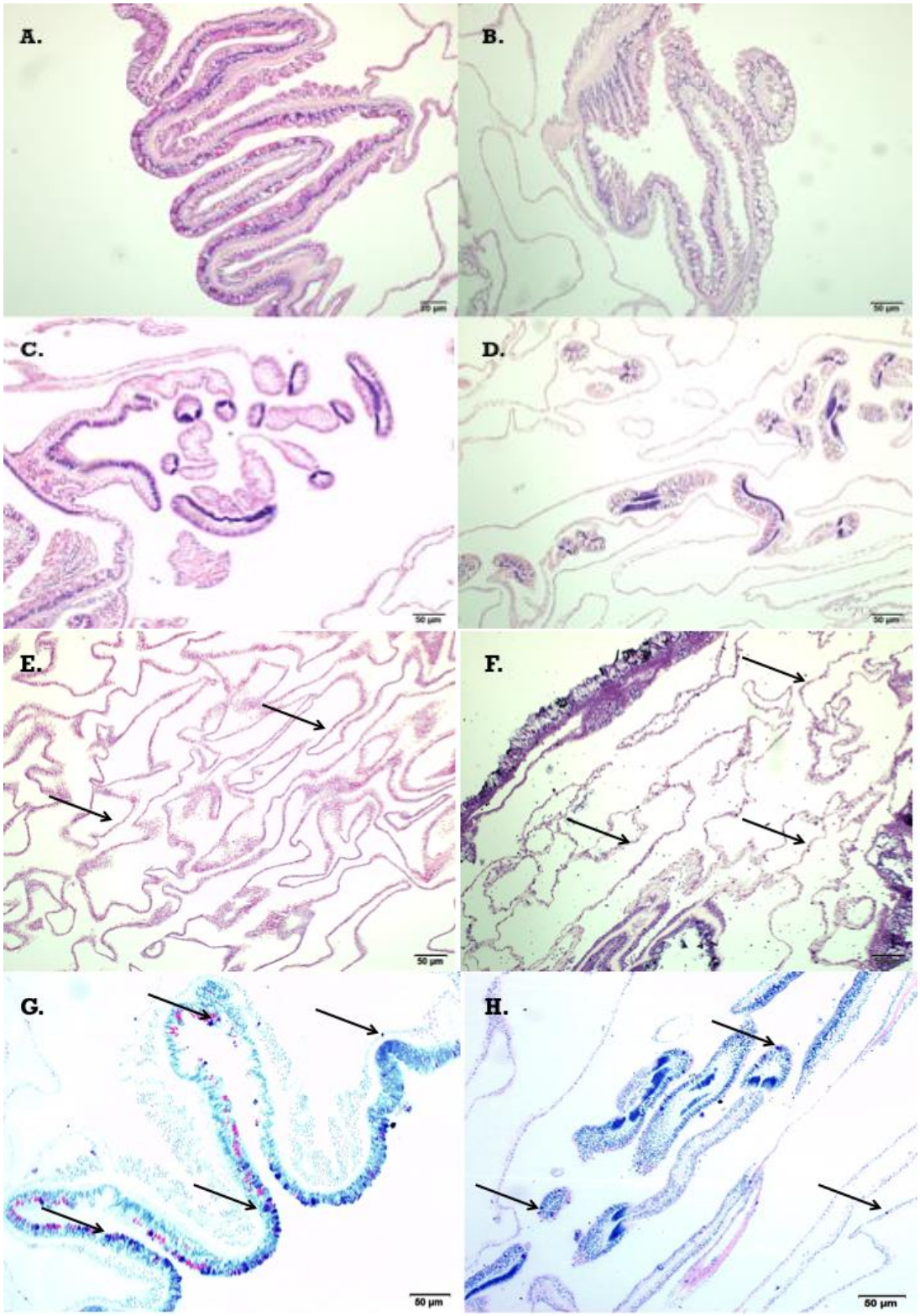

Figure 2. Histological observations of apparently healthy *A. cervicornis* collected in 2012. (A & B) Comparison of tentacles noting the attenuated mesoglea and reduction in zooxanthellae of the AH sample in worse condition (B);(C&D) Comparison of cnidoglandular bands showing the poorer condition of the mesenteries in (D); (E&F) Basal body wall condition variation in apparently healthy *A. cervicornis* samples; (G&H), RLOs were present in the (G) surface body wall, and (H) cnidoglandular bands and gastrodermis of apparently healthy *A. cervicornis* samples.

granular gland cells that aid in food digestion were also present within the cnidoglandular bands. There were minimal gaps and few areas present where cells were lysing or sloughing off from the gastrodermis, mesoglea, and calicodermis of the basal body wall, but the calicodermis appeared to be attenuated in some areas. Multifocal RLO infections were observed in the epidermis of the AH samples. These infections tended to be more prevalent in the polyp tentacles rather than along the surface body wall. In most cases, few RLOs were observed in the cnidoglandular bands of the mesenteries, and few were observed within the mucocytes of the gastrodermis.

The mean histopathological scores for all parameters observed in HD *A. cervicornis* tissue ranged from fair to poor (3–4) (Table 2). The overall condition of HD samples was variable. Half of the HD samples were in good to fair condition (2–3), while the other half ranged from poor to very poor (4–5). Although these samples were collected from normally pigmented branches on the opposite side of a colony from a tissue lesion, a quarter of these samples' overall condition was very poor (ranking of 5).

Histological examinations of the HD samples that were in good to fair condition, resembled the condition of the histological parameters observed for AH samples. There was no longer a clear structure of the cnidoglandular bands of the mesenteries and cells were no longer ciliated or adhering to one another in the HD samples that were in poor to very poor condition. Vacuolation was observed in the cnidoglandular bands, mucocytes within the cnidoglandular bands were hypertrophied, cells had been lost, and dissociation of mesenterial filaments was also observed. Zooxanthellae were less abundant and were found loosely occupying the gastrodermis compared to the tightly packed cells observed

in AH samples. Both the gastrodermis and calicodermis were severely atrophied, zooxanthellae were released as gastrodermal cells lysed and sloughed off the mesoglea, and the two dermal layers were necrotic and dissociating from one another in many areas.

The mean histopathological scores for all parameters observed in diseased *A. cervicornis* tissue also ranged from fair to poor (3–4). However, these scores showed that diseased tissues were in worse condition than the HD samples, except in the case of epidermal RLOs (M=3.3, SD=0.8), and mesenterial filament RLOs (M=2.9, SD=1.2) (Table 2). There were numerous hypertrophied mucocytes and large gaps along the epidermis where mucocytes had been lost. The increase in condition scores for RLOs does not represent a decrease in infection prevalence. Instead, these scores can be attributed to the loss of epidermal and mesenterial filament mucocytes in the diseased tissues. Once again zooxanthellae abundance was reduced and inconsistent, but these cells were not absent and accounted for providing the remaining tissue with a normally pigmented appearance. The cells of the cnidoglandular bands showed varying degrees of cell loss, necrosis, lysing, vacuolation, and many bands were dissociating entirely. There was much cellular debris present, particularly in conjunction with the tissue-loss margin. In the most severe cases, tissues of the diseased samples had little cellular architecture left and simply looked like a conglomeration of dissociated cells (Figure 3 and Figure 4).

Diseased tissues were examined further on a finer spatial scale by examining the HDD, TLM, and DS portions of a diseased branch separately where applicable (Table 3). Although a general decline in tissue condition was observed when comparing AH, HD, and D samples, this was not the case when examining the diseased branches in more

detail. The overall condition of HD and HDD samples was quite inconsistent. These two sample types had the most variation in severity indices and condition scores compared to

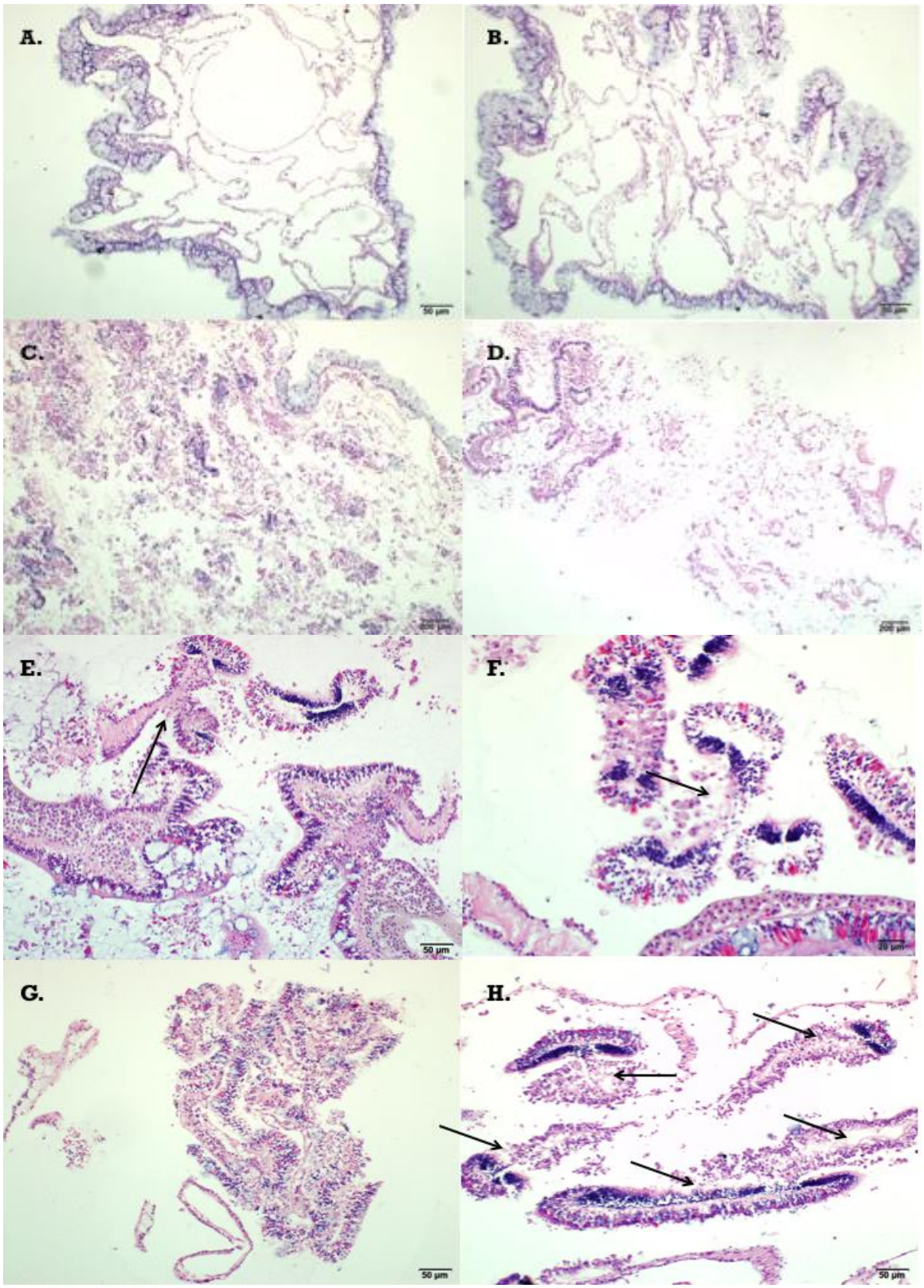

Figure 3. Histological comparisons of diseased *A. cervicornis* samples. (A&B) General condition of diseased *A. cervicornis* samples; (C&D) Tissue components are necrotic and lysing, little cellular architecture remains; (E-H) Cnidoglandular bands and mesenteries are dissociating, mucocytes are hypertrophied, cells have been lost, and gastrodermis is detaching from the mesoglea.

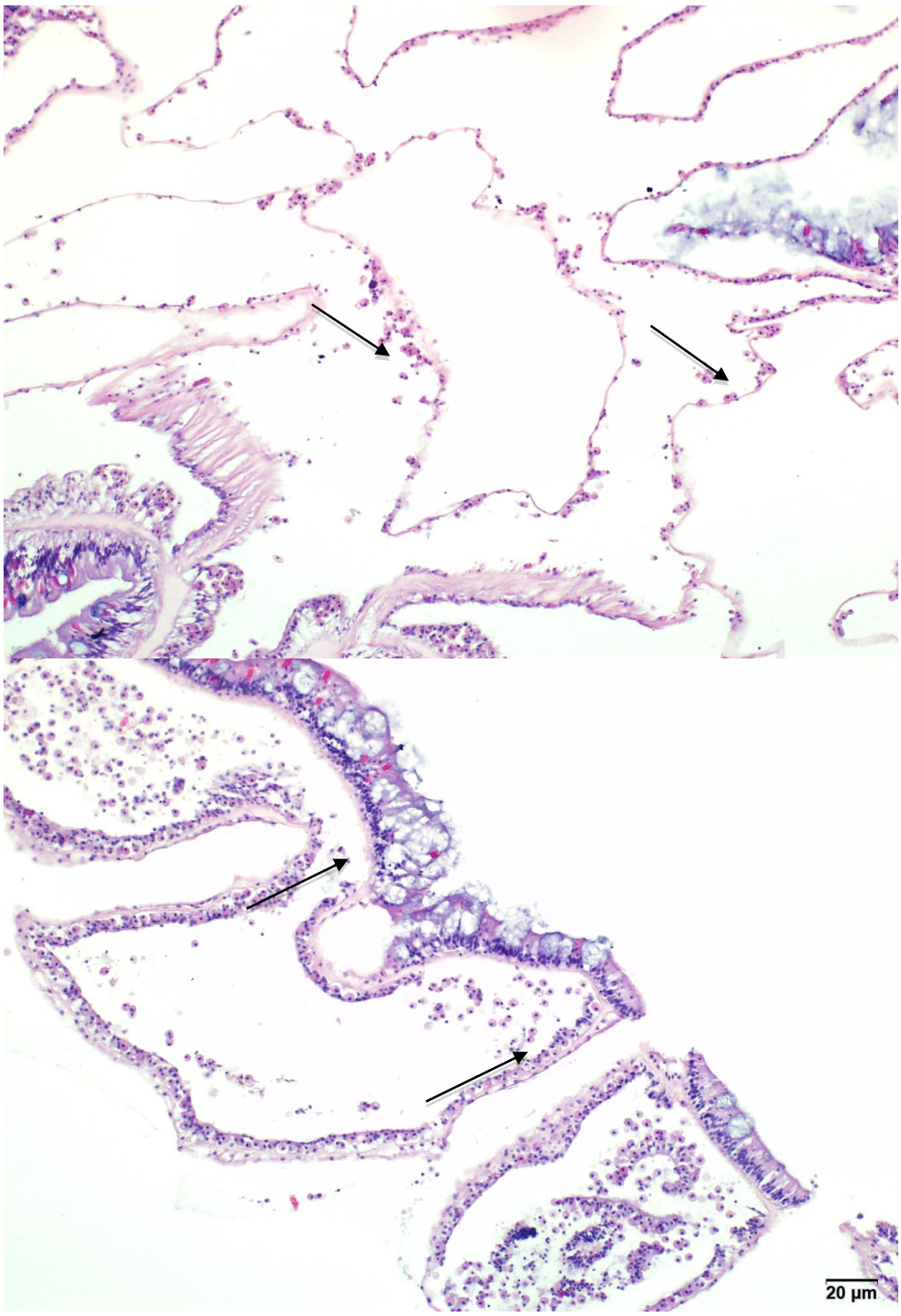

Figure 4. Histological observations of the (A) zooxanthellae being released as gastrodermal cells lyse and sloughoff the mesoglea of a diseased *A. cervicornis* sample, and (B) a tissue-loss margin sample showing a reduction in zooxanthellea abundance where zooxanthellea are being released into the gastrovascular canals.

Table 3. Summary statistics for histopathological observations on all apparently healthy (AH) (n=11) and healthy-on-diseased (HD) (n=12) *A. cervicornis* samples, as well as samples that included a trimmed section of only the healthy-on-diseased portion of the diseased branch (HDD) (n=8), a trimmed partition that contained the tissue-loss margin (TLM) (n=14), and a trimmed section of only denuded skeleton (DS) (n=15) *A. cervicornis* tissue samples. Condition scores applied were 0 = excellent, 1 = very Good, 2 = good, 3 = fair, 4 = poor, and 5 = very poor; whereas severity scores were categorized as follows 0 = within normal limits, 1 = minimal change, 2 = mild changes, 3 = moderate changes, 4 = marked changes, and 5 = severe tissue changes.

Sample type	**AH**			**HD**			**HDD**			**TLM**			**DS**		
Parameter	**Mean**	**SD**	**Range**	**Mean**	**SD**	**Range**	**Mean**	**SD**	**Range**	**Mean**	**SD**	**Range**	**Mean**	**SD**	**Range**
General Condition 10x	1.9	1.0	1–4	3.7	1.1	2.0–5.0	3.8	1.1	2.0–5.0	4.6	0.4	4.0–5.0	4.0	0.0	4.0
Zooxanthellae 10x	1.8	1.0	1–4	2.8	0.6	2.0–4.0	2.7	0.8	2.0–4.0	3.6	0.4	3.1–4.7	3.3	0.4	3.0–3.5
Epidermal Mucocytes Condition	1.9	0.9	1–3.3	3.5	1.1	2.0–5.0	3.7	1.1	2.0–5.0	4.4	0.6	3.3–5.0	4.0	0.0	4.0
Mesenterial Filament Mucocytes	2.8	0.8	2–4	3.4	1.4	1.0–5.0	3.1	1.5	1.0–5.0	4.2	0.4	3.5–5.0	3.0	Undef	3.0
Degeneration Cnidoglandular Bands	1.5	1.4	0–4	3.7	1.2	2.0–5.0	3.3	1.3	1.0–4.3	4.2	0.6	3.1–5.0	4.0	Undef	4.0
Dissociation of Mesenterial Filaments	1.0	1.4	0–4	3.5	1.2	2.0–5.0	2.3	1.6	0.0–4.0	3.5	1.1	1.3–5.0	4.0	Undef	4.0
Costal Tissue Loss	1.9	1.1	1–4	3.8	1.2	2.0–5.0	3.0	1.4	1.0–5.0	4.1	0.6	2.8–5.0	3.0	Undef	3.0
Calicodermis Condition	0.6	1.0	0–3	3.8	1.2	2.0–5.0	3.1	1.1	1.0–4.0	4.0	0.7	2.3–5.0	3.5	Undef	3.5
Epidermal RLOs	3.4	0.5	3–4	3.5	1.0	2.0–5.0	3.3	1.1	2.0–5.0	3.4	0.8	2.4–4.7	2.0	Undef	2.0
Filament RLOs	2.7	1.2	0–4	3.6	0.8	2.0–5.0	2.6	1.6	0.0–4.5	2.9	1.5	0.0–5.0	1.0	Undef	1.0

other sample types. It was surprising to see that some of the HD branches were in poorer condition than the HDD portion of the diseased branch. The mean condition and severity scores for mesenterial filament mucocytes (M=3.4, SD=1.4 and M=3.1, SD=1.5, respectively), degeneration of cnidoglandular bands (M=3.7, SD=1.2 and M=3.3, SD=1.3, respectively), dissociation of mesenterial filaments (M=3.5, SD=1.2 and M=2.3, SD=1.6, respectively), costal tissue loss (M=3.8, SD=1.2 and M=3.1, SD=1.1, respectively), calicodermis condition (M=3.8, SD=1.2 and M=3.3, SD=0.8, respectively), epidermal RLOs (M=3.5, SD=1.0 and M=3.3, SD=1.1, respectively), and filament RLOs (M=3.6, SD=0.8 and M=2.6, SD=1.6, respectively) were all higher for HDD samples than HD samples.

TLM samples also varied in condition scores and severity indices, but the mean scores for each TLM parameter were consistently worse than the HD and HDD scores apart from epidermal (M=3.4, SD=0.8, M=3.5, SD=1.0 and M=3.3, SD=1.1, respectively), and filament RLOs (M=2.9, SD=1.5, M=3.6, SD=0.8 and M=2.6, SD=1.6, respectively). Once again, these differences reflect the loss of epidermal and mesenterial mucocytes. There were only two DS samples that had enough tissue present for observation, only accounting for 13 percent of the samples. All samples that contained a tissue-loss and denuded skeleton were enrobed in agarose prior to embedding. However, the enrobed samples proved to be a great challenge for slide reading as our samples were greatly shrunken unfortunately (Figure 5). Therefore, the condition and severity scores for DS samples are not a clear representation of the condition of DS samples which dominantly lacked tissue all together.

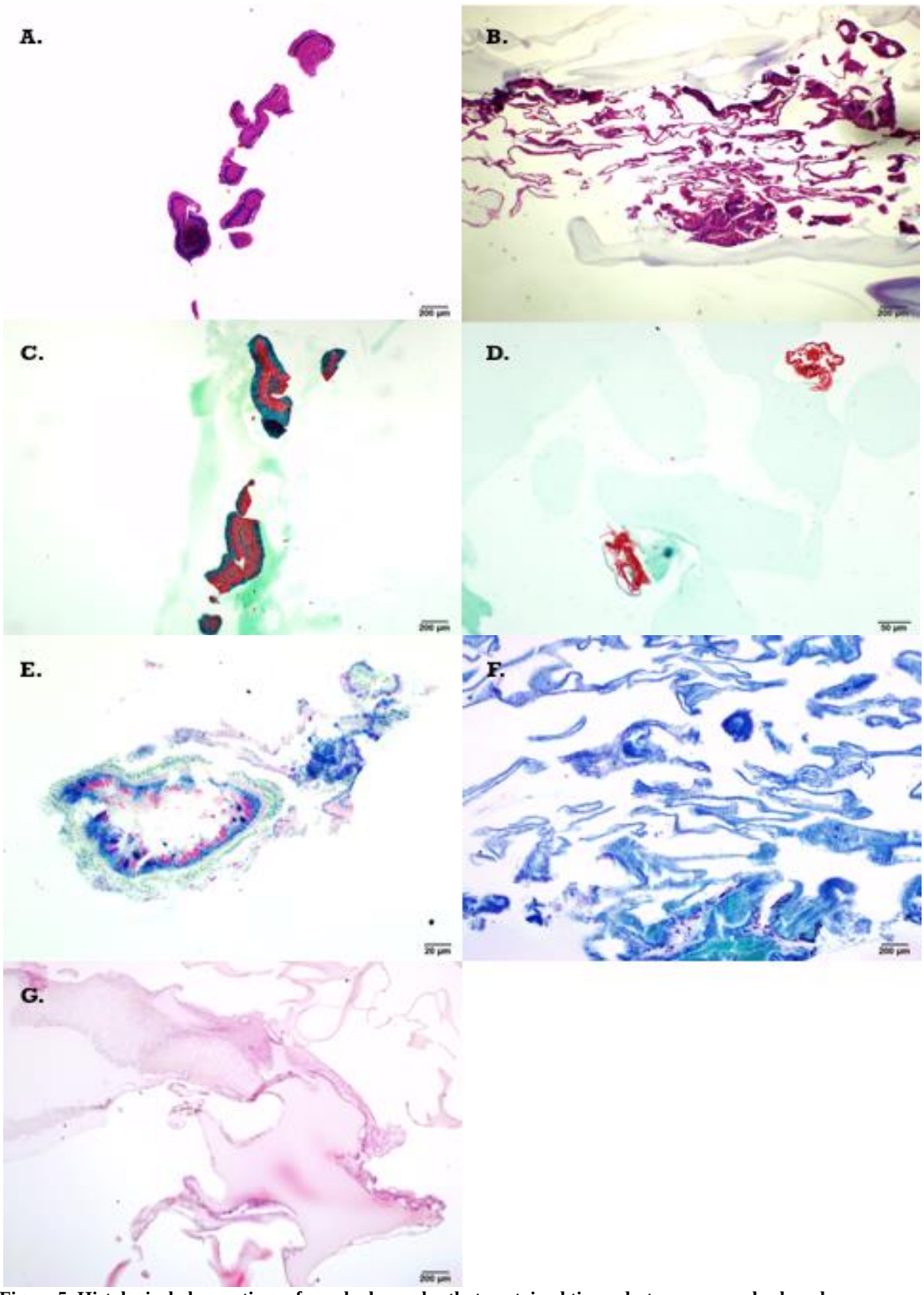

Figure 5. Histological observations of enrobed samples that contained tissue, but were severely shrunken, stained with (A&B) H&E (C&D) MMP, and (E&F) Geimsa. (G) Denuded skeleton samples predominantly contained very few cells if any at all.

Histopathological comparisons among sample types

The observed histological parameters for apparently healthy and diseased *A. cervicornis* tissues were compared first (Figure 6). Histological scores for HD, HDD, TLM, and DS were all included for the diseased category to account for all of the samples that were collected from each diseased colony. All apparently healthy and diseased scores were significantly different for each histological parameter except epidermal (p=0.178) and filament RLOs (p=0.467) (Table 4). RLOs were observed in all samples regardless of sample type and prevalence varied little (Figure 7).

Parameter scores for AH, HD, and diseased samples (HDD, TLM, and DS combined) were compared to test for differences in tissue condition. Six histological parameters were significantly different between AH and HD tissues, while only the general condition (p=0.002) and zooxanthellae condition (p=0.021) scores were significantly different between HD and diseased tissues (Table 5). Despite the fact that HD samples were analyzed separately from diseased samples, all AH and diseased scores were once again significantly different for each histological parameter except epidermal (p=0.078) and filament RLOs (p=0.091).

To examine the diseased samples in more detail, all five sample types (AH, HD, HDD, TLM, and DS) were compared to test for histological differences between the tissue types (Table 6 and Figure 8). AH samples were significantly different from HDD samples for four of the observed histological parameters: general condition (p=0.009), epidermal mucocyte condition (p=0.006), costal tissue loss (p=0.006), and calicodermis condition (p=0.039). AH and TLM samples had the greatest number of histological parameters that were significantly different. All AH and TLM scores were significantly

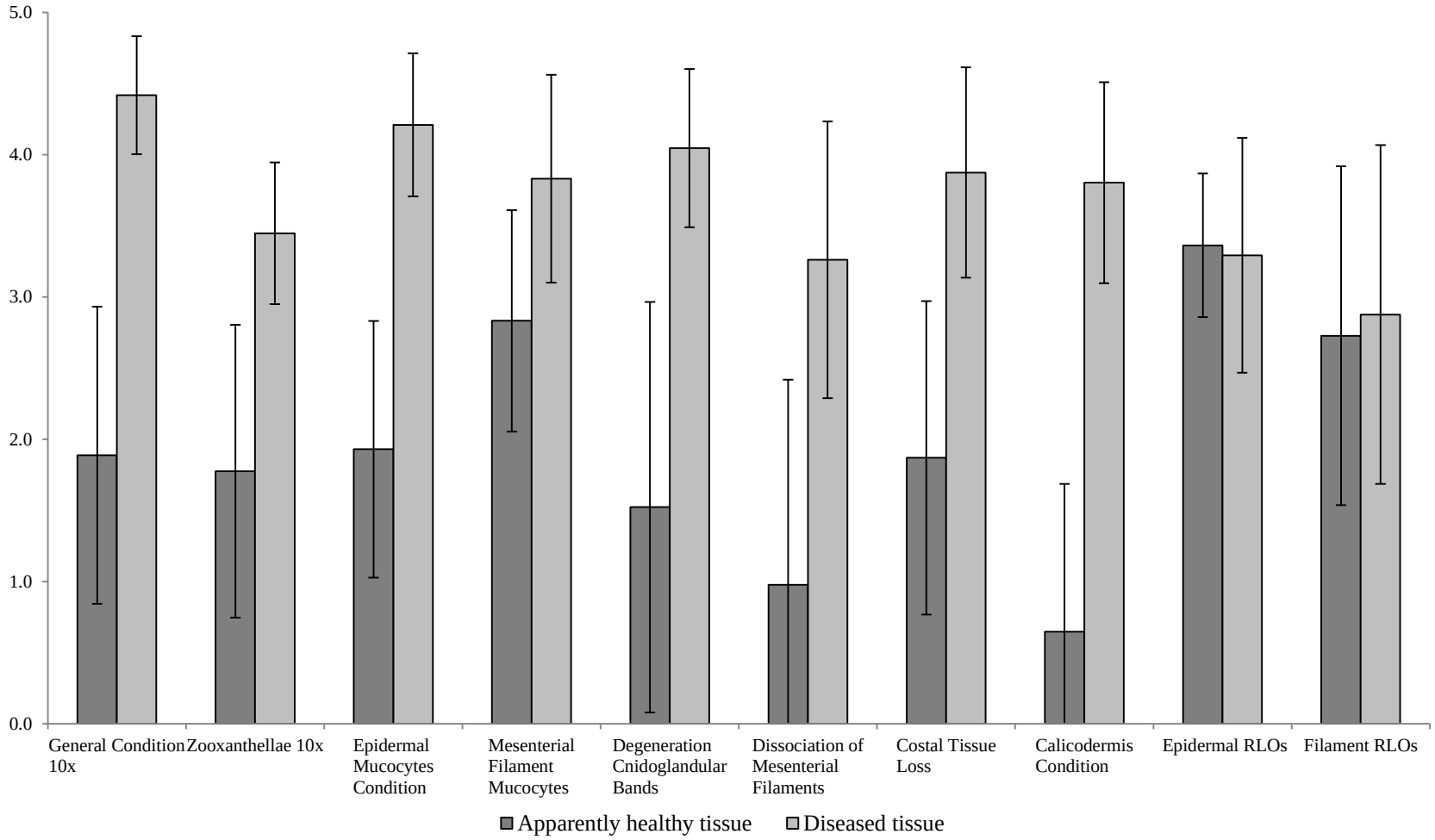

Figure 6. Mean histology parameter scores for apparently healthy and diseased *A. cervicornis* samples.

Table 4. Summary of Mann-Whitney-Wilcoxon test results comparing histological observations between apparently healthy and diseased samples. Highlighted p-values equal p<0.01.

Parameter	p-value
General Condition 10x	**7.496E-15**
Zooxanthellae 10x	**4.635E-10**
Epidermal Mucocytes Condition	**6.187E-12**
Mesenterial Filament Mucocytes	**0.001**
Degeneration Cnidoglandular Bands	**7.956E-10**
Dissociation of Mesenterial Filaments	**7.524E-08**
Costal Tissue Loss	**9.067E-12**
Calicodermis Condition	**5.878E-11**
Epidermal RLOs	0.178
Filament RLOs	0.467

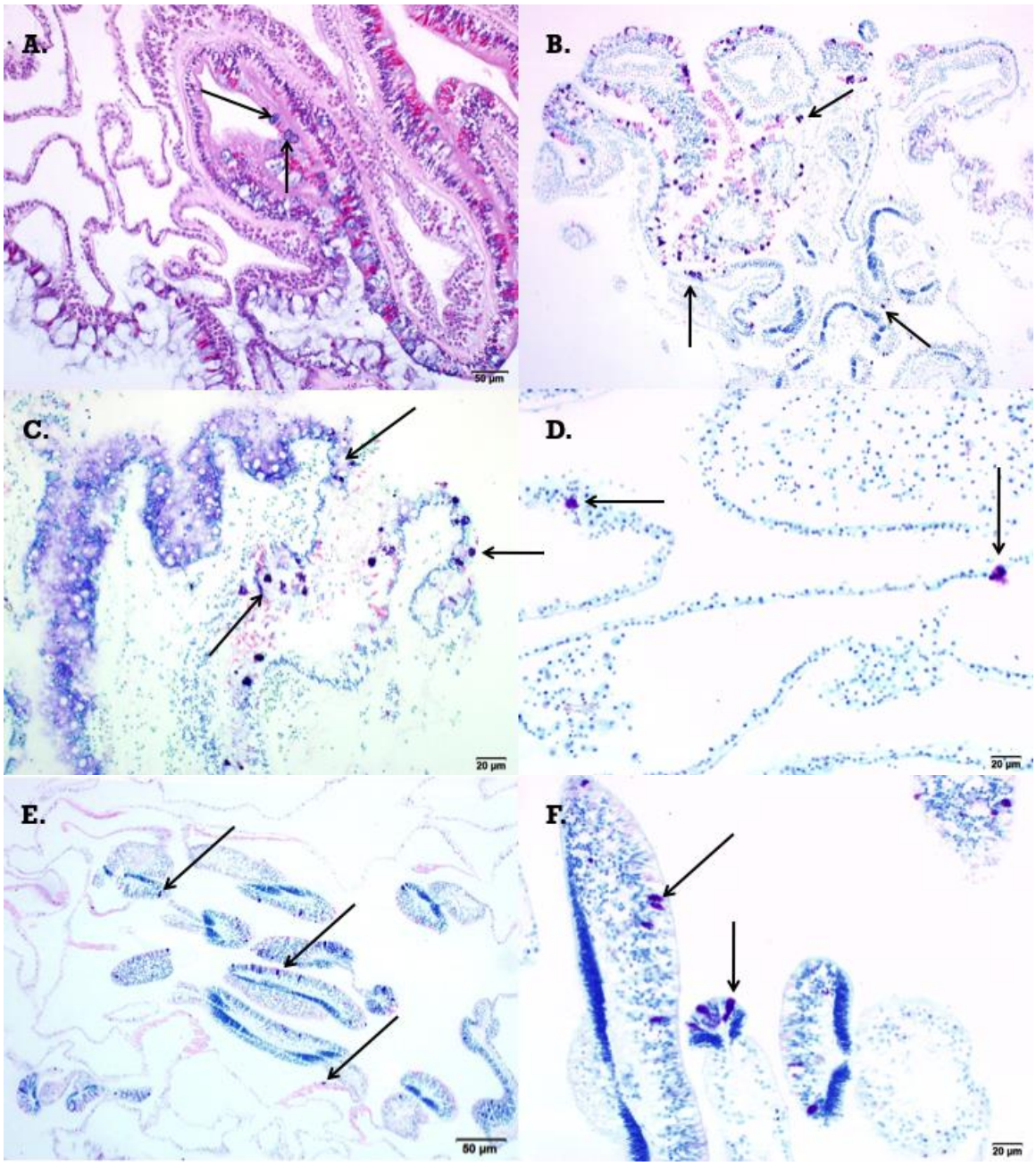

Figure 7. (A) Rickettsiales-like organisms are observable in H&E stained tissue sections, but H&E does not highlight these reticulate bodies as Giemsa does; (B) A severe RLO infection in the tentacles and cnidoglandular bands of *A. cervicornis*. Note that no RLOs are observed in the epidermis of the surface body wall; (C) RLOs were observed in mucocytes that were not secreting a large amount of mucus; (D) RLOs observed within mucocytes of the gastrodermis; (E-F) RLO infection of the cnidoglandular bands.

Table 5. Summary of Mann-Whitney-Wilcoxon test results comparing histological observations between apparently healthy, healthy-on-diseased, and diseased samples. Highlighted p-values equal p<0.05.

Parameter	AH vs. HD	AH vs. D	HD vs. D
General Condition 10x	**0.009**	**6.318E-08**	**0.021**
Zooxanthellae 10x	**0.038**	**2.509E-05**	**0.002**
Epidermal Mucocytes Condition	**0.014**	**1.837E-07**	0.052
Mesenterial Filament Mucocytes	0.958	**0.013**	0.292
Degeneration Cnidoglandular Bands	0.113	**2.985E-04**	0.694
Dissociation of Mesenterial Filaments	**0.015**	**0.001**	0.548
Costal Tissue Loss	**0.002**	**9.128E-06**	0.789
Calicodermis Condition	**0.008**	**5.243E-06**	0.770
Epidermal RLOs	1.000	0.567	0.078
Filament RLOs	0.219	0.922	0.091

Table 6. Summary of Mann-Whitney-Wilcoxon test results comparing histological observations among all sample types. Highlighted p-values equal p<0.05.

Parameter	AH vs. HD	AH vs. HDD	AH vs. TLM	AH vs. DS	HD vs. HDD	HD vs. TLM	HD vs. DS	HDD vs. TLM	HDD vs. DS	TLM vs. DS
General Condition 10x	**0.009**	**0.009**	**7.665E-08**	**0.022**	0.720	**0.007**	0.891	**0.013**	1.000	0.125
Zooxanthellae 10x	**0.038**	0.294	**2.737E-06**	0.067	1.000	**3.721E-04**	0.218	**0.037**	0.667	0.998
Epidermal Mucocytes Condition	**0.014**	**0.006**	**3.950E-07**	**0.022**	0.607	0.055	0.527	0.304	1.000	0.157
Mesenterial Filament Mucocytes	0.958	0.848	**0.003**	1.000	0.555	0.130	0.800	0.051	1.000	0.684
Degeneration of Cnidoglandular Bands	0.113	0.078	**3.189E-04**	0.571	0.602	0.535	1.000	**0.029**	1.000	1.000
Dissociation of Mesenterial Filaments	**0.015**	0.091	**0.001**	0.143	0.537	0.544	1.000	0.212	0.727	0.810
Costal Tissue Loss	**0.002**	**0.006**	**1.080E-05**	0.222	0.636	0.910	0.800	0.514	1.000	0.625
Calicodermis Condition	**0.008**	**0.039**	**3.186E-06**	0.244	0.549	0.619	0.727	**0.005**	1.000	0.294
Epidermal RLOs	1.000	0.813	0.480	0.778	0.307	0.121	0.100	0.564	0.455	0.316
Filament RLOs	0.219	0.457	0.987	0.429	0.790	0.064	0.200	0.817	0.636	1.000

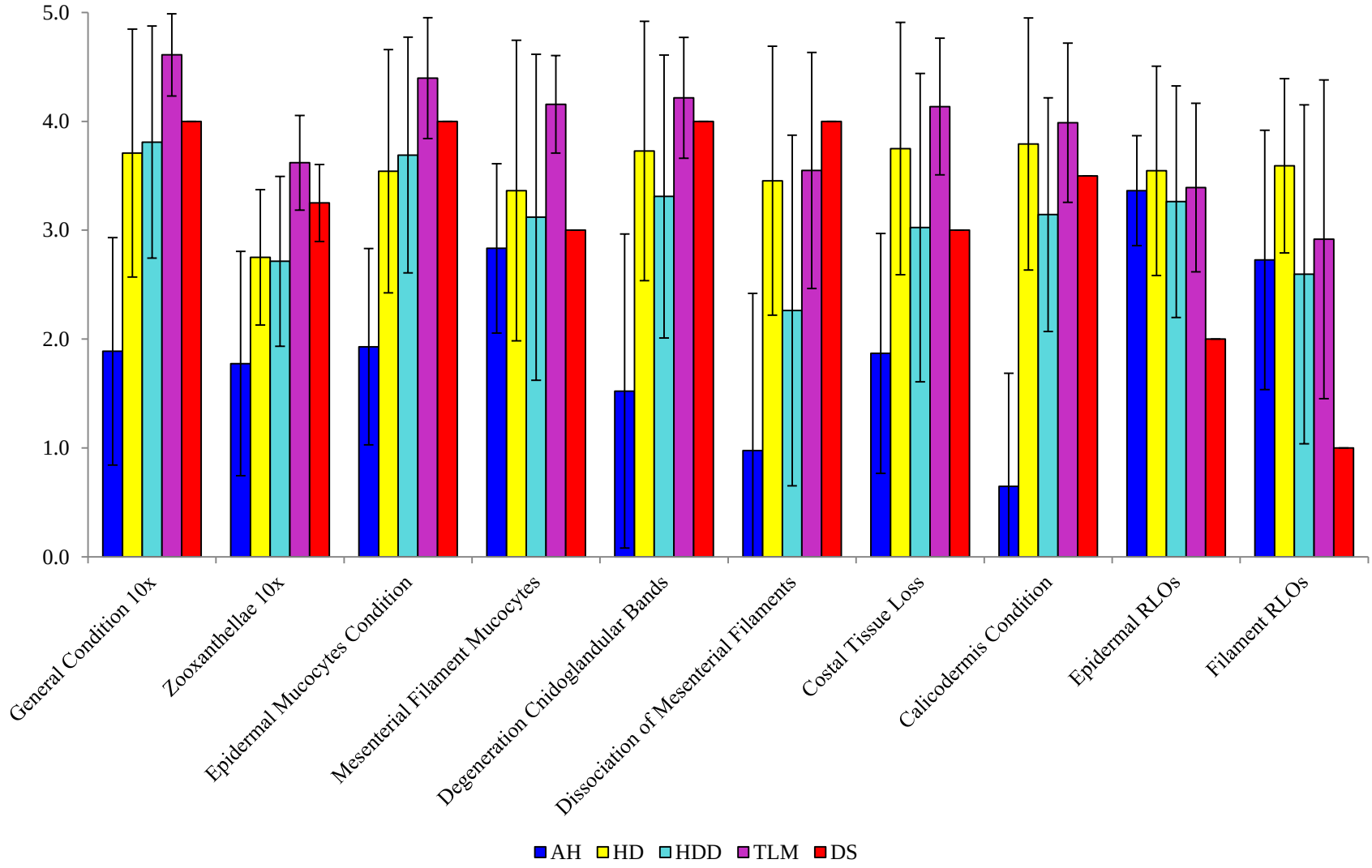

Figure 8. Mean histology parameter score comparisons for all *A. cervicornis* sample types.

different for each histological parameter except epidermal (p=0.480) and filament RLOs (p=0.987). Although two parameters were significantly different between AH and DS samples, general condition (p=0.022) and costal tissue loss (p=0.022), the DS data only included pieces of tissue from two samples and therefore these results were not informative.

In addition to AH samples, the only other sample type that was significantly different from HD samples was TLM samples. However, only two histological parameters were significantly different between HD and TLM samples: general condition (p=0.007) and zooxanthellae condition (p=3.721E-04). TLM samples also had four parameters that were significantly different from HDD samples: general condition (p=0.013), zooxanthellae condition (p=0.037), degeneration of cnidoglandular bands (p=0.029), and calicodermis condition (p=0.005). DS were not significantly different from any other sample type other than AH samples.

Histopathological comparisons between white-band disease and rapid tissue loss

All histological parameters were significantly different between WBD (n=16) and RTL (n=3) samples, except epidermal mucocyte condition (p=0.252), calicodermis condition (p=0.067), and epidermal RLOs (p=0.647) (Table 7 and Figure 9). Additionally, branches that were touching the sediment and exhibited atypical branch tip-to-colony base WBD disease progression were of interest. However, there were no significantly different histological parameters between coral colonies that exhibited base-to-branch tip disease progression (n=13) and branch tip-to-colony base disease progression (n=3) (Table 8).

Table 7. Summary of Mann-Whitney-Wilcoxon test results comparing histological observations between WBD and RTL samples. Highlighted p-values equal p<0.05.

Parameter	p-value
General Condition 10x	**0.002**
Zooxanthellae 10x	**0.021**
Epidermal Mucocytes Condition	0.252
Mesenterial Filament Mucocytes	**2.502E-04**
Degeneration Cnidoglandular Bands	**0.001**
Dissociation of Mesenterial Filaments	**0.001**
Costal Tissue Loss	**2.712E-06**
Calicodermis Condition	0.067
Epidermal RLOs	0.647
Filament RLOs	**0.001**

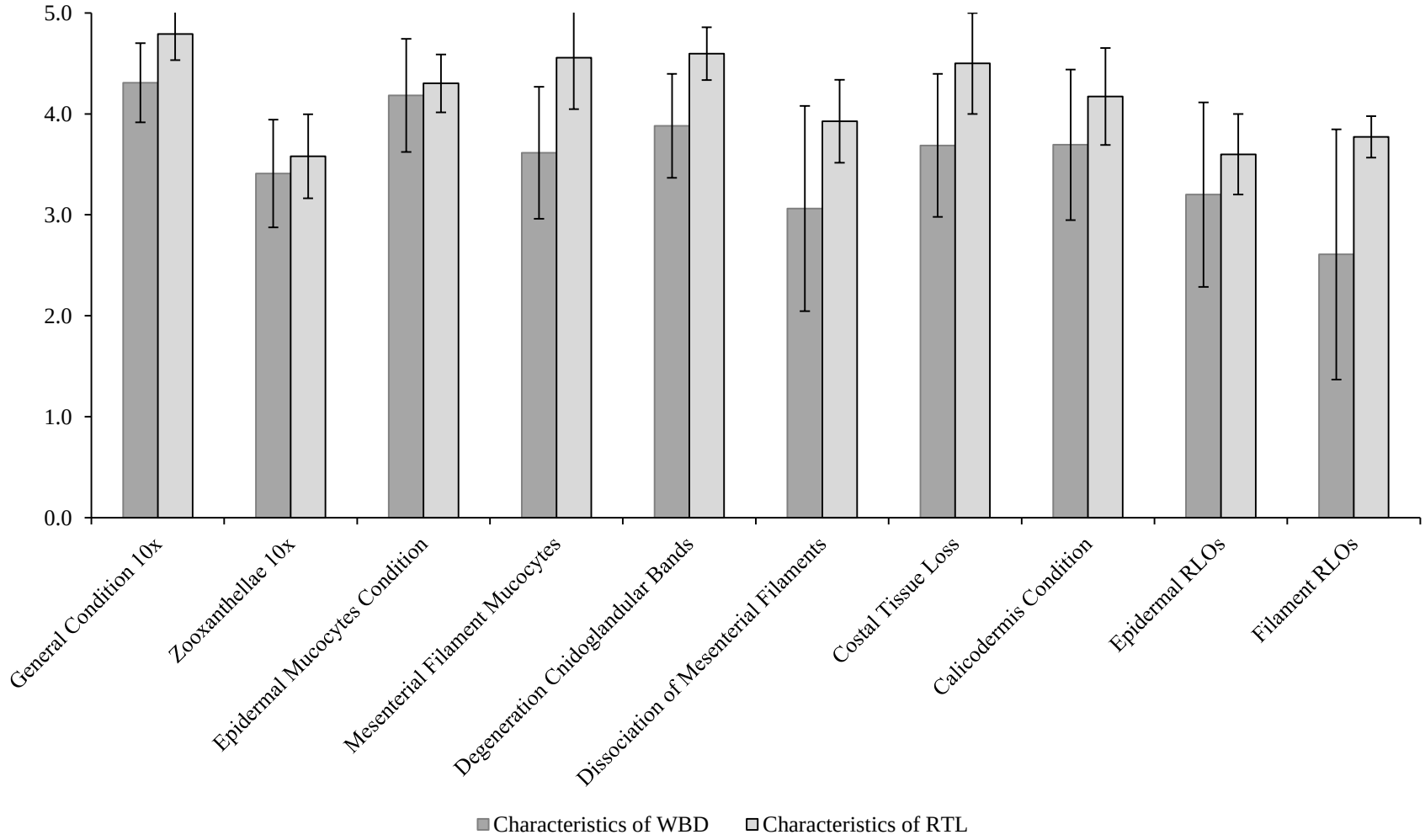

Figure 9. Mean histology parameter score comparison of tissues exhibiting WBD and RTL

Table 8. Summary of Mann-Whitney-Wilcoxon test results comparing histological observations between WBD-affected tissues exhibiting coral colony base to branch tip disease progression and branch tip to colony base progression. Highlighted p-values equal p>0.05.

Parameter	p-value
General Condition 10x	0.185
Zooxanthellae 10x	0.384
Epidermal Mucocytes Condition	0.605
Mesenterial Filament Mucocytes	0.634
Degeneration Cnidoglandular Bands	0.632
Dissociation of Mesenterial Filaments	0.233
Costal Tissue Loss	0.103
Calicodermis Condition	0.652
Epidermal RLOs	0.140
Filament RLOs	0.069

Discussion

This study histopathologically characterized apparently health, healthy-on-diseased, and diseased *A. cervicornis* tissue. The first step of this study was to characterize cellular features and identify what was considered to be within the normal range of healthy. There was some variation in sample condition when characterizing apparently healthy coral samples. In general, AH samples were similar to one another when grouped by sample year, but the 2011 AH samples appeared to be in better condition than the 2012 samples. Miller et al. (2014) reported that Conch Shallow and Little Conch reefs showed among the highest disease prevalence during their 2011 and 2012 surveillance study. Of the three AH samples collected in 2012, one sample was collected from Conch Shallow and anther was collected from Little Conch reef, which may account for the drastic declines in tissue health observed in these specific samples. Furthermore, one of the AH samples examined was in worse condition than several of the HD, HDD, and even TLM samples.

Apparently healthy histological parameter scores were significantly lower (healthier) than all other sample types (HD, HDD, TLM) in four key areas: general tissue condition, epidermal mucocyte condition, costal tissue loss, and calicodermis condition. Since only 13 percent of the samples were represented in the DS data, this sample type was disregarded as one of the diseased sample types. Departures from healthy conditions were seen in several of the cellular features of the diseased samples (HD, HDD, and TLM), with TLM samples having the most number of significantly different histological parameters from AH samples. Tissue-loss margin samples showed the most prominent signs of disease, making it the most severe and advanced disease. However, parameter

scores for HD samples were lower than HDD samples thus, the idea of pathogenesis moving from TLM towards the HDD tissue was not supported.

Healthy-on-diseased and HDD samples were most similar to one another. No histological parameters were significantly different between the two tissue types despite the fact that the HD samples were collected from a normally pigmented coral branch on the opposite side of the coral colony from where a tissue lesion was observed. HD and TLM samples were similar across the majority of the histological parameters, differing only in general and zooxanthellae condition. This was most likely attributed in the high variance of HD sample condition scores and severity indices. General and zooxanthellae conditions were also significantly different between HDD and TLM samples.

Despite the presence of zooxanthellae in all samples (albeit some areas of the TLM were devoid of zooxanthellae), many of the dinoflagellate cells were necrotic. Zooxanthellae abundance in diseased samples was inconsistent, karyolysis of some cells was observed, and pyknotic nuclei were observed in others. In some diseased samples, there were large areas of gastrodermis that lacked zooxanthellae. Despite these declines in zooxanthellae condition, the remaining cells were still responsible for providing the HD and HDD sections of coral with what is considered to be its normally pigmented golden color. However, the significantly reduced density of zooxanthellae is an indicator that the amount of energy available to the coral and metabolic capacities were reduced and cellular repair and growth rates were impaired (Hatcher 1988).

The cnidoglandular bands were significantly more degenerated and calicodermis condition was significantly worse in TLM samples when compared to HDD samples.

Mesenterial filaments are important to the metabolic function of the coral because these cells are involved in digestion. As both the cnidoglandular bands deteriorate and mesenterial filaments dissociate, a coral's ability to properly carry out digestion and absorb nutrients is reduced. Fewer nematocysts were also seen in TLM samples compared to AH and other diseased samples. Nematocytes produce nematocysts, which are responsible for delivering toxins that either help entangle prey or repel attackers.

Histological features of *A. cervicornis* observed in this study have been characterized previously. Similar to Miller et al. (2014), RLOs were present in all samples. Multifocal infections appeared to be more prevalent within the tentacles than along the surface body wall of the coenenchyme. RLOs were not observed in epidermal mucocytes that were secreting a large amount of mucus, which might explain why RLOs were more prominent in contracted tentacles opposed to the surface body wall. RLOs were also observed in the mucocytes of cnidoglandular bands and gastrodermal mucocytes. Increases in RLO abundance were correlated with an decrease in coral health. The more prevalent the RLOs were in the internal polyp structures, the worse the parameters scores were for those conditions typically characterized by a lack of adhesion in cells and dissociation of structural components. The dissociation of cnidoglandular bands results in a coral's inability to obtain energy through digestion (Peters 1984). Furthermore, Miller et al. (2014) hypothesized that the RLO infections might alter *A. cervicornis* mucous secretions, thus increasing susceptibility to other environmental stressors and tissue loss.

Histological features of WBD- and RTL- affected *A. cervicornis* have been characterized previously. Miller et al. (2014) found no differences between WBD- and RTL-affected colonies. All histological parameters between WBD and RTL diseases were different except epidermal mucocytes condition, epidermal RLO abundance, and calicodermis condition. However, no one histological parameter stood out consistently as a key marker of disease across sample or disease types.

All findings from this study support the growing evidence that tissue-loss diseases significantly affect the biological function of *A. cervicornis* as the functions involved in feeding, digestion, defense, prey capture were compromised by both WBD and RTL (Peters et al. 1986; Work et al. 2008a). *A. cervicornis* colonies in the Upper Florida Keys have a high prevalence of tissue-loss diseases. There have been continuous disease reports in the Upper Florida Keys since this study commenced. Without looking at corals histologically, a grave assumption is being made about the health of corals, because even grossly apparently healthy colonies may have microscopic changes indicating impairment before tissue loss is visibly detected. Therefore, making assumptions about coral health based on gross observations is incorrect and diseased samples should be histologically examined on a finer scale.

Most molecular-based coral disease studies have focused comparing the microbial communities associated with apparently healthy and diseased coral tissues to test for community differences. In these studies, coral colonies are assumed to be healthy as long as there is no tissue loss lesion present. However, the histopathological analysis of this study showed this not to be true. Two out of the three apparently healthy coral tissues

examined in this study exhibited tissue deterioration and necrosis. There were also many cases where the HD tissue exhibited signs of greater tissue decline than the HDD and TLM portions of a diseased coral branch. The data show that it is necessary for future coral disease studies to first examine samples histopathologically to categorize the samples properly, and then conduct molecular investigations. Using a microscopically based severity index of coral health instead of classifying samples based on the gross presence or absence of a tissue lesion may lead to more informative results. Future analysis of the molecular results obtained in this study will reassign the samples by condition based on the histology. This study was at a disadvantage when the pilot study for this project only tested for molecular differences among samples to determine whether the study was plausible. Then histopathological and molecular analyses were carried out simultaneously, so the assignment of disease category for the samples used in the molecular analyses described in the following chapters was based on the field signs of tissue loss at the time of sample collection. As shown here, it is more important for future studies to begin with histological examinations and then move into biodetection methodology.

CHAPTER 2: MOLECULAR APPROACHES FOR CHARACTERIZING MICROBIAL COMMUNITIES ASSOCIATED WITH APPARENTLY HEALTHY AND TISSUE-LOSS DISEASE-AFFECTED ACROPORIDS

Introduction

Coral reefs are dramatically changing as coral cover continues to decline worldwide. Nineteen percent of the world's original coral reef area has already been lost and there have been novel shifts in community reef structure as a result (Wilkinson 2008). Assessments predict that an additional 15 percent of coral reefs are considered to be at dangerously high risks for population collapse in the next 10–20 years and a final 20 percent are under threat of being lost in 20–40 years (Wilkinson 2008). Coral diseases have been identified as one of the greatest causes for reef decline globally (Harvell et al. 2007; Hoegh-Guldberg et al. 2007), and the coral holobiont has been studied intensively with regards to these diseases (Rosenberg et al. 2007b; Vega Thurber et al. 2009).

The causal agent(s) or pathogen(s) of a disease may include viruses, microorganisms, or other substances (Sutherland et al. 2004). Investigations of coral diseases have predominately focused on identifying a bacterial pathogen by using culture-dependent and/or culture-independent techniques (Ritchie and Smith 1997; Rohwer et al. 2001, 2002; Pantos et al. 2003; Bourne and Munn 2005; Pantos and Bythell

2006; Ritchie 2006; Lampert et al. 2008; Daniels et al. 2011). However, species composition findings from culture-dependent and culture-independent analyses have yielded significantly different results (Fuhrman and Campbell 1998; Rohwer et al. 2001).

Coral diseases have mainly been investigated by traditional culture-based methods (Amann et al. 1995), but attempts to isolate and cultivate pathogens have failed or yielded controversial results (Beleneva et al. 2005). Culture-based methods underestimate the true diversity of bacteria and are biased towards a very small percentage (less than 1%) of microbial associates that readily grow on culture media (Amann et al. 1995; Suzuki et al. 1997; Rohwer et al. 2001). However, it has been argued that information garnered from living and active cells is necessary to biochemically classify and analyze the bacterial portion of the coral holobiont (Beleneva et al. 2005). Furthermore, putative pathogens are not detectable by most culture-independent studies with regards to Koch's second postulate, if isolation of the agent using either culture or nonculture-dependent approaches from every case with similar signs is not possible (Koch 1882).

Culture-independent techniques began being employed systematically to study the microbiota of coral reefs in the early 2000s (Rohwer et al. 2001, 2002; Frias-Lopez et al. 2002). Since the majority of marine microorganisms are not culturable due to the lack of appropriate media, culture-independent methods are more-widely used today to overcome these limitations (Fuhrman and Campbell 1998; Rappé and Giovannoni 2003). However, conventional sequencing methods have their own limitations. Determining the nucleotide sequences in the genomes of numerous microorganisms contained in environmental

samples was beyond the scope of traditional Sanger sequencing methods (Hajibabaei et al. 2011). Advances in sequencing technology with deoxyribose nucleic acid (DNA) barcoding led to the identification of unknown organisms in large-scale, broad-scope biosystematics projects, but microoorganisms present in low numbers were not always represented in polymerase chain reaction (PCR) products (Wintzingerode et al. 1997). In many cases, only the complexity and diversity of the most dominant taxa found in microbial communities were described with Sanger sequencing (Sunagawa et al. 2009, 2010), but undetected microbial taxa found at low abundances are known to account for much of the total diversity found in marine systems (Sogin et al. 2006).

The desire to continue reducing the cost associated with DNA sequencing at an exponential rate consistent with Moore's Law has resulted in a variety of new sequencing technology (Moore 1965; Rothberg et al. 2011, 2012; Merriman et al. 2012). Through the development of high-throughput sequencing techniques, the diversity of previously undetected rare taxa can be examined and has provided novel insights about underestimated polymicrobial communities (Sogin et al. 2006; Sunagawa et al. 2010). Next-generation sequencing (NGS) technologies have considerably increased our understanding of microbial diversity, population structure, functional potential, and geographic distribution (Pedrós-Alió 2006; Sogin et al. 2006).

Several high-throughput sequencing technologies, such as multitag pyrosequencing (MTPS), have revolutionized genomic analyses of environmental samples using different chemistry and detection techniques. This multitag technology was developed at George Mason University and allows the pooling and sequencing of

hundreds of samples at one time. MTPS technology has exponentially increased sequencing capabilities from what was once several hundred reads per sample using a Sanger sequencer to tens of thousands of sequencing reads per sample using MTPS (Shokralla et al. 2012). NGS systems are simpler, faster, and more cost-effective and the data have been shown to be comparative to data from platforms such as Sanger sequencing (Sunagawa et al. 2009; Rothberg et al. 2011; Bayer et al. 2013; Stillman and Armstrong 2015).

Unlike dideoxy sequencing, DNA is synthesized during pyrosequencing. The addition of a nucleotide by DNA polymerase releases a pyrophosphate (PPi), and the emitted light is recorded (Ronaghi et al. 1996). MTPS was carried out on a GS Junior 454 Sequencing System (Roche, Branford, CT) that had a 125,000 sequence read capacity and took 10 hours to run. More recently, Life Technology's Ion Torrent™ technology (Frederick, MD) became available at The MicroBiome Analysis Center (MBAC) (Manassas, VA). Ion Torrent™ uses the simplest sequencing chemistry possible, allowing for the natural detection of nucleotide additions and eliminating the need for expensive optics and complex chemistries for DNA detection. In this technology, a complementary metal-oxide-semiconductor (CMOS) sensor array chip collects all data necessary for simple, on-chip, sequencing chemistry (Merriman et al. 2012). In this case, the chip contains a pH-sensitive field-effect transistor (pHFET) in order to obtain sequence data by directly detecting hydrogen ions. This all-electronic detection system has greatly reduced the cost of this sequencing technique, which only takes three hours to run and produces more scalable data (Rothberg et al. 2011).

Both MTPS and Ion Torrent™ technologies are emulsion PCR-based (emPCR), or amplicon sequencing technologies. This study used MTPS and Ion Torrent™ (the latter became available after the study began) NGS to conduct a taxonomical comparison of bacterial communities associated with (1) apparently healthy and diseased *A. cervicornis* tissue and (2) coral tissue and reef sediment using the Ribosomal Database Project (RDP 10) Bayesian Classifier (Chapters 3 and 4) and a phylogenetic community analysis of the same samples using quantitative insights into microbial ecology (Qiime) open-source bioinformatics pipeline and the unique fraction metric (UniFrac) (Chapter 5). The following section is an overview of the molecular techniques used to obtain data for the aforementioned bioinformatic analyses conducted in the following three chapters.

Methods

Sample collection

Field site descriptions, coral-tissue sample collection, and tissue preservation were discussed in the methods section of Chapter 1. In addition to coral fragments, reef-sediment samples were also collected for molecular analysis to investigate whether the surrounding sediment serves a source of a potential pathogen(s). A corresponding sediment sample was collected from the base of apparently healthy (AH) colonies. Healthy-on-diseased (HD) sediment samples were taken either where HD coral branches were touching the sediment or directly under the HD area of that colony. Diseased (D) sediment samples were collected similarly to HD samples (see Appendix I). Once on the boat, seawater was carefully decanted from the sediment samples and RNAlater® (Life Technologies, Frederick, MD) was added for DNA stabilization (Gray et al. 2013).

Sampling techniques were standardized for the 2012 field season, as samples were collected randomly and opportunistically during the 2011 pilot study. Although coral-tissue and sediment samples were collected and transported to the laboratory following the same methodology as the 2011 field season, coral subsamples for molecular analysis were preserved in a different manner. Bacteria from the mucosal biofilm were found in the RNAlater® solution in the 2011 samples. To prevent cross-contamination in the 2012 samples, the diseased-tissue samples were aseptically subdivided into the following sections prior to preservation in RNAlater®: healthy-on-diseased portion (normally pigmented) of the diseased tissue sample (HDD), tissue-loss margin (TLM), and denuded skeleton (DS) (Figure 10). However, all three sections were not always present in the coral fragments that were collected (see Appendix II). Sediment and coral-tissue samples for molecular analysis were transported to MBAC. All tissue and sediment samples were kept at -20°C until processing.

Many studies have shown that the surrounding water column was significantly different than the coral tissue and have found very little microbial overlap or contamination from the surrounding seawater (Rohwer et al. 2001, 2002; Frias-Lopez et al. 2002; Bourne and Munn 2005; Kvennefors et al. 2010; Daniels et al. 2011). Therefore, seawater samples were not collected for this study.

Genomic DNA extraction

Tissue and sediment samples were first thawed to room temperature. RNAlater® was then decanted from both tissue and sediment samples after centrifugation at 14,000 x g (~14,000 rpm) for 30 s. Using less tissue than the recommended 500 mg for the reef-

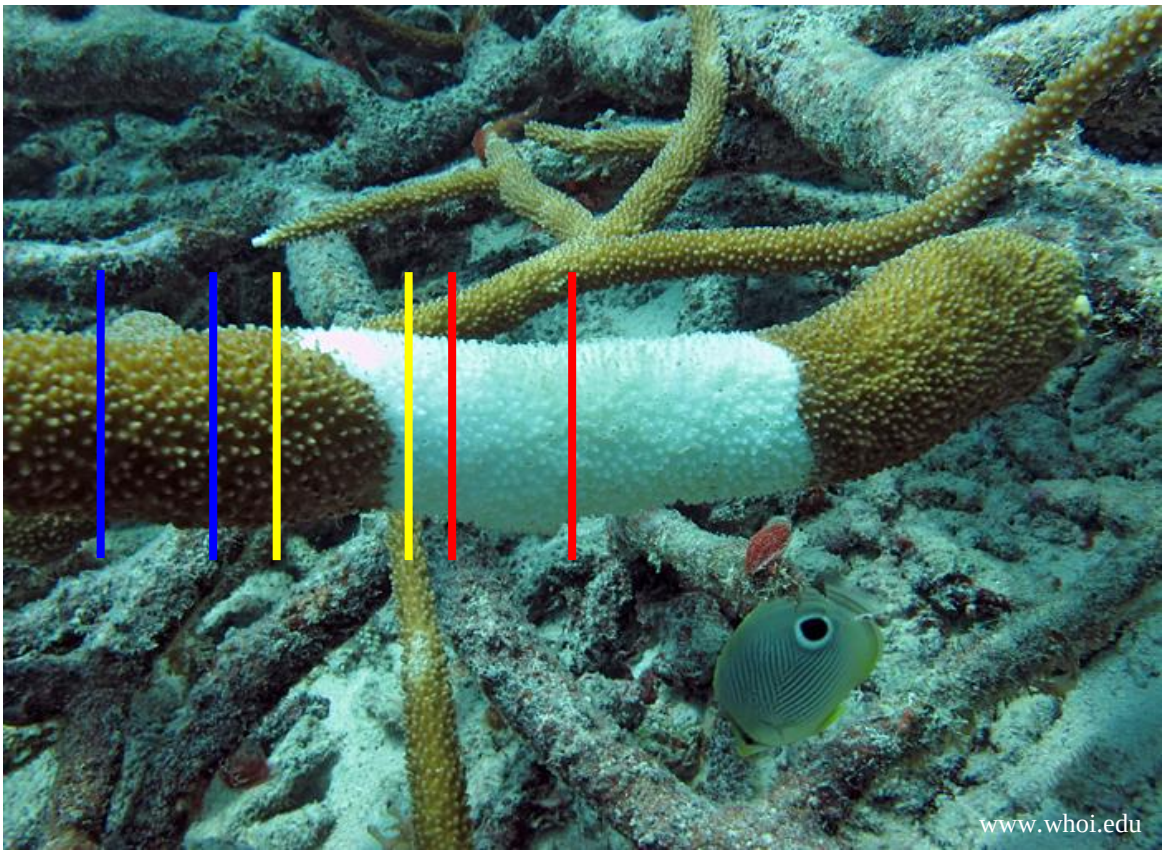

Figure 10. Figure depicts appropriate subsampling margins of diseased *A. cervicornis* branches for processing after collection. Blue represents the healthy-on-diseased section of a diseased branch (HDD); yellow represents the tissue-loss margin (TLM); and red represents denuded skeleton (DS).

sediment samples and coral-tissue samples, particularly the H and HD samples, resulted in higher DNA yields. Therefore, approximately 150–250 mg sections of coral tissue and skeleton or reef sediment were transferred into a Lysing Matrix E tube provided in the FastDNA® SPIN Kit for Soil (MP Biomedicals, Santa Ana, CA). Coral-tissue sections were transferred directly into the Matrix tubes using disinfected forceps, and sediment samples were directly transferred into the Matrix tubes using a 2-mL pipette, for which the tips were trimmed to enlarge the opening.

Whole-community genomic DNA was extracted from all samples using the bead beating method of the FastDNA® SPIN Kit for Soil (Sekar et al. 2006, 2008; Myers et al. 2007; Richardson et al. 2007; Voss et al. 2007; Lampert et al. 2008; Polson et al. 2008). This methodology extracts DNA from all microbial cells in the sample. Extractions were conducted following the manufacturer's protocol with the following modifications. In order to normalize bead-beating efficiency, a Savant/BIO 101® FastPrep® FP120 (Thermo Savant, Holbrook, NY) was used at speed 5.5 for 30 seconds (s) for all DNA extractions. To maximize cell lysis and increase DNA yield, samples were placed back into the FastPrep® FP120 after the initial 30 s of bead beating and processed two additional times for 30 s at the same speed of 5.5. Additionally, samples were also washed with SEWS-M wash solution two additional times to remove most of the inhibitory organic acids that can sometimes interfere with subsequent amplification steps. DNA dilutions (1:5, 1:10, or 1:50) were prepared depending on the concentration of DNA. The genomic DNA was visualized by electrophoresis on a 1% agarose gel in Tris-Acetate-EDTA (TAE) buffer and added ethidium bromide (EtBr) using a

Transilluminator 4000 (Stratagene, La Jolla, California). A Lambda DNA-HindIII ladder (Thermo Fisher Scientific, Inc., Waltham, MA) was used as the DNA size marker on the gel. The results of a polymerase chain reaction (PCR) was the most effective method for determining which DNA concentration yielded the most amplified product (Suzuki et al. 1998). The original DNA and DNA dilutions were kept at -20°C until used for PCR and were transferred to an -80°C freezer for long-term storage.

Polymerase chain reaction

Genomic DNA extracted from coral-tissue and reef sediment was used for amplification of two hypervariable regions (V1 & V2) of the 16S rRNA gene using the following primers: Tagged L27F (5′-AGA GTT TGA TCM TGG CTC AG-3′) and FAM (6-carboxyfluorescein) 355R (5′-GGT GCC TCC CGT AGG AGT-3′) (Life Technologies, Frederick, MD). PCR mixture concentrations and cycling parameters were the same for both amplicon length heterogeneity PCR (LH-PCR) and NGS, since the forward primers were individually tagged with unique barcodes necessary for NGS, and the reverse primer was fluorescently labeled for LH-PCR.

A master mix containing the following concentrations of PCR mixtures was prepared: DEPC water, l X PCR Rx. buffer for Taq Gold, 200 μM Mg mix, 0.5 units of AmpliTaq Gold® DNA Polymerase (5 units/μl) (Life Technologies, Frederick, MD), 0.1% bovine serum albumin (BSA) (Promega, Madison, WI), 0.025 mM of each deoxynucleotide triphosphate (dNTPs) (Promega, Madison, WI), and 0.5 μM of each of the forward and reverse primers. Approximately 10 ng of genomic DNA was added to the master mix for a final 20-μl reaction. PCR reactions were carried out using an Applied

Biosystems® (ABI) GeneAmp® PCR System 9700 (Life Technologies, Frederick, MD). The PCR program began with an initial denaturation step at 95°C for 11 min to activate the Taq DNA polymerase, which avoids non-specific amplification. The program continued with 32 cycles where each cycle included a denaturation step at 95°C for 30 s; an annealing step at 48°C for 30 s; and an extension step at 72°C for 1 min plus 5 s per cycle. A final extension step at 72°C for 30 min was added to ensure extension of all PCR fragments. Reactions were held at 4°C in the thermocycler until amplicons could be stored at 4°C for further processing. All PCR products were verified using 1% EtBr-stained agarose gels in TAE buffer for visualization. At least two replicates of PCR products were obtained for each sample for comparison and quality control.

Length heterogeneity polymerase chain reaction

PCR amplicons for each sample were analyzed using LH-PCR. LH-PCR is used to produce genetic fingerprints that differentiate organisms based on natural variation in the sequence lengths or composition of hypervariable regions within conserved 16S rRNA genes. The amplicons that are produced by LH-PCR may vary in base pair (bp) length and composition and can be indicative of different operational taxonomic units (OTUs) to show the diversity and relative abundance of a microbial community (Suzuki et al. 1998). Using these genetic fingerprints, the bacterial community structure associated with each coral tissue type (AH, HD, HHD, TLM, and DS) and reef-sediment samples (AH, HD, D) can be compared. A single OTU can be representative of an individual microbe. However, it is also possible for distantly related organisms to have identical amplicon lengths but vary in sequence (Mills et al. 2003). Therefore, LH-PCR

only assesses the similarity or dissimilarity among bacterial communities as a whole and molecular sequences of the amplified variable regions must be examined for taxonomic identification (Voss et al. 2007; Sekar et al. 2008).

PCR amplicons were diluted with deionized water relative to intensity of the product visualized on an EtBr-stained agarose gel. In this study, 1:10 and 1:20 dilutions were made of the selected PCR products. The diluted samples were then added in 1:10 ratio to a mix of Internal Lane Standard-600 (ILS-600) (Promega, Madison, WI) and highly deionized (Hi-Di™) Formamide (Life Technologies, Frederick, MD) (made in a 1:20 ratio) to be analyzed by the ABI 3130xl capillary sequencer (Life Technologies, Frederick, MD). ILS-600 is a size standard similar to the lambda ladder that is used when running agarose gels during electrophoresis. Hi-Di™ Formamide keeps both the ILS-600 and samples in a denatured state after an initial heating step (3 min at 95°C). Essentially, the Hi-Di™ formamide binds to the nitrogenous bases in DNA to disrupt the hydrogen bonds from reforming, keeping DNA in its denatured state. The PCR products were then separated on a capillary electrophoresis ABI 3130xl genetic analyzer.

The OTUs were quantified based on the intensity of fluorescence emitted and these results were depicted on electropherograms (profiles). LH-PCR profiles from each duplicate sample were analyzed using Applied Biosystems® GeneMapper® software (Version 4.1) (Life Technologies, Frederick, MD). Duplicate profiles for each sample type contained identical information and confirmed the products of the fingerprinting analysis. The size and relative abundance of amplicons in the electropherograms for each duplicate PCR from the same sample were determined for each profile. Profiles for

sample replicates were compared for quality control before pooling the amplicons for NGS analysis.

Next-generation sequencing

Amplicons for each sample were pooled and the pool was purified using the Agencourt® AMPure® XP PCR Purification solution (Beckman Coulter, Pasadena, CA) using the manufacturer's protocol. The goal of the purification step is to immobilize the DNA to the magnetic bead using a buffer so that everything else will be washed away. Purification was repeated a second time, and amplicons from the second clean-up were used for NGS. Five microliters of the original pool and both purified PCR products were run on a 1% EtBr-stained agarose gel for visualization and quantification. The original pool, first clean-up, and second clean-up were also fingerprinted for quality control. Pooling, clean-ups, and fingerprinting for quality control were performed prior to both MTPS and Ion Torrent™ NGS. The purified sample was then quantified for emPCR. The pools and both purified samples were diluted in TE buffer pH 8.0 (5 µl of sample added to 145µl TE) and quantified on a Multimode Analyzer based on the FAM label and the protocol discussed in Sikaroodi and Gillevet (2012).

Multitag pyrosequencing and emulsion PCR

To taxonomically identify the bacterial communities within each OTU, multitag pyrosequencing (MTPS), was performed on 24 samples using a GS Junior 454 Sequencing System (Roche Branford, CT). Pyrosequencing performs sequencing-by-synthesis, which allows the sequencing of a single strand of DNA by synthesizing the complementary strand enzymatically one base pair at a time. Sequencing-by-synthesis is

based on the detection of nucleotide incorporation, in this case by the release of a PPi, using primer-directed polymerase extension (Ronaghi et al. 1996).

Emulsion PCR was first carried out following the emPCR Amplification Method Manual - Lib-L Multiple-Prep (MV) for GS Junior Titanium Series (Roche, Branford, CT). emPCR amplifies a single DNA fragment that is linked with a titanium adapter and bound to a microbead in an aqueous-oil emulsion. The same forward and reverse primers used for LH-PCR (Tagged L27F and FAM 355R) were used for MTPS as adapters A and B were already included. Specifically, the forward primers included a Roche 454 A-Adapter, a seven bp unique tag, and the 27F rRNA universal bacterial primer in the 5′ to 3′ direction, whereas the reverse primer consisted of a Roche 454 B-adapter and the 355R reverse rRNA universal bacterial primer. The emulsion was amplified to create millions of copies of each single-stranded library fragment using a MJ Research PTC-200 thermal cycler (GMI, Minneapolis, Minnesota) following the conditions described in (Sikaroodi and Gillevet 2012). The emulsion was broken and all beads that retained amplified fragments were loaded onto a GS Junior Titanium PicoTiterPlate (Roche, Branford, CT) for sequencing. Manufacturer's protocols were followed for emPCR, breaking of the emulsion, and sequencing.

A sequencing primer was first hybridized to the amplified single-stranded DNA fragments in preparation for synthesis of the complementary strand. Polymerase then catalyzes the incorporation of nucleotide(s) into the complementary strand through a sequence of enzymatic reactions. After nucleotide incorporation, a PPi is released and is converted into ATP by ATP sulfurylase. The required energy is then provided to

luciferase, oxidizing luciferin to produce oxyluciferine and therefore generate light (Figure 11). Because each nucleotide is added stepwise to the primed DNA template, the incorporated nucleotides are known and the sequence of the template can be determined (Ronaghi 2001).

Ion Personal Genome Machine™ for next-generation sequencing

Ion Torrent™ NGS directly translates chemically encoded information into digital information on the CMOS sensor array chip. The PGM™ sequencer floods the CMOS chip with each nucleotide one at a time. If a nucleotide is complementary to the template base, it is then incorporated into the nascent strand. The addition of a base results in the hydrolysis of the incoming nucleotide triphosphate and a proton is released. The charge from that proton changes the pH of the solution, which is detected by a sensor at the bottom of each well and converted to a voltage. The sequencer then calls a base, going directly from chemical information to digital information (Rothberg et al. 2011).

Similar to MTPS, samples were pooled, fragmented, ligated to appropriate Ion Torrent™ adapters, and amplified onto beads for Ion Torrent™ NGS. LH-PCR products for each sample were once again pooled and purified using the Agencourt® AMPure® XP PCR Purification protocol. The same forward and reverse primers used for LH-PCR (Tagged L27F and FAM 355R) were used again but included titanium adapters A and P1 (a different B adapter), respectively.

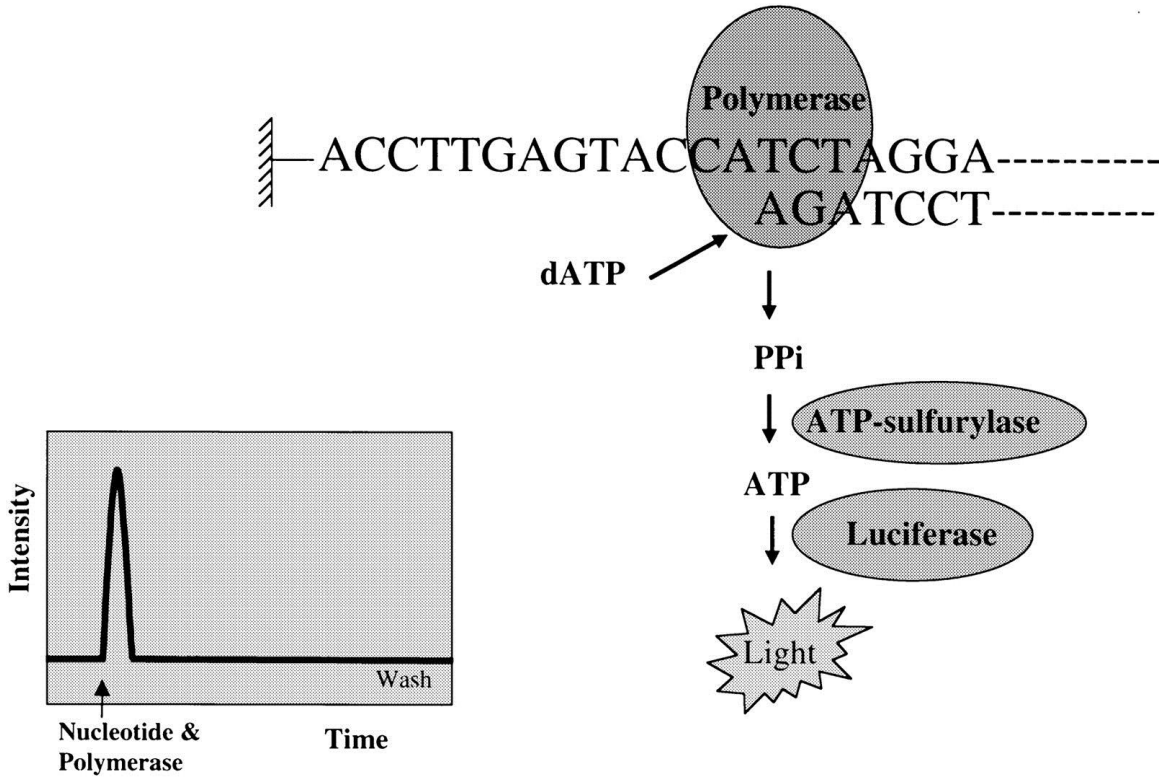

Figure 11. Schematic representation of the progress of the enzyme reaction in solid-phase pyrosequencing (Ronaghi 2001)**.**

CHAPTER 3: CHARACTERIZATION AND COMPARISON OF BACTERIAL COMMUNITIES ASSOCIATED WITH APPARENTLY HEALTHY AND TISSUE-LOSS DISEASE-AFFECTED *ACROPORA CERVICORNIS* TISSUES

Introduction

Microorganisms dominate the oceans' total biomass (Whitman et al. 1998) and are arguably the most abundant and diverse component of coral reef ecosystems (Rohwer et al. 2002). Investigations between coral hosts and a range of symbiotic microorganisms began in the early 1970s. These studies demonstrated that microbial communities are found in association with what was then described as the coral surface microlayer (CSM) (DiSalvo 1971a, 1971b; DiSalvo and Gundersen 1971; Coles and Strathmann 1973; Sorokin 1973; Benson and Muscatine 1974; Lewis and Price 1975; Mitchell and Chet 1975; Richman et al. 1975; Ducklow and Mitchell 1979). Further studies showed that a dynamic microbiota (Knowlton and Rohwer 2003; Ritchie and Smith 2004; Reshef et al. 2006; Rosenberg et al. 2007b) comprised of endosymbiotic dinoflagellates (Rowan 1998; Lajeunesse 2005), bacteria (Rohwer et al. 2002; Bourne and Munn 2005), Archaea (Kellogg 2004; Wegley et al. 2004), endolithic fungi and algae (Bentis et al. 2000), and protozoa (e.g., ciliates and coccidia) (Peters 1984) occupy ecological niches within the coral surface mucopolysaccharide layer (SML) (Ritchie 2006), on and within coral tissue

(Santavy 1995; Frias-Lopez et al. 2002; Ainsworth et al. 2006; Lesser et al. 2007), and its skeleton (Li et al. 2014).

Corals form long-term, host-specific bacterial associations (Ritchie and Smith 1997; Rohwer et al. 2001, 2002; Pantos et al. 2003; Kvennefors et al. 2010), but the degree to which the coral host relies on such symbiosis is unknown. Bacterial communities have been shown to play a role in the cycling of nutrients (Williams et al. 1987; Shashar et al. 1994; Lesser et al. 2004; Lema et al. 2012) and carbon (Ritchie and Smith 1995, 1997), while others provide antibiotic capabilities (Castillo et al. 2001; Ritchie 2006) and antimicrobial properties (Koh 1997; Ritchie and Smith 2004; Geffen and Rosenberg 2005; Kelman et al. 2006; Nissimov et al. 2009; Kvennefors et al. 2010). Despite these discoveries, little is known about what mechanisms control these unique associations.

Microbial communities have been studied extensively during the past 20 years with regards to coral health (Ritchie and Smith 1995, 1997; Santavy et al. 1995; Koh 1997; Santavy and Peters 1997; Richardson 1998; Rohwer et al. 2001; Rosenberg et al. 2007b; Vega Thurber et al. 2009). In the last 40 years, Caribbean coral reefs have declined dramatically due to the synergistic effect of multiple stressors contributing to biotic and abiotic diseases, including climate change and anthropogenic factors (Goreau et al. 1998; Richardson 1998; Harvell et al. 1999; Green and Bruckner 2000; Carpenter et al. 2008). Diverse bacterial coral diseases occur globally, and the number of coral diseases identified have increased exponentially over the last three decades, as well as the number of reported disease events or outbreaks, and the number of coral species being

affected by disease (Richardson 1998; Harvell et al. 1999; Green and Bruckner 2000; Hughes et al. 2003; Pandolfi et al. 2003; Rosenberg and Loya 2004; Sutherland et al. 2004; Weil 2004; Williams and Miller 2005; Vollmer and Kline 2008).

Research efforts investigating coral diseases have focused predominately on identifying a single infectious agent. Although numerous pathogenic sources have been suggested, *Vibrio shiloi* (Kushmaro et al. 2001) and *Vibrio* ribotypes (Cervino et al. 2008) for bacterial bleaching; *Serratia marcescens* for white pox disease (Patterson et al. 2002); African dust for aspergillosis (Garrison et al. 2003); *Aurantimonas coralicida* (Denner et al. 2003) and *Thalassomonas loyana* for white plague disease type II (WPL-II) (Thompson et al. 2006), there is still no consensus on pathogens and the causative agents of most coral diseases remain unknown (Lesser et al. 2007; Rosenberg and Kushmaro 2011). Multiple factors in addition to pathogen exposure likely result in onset of disease since several studies have detected proposed pathogenic microorganisms in apparently healthy coral tissue (Ritchie 2006; Sweet et al. 2012).

Coral disease origins have also been thought to involve an imbalance in the polymicrobial structure and diversity of the communities associated with the host (Harvell et al. 2007; Lesser et al. 2007). Perhaps specific bacteria-coral associations are disrupted on infection and beneficial relationships may be lost or compromised at the onset of infection (Pantos and Bythell 2006). Several studies have shown shifts in bacterial communities associated with coral during disease events (Ritchie and Smith 1995; Patterson et al. 2002; Garrison et al. 2003; Pantos et al. 2003; Frias-Lopez et al. 2004; Pantos and Bythell 2006; Ritchie 2006; Sunagawa et al. 2009; Cárdenas et al.

2012; Roder et al. 2014). Ritchie (2006) observed an environmental shift from beneficial bacteria to *Vibrio*-dominated *A. palmata* mucus, which resulted in the loss of antibiotic protective qualities of the mucus. Despite the known importance of coral-microbial associations, there is a lack of baseline information for these associations in both apparently healthy and diseased corals (Sweet et al. 2011).

Before 1980, acroporid corals used to dominate shallow Caribbean reefs, but were reduced to smaller scattered patches after large-scale epizootic events in the mid-1970s (Bruckner 2002). These events resulted in an 80 percent population reduction in *A. cervicornis* across the Caribbean and tropical western Atlantic Ocean (Harvell et al. 2002; Rosenberg and Ben-Haim 2002; Sutherland et al. 2004) and a 98 percent decline in the Florida Keys specifically (Miller et al. 2003), resulting in the species listing of threatened under the United States Endangered Species Act (Hogarth 2006). Three pantropical tissue-loss diseases affecting *A. cervicornis* have been described: white-band disease (WBD) type I (WBD-I) (Gladfelter 1982), WBD type II (WBD-II) (Ritchie and Smith 1998), and rapid tissue loss (RTL) (Williams and Miller 2005). These diseases are considered one of the most important threats to *A. cervicornis* populations today, but there is still no clear understanding about the epizootiology, etiology, and pathology of the tissue-loss diseases affecting *A. cervicornis*.

It has been presumed that WBD is caused by a bacterial infection, but there has been some debate whether coral diseases are infectious. Richardson (1998) suggested that WBD was a biochemical response, or a "shut-down-reaction," to some type of trauma to the coral rather than pathogen-induced (Richardson 1998). Distinct differences between

the bacterial communities associated with apparently healthy and diseased acroporid tissues has lead to the suggestion that bacteria are more than opportunistic invaders (Casas et al. 2004; Pantos and Bythell 2006; Vollmer and Kline 2008). Antibiotic treatments tested by Kline and Vollmer (2011) verified that WBD was an infectious disease caused by bacteria, and was not an opportunistic infection as suggested by (Lesser et al. 2007). Furthermore, experiments showed that WBD could be transmitted through direct contact with infected coral tissue and diseased homogenates (Kline and Vollmer 2011). Aquarium-based transmission experiments also revealed that the corallivorous snail, *Coralliophila abbreviata*, served as a vector and reservoir for the transmission of the WBD pathogen(s) (Williams and Miller 2005; Gignoux-Wolfsohn et al. 2012). Gignoux-Wolfsohn et al. (2012) also detected waterborne transmission of WBD to previously injured coral colonies, but not intact ones.

After almost four decades, no causative agents have been definitively identified for WBD-I. Histological examinations of WBD-I tissues have revealed the presence of Gram-negative bacterial colonies in both diseased and apparently healthy *A. palmata* tissue samples (Peters et al. 1983). However, no specific causative pathogen could be established because diseased-tissue samples were also found that did not have these bacterial aggregates. (Ritchie and Smith 1998) identified *V. harveyi (carchariae)* as the putative pathogen of WBD-II, but Pantos and Bythell (2006) noted that no vibrios were detected in WBD-I diseased tissue using culture-independent techniques. Instead, Pantos and Bythell (2006) detected α-proteobacteria related to *Roseobacter* in WBD-I diseased tissues that was absent in apparently healthy tissue.

Rickettsiales-like bacteria, particularly in the SML, have also been associated with WBD-I (Casas et al. 2004). However, (Kline and Vollmer 2011) showed that Rickettsiales-like bacteria are not likely involved in causing WBD-I, as the antibiotic ampicillin which is not effective against obligate intracellular bacteria such as *Rickettsia,* effectively suppressed disease transmission. (Kline and Vollmer 2011) also suggested that WBD-I was caused by transmissible Gram-positive infectious bacteria. Most recently, Sweet et al. (2014) confirmed that WBD is a polymicrobial disease and detected differences in the bacterial community associated with apparently healthy and diseased tissues using culture-independent analyses and antibiotic treatments. Sweet et al. (2014) proposed a histophagus ciliate, *Philaster lucinda,* and three candidate bacterial pathogens, *V. harveyi (carchariae), Lactobacillus suebicus,* and *Bacillus* sp. as potential primary pathogens of WBD. Furthermore, *P. lucinda, V. harveyi (carchariae),* and *Bacillus* sp. have all been indicated as potential causative agents in similar tissue-loss diseases: white syndrome (WS) (Sweet and Bythell 2012), WBD-II (Gil-Agudelo et al. 2006), and WBD in Indonesian acroporids (Hakim et al. 2012).

With regards to WBD-II, no causative agent or pathogen has been identified, but the disease was associated with the presence of *V. harveyi (carchariae)* in SML samples collected from the bleaching margin (Gil-Agudelo et al. 2006)**.** *Vibrio* bacteria were isolated from infected *A. cervicornis* colonies from Puerto Rico and were able to cause WBD-II signs in previously healthy corals (Ritchie and Smith 1998). Ritchie and Smith (1998) were able to satisfy Koch's first postulate, which states that the presumed pathogen must be always be found in association with a particular disease (Koch 1882).

However, *V. harveyi (carchariae)* could not be reisolated and no definitive identification has been documented. Lastly, very little is known about RTL, but this tissue-loss disease was found to be transmissible by *C. abbreviata* (Williams and Miller 2005). The role of microorganisms in most coral diseases including WBD and RTL has simply not been elucidated (Richardson 1998).

Recognizing disease requires an understanding of what "good health" is by defining a normal range of gross, microscopic, physiological, biochemical, and behavioral attributes or functions in a coral species (Peters 1984). Despite efforts, apparently healthy communities remain largely uncharacterized (Bourne and Munn 2005), and little research has examined *A. cervicornis* bacterial communities specifically. Precise disease diagnosis and potential prevention of future outbreaks requires fundamental knowledge of the composition and distribution of the microbial communities associated both with healthy and diseased colonies (Beleneva et al. 2005). A baseline for bacterial diversity associated with healthy coral tissues still needs to be established to understand the bacterial roles in the coral holobiont and to be able to better understand coral disease ecology at large (Cook 2009; Kvennefors et al. 2010; Sharp et al. 2010). This study (1) taxonomically characterized bacterial communities associated with apparently healthy *A. cervicornis*, (2) compared bacterial communities associated with apparently healthy and diseased *A. cervicornis* tissues, (3) identified potential biomarkers of tissue-loss diseases affecting *A. cervicornis*, and (4) discussed key taxa related to tissue-loss disease, using two culture-independent next-generation sequencing (NGS)

technologies. It is the first to use Ion Torrent's PGM technology to sequence 16S rRNA amplicons from *A. cervicornis* samples.

Methods

Sample information

Fifty-eight coral samples from seven coral reefs across the Upper Florida Keys, USA (see Chapter 1, Table 1 and Figure 1), were collected from a single host species, *A. cervicornis*. Eight apparently healthy (AH) samples, 8 healthy-on-diseased (HD) samples (HD samples were collected from normally pigmented branches of a diseased colony), 11 healthy-on-diseased portions of the diseased branch (HDD) samples (HDD samples refer to the normally pigmented section of tissue located on a coral branch that contains a disease lesion), 16 tissue-loss-margin (TLM) samples, and 15 denuded skeleton (DS) samples (see appendices II and III) were analyzed using NGS. Field site descriptions, coral-tissue sample collection, and sample fixation for molecular analysis were discussed in the methods section of Chapter 1, and all molecular techniques used were described in the methods section of Chapter 2.

RDP 10 analysis

De-multiplexed sequences from both multitag pyrosequencing (MTPS) and Ion Torrent™ were assigned taxonomic identifications using the Ribosomal Database Project (RDP) 10 Bayesian Classifier (Version 1.2) available on MBAC's Galaxy portal, an open source, web-based platform for data intensive research. Taxonomic classifications were examined using a relative abundance cut-off of 1 and 0.1 percent, and with a classification bootstrap confidence of 0.80. The resulting abundance tables were compared for five samples (17, 65, 70, 72, and 83) that were sequenced using both MTPS

and Ion Torrent™ to determine whether sequence reads were different. The resulting relative abundance tables and taxonomic classifications were also compared at each cut-off level to determine how much of the taxonomic diversity of the associated bacterial communities was comprised of rare taxa. Lastly, the average relative abundance of the bacteria associated with the samples was examined at all taxonomic levels (phylum to genus) to determine the appropriate taxonomic resolution needed to clearly represent any patterns of similarity or dissimilarity in bacterial community composition.

Bray Curtis principal coordinate analysis

Principal coordinate analyses (PCOs) were conducted on the RDP 10 data using the MultiVariate Statistical Package (MVSP) (Version 3.1) to make taxonomic comparisons among coral sample types. Specifically, Bray-Curtis ordination was used to identify relationships among sample types by comparing the relative bacterial abundances among the various coral-tissue sample types. The similarity matrix ranges from 0–1, where zero means that the two datasets are completely unrelated and one means that the two datasets are an identical match. Bray-Curtis similarity matrices were calculated and used to compare bacterial communities associated (1) among all coral sample conditions (AH, HD, HDD, TLM, DS); and (2) among collapsed coral health states, (AH, HD, D).

Linear discriminant analysis effective size estimation

Advancements in sequencing technologies have made the detection of microbial biomarkers easier for microbial community comparisons (Zhang et al. 2010). The presence of pathogenic microorganisms within a community can signal disease, while increases and decreases in community diversity can also serve as potential biomarkers (Lecuit et al. 2004; Segata et al. 2011). These abnormal shifts in the microbiome are

termed dysbiosis. Metagenomic studies seek to identify specific organisms or operational taxonomic units (OTUs) whose relative abundances differ between two or more groups of samples. However, few bioinformatic methods available can successfully compare the communities found in different sample classes (Segata et al. 2011).

Metagenomic studies are challenged by the ability to detect an organism(s) that consistently explains the differences between two or more microbial communities due to the high dimensionality of the data (Clarke et al. 2008). These studies are further complicated by the fact that rare taxa are known to account for much of the total diversity found in marine systems (Pedrós-Alió 2006; Sogin et al. 2006) and the fact that the data distribution is non-parametric. Most statistical tests for microbial community analysis rely on cluster analyses based on PCOs. Although they successfully detect relatedness among samples, PCOs are unable to identify the biological features responsible for these relationships, whereas metastats perform binary statistical analysis with biomarker discovery. Linear Discriminant Analysis (LDA) coupled with Effective Size estimation (LEfSe) is the preferred method of biomarker discovery and provides biological class explanations by coupling statistical tests for significance with tests for encoding biological consistency, and effect-size estimation of the predicted biomarkers (Segata et al. 2011).

LEfSe is an algorithm that supports high-dimensional class comparisons to predict metagenomic biomarkers by detecting differences in genomic features, such as taxa, that explain most of the effect and are both differentially abundant and biologically meaningful (Segata et al. 2011). LEfSe first identifies features with significant

differential abundance using the non-parametric Kruskal-Wallis (KW) sum-rank test (Kruskal and Wallis 1952). Biological consistency is next investigated using pairwise tests among subclasses using the (unpaired) Wilcoxon rank-sum test (Wilcoxon 1945). Lastly, LEfSE estimates effect size of each differentially abundant feature using LDA (Fisher 1936). LEfSe was used to identify indicator bacterial taxa that were differentially abundant or depleted through pairwise comparisons of all sample types.

Results

Sequencing and quality control

A total of 808,703 sequences were obtained from 58 coral fragments processed using MTPS (61,557sequences) and Ion Torrent™ (741,353 sequences) sequencing methods. Sample reads ranged from 122 to 79,694 with an average of 17,352 reads per sample. Twelve samples had less than 1,000 reads and were dropped from the study (5,703 sequences), retaining a total of 802,910 sequences for this analysis. The sequences for six AH, five HD, six HDD, 14 TLM, and 15 DS samples were examined for this study (n=46). De-multiplexed sequences from both MTPS and Ion Torrent™ were assigned taxonomic identifications using the RDP 10 Bayesian Classifier available on MBAC's Galaxy portal. The RDP 10 Classifier provided a hierarchical description and average relative abundances of the coral-associated bacteria that spanned from phylum to genus.

Samples were initially pyrosequenced as the Ion Torrent™ technology was not available yet at George Mason University's (GMU) MicroBiome Analysis Center (MBAC). Pyrosequencing is already a widely accepted approach, and Ion Torrent™ data

have been shown to be comparable (Yergeau et al. 2012). However, no previous studies have compared the results of these two technologies while investigating coral diseases. No major differences in the average relative abundance of coral-associated bacteria were observed when comparing sequencing techniques at any taxonomic level (Figure 12). These results confirm that the sequence data obtained using both NGS technologies were comparable and that it was appropriate for the data to be concatenated and analyzed together.

Rare taxa abundance and diversity

In total, the bacterial communities associated with coral fragments collected from the Upper Florida Keys were composed of 11 phyla comprised of 19 classes, 43 orders, 89 families, and 153 genera, when examined using a 1 percent relative abundance cut-off. Twenty-four phyla comprised of 42 classes, 86 orders, 192 families, and 352 genera were identified when examined using a 0.1 percent relative abundance cut-off. Although 13 more phyla were identified using the 0.1 percent cut-off, these additional phyla accounted for less than one percent of the total number of sequence reads (2,771 sequences), and the dominant phyla present in each sample type were the same (Figure 13).

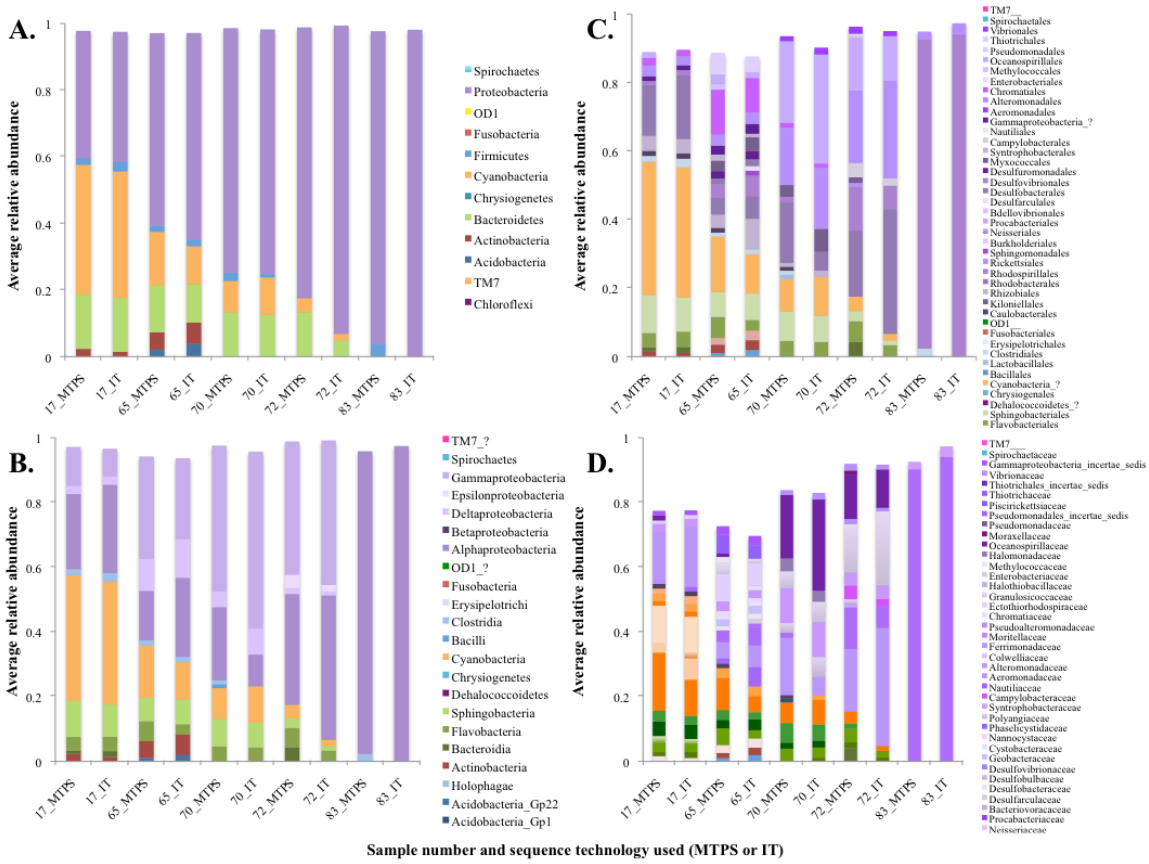

Figure 12. Comparison of the average relative abundance of bacterial communities associated with coral tissue (17, 70, 72, and 83) and reef sediment (65) at the (A) phylum level (n=12); (B) class level (n=23); (C) order level (n=50); and (D) family level (n=115); using multitag pyrosequencing (MTPS) and Ion Torrent™ sequencing technologies (Bootstrap P = 0.80, Cutoff = 0.01).

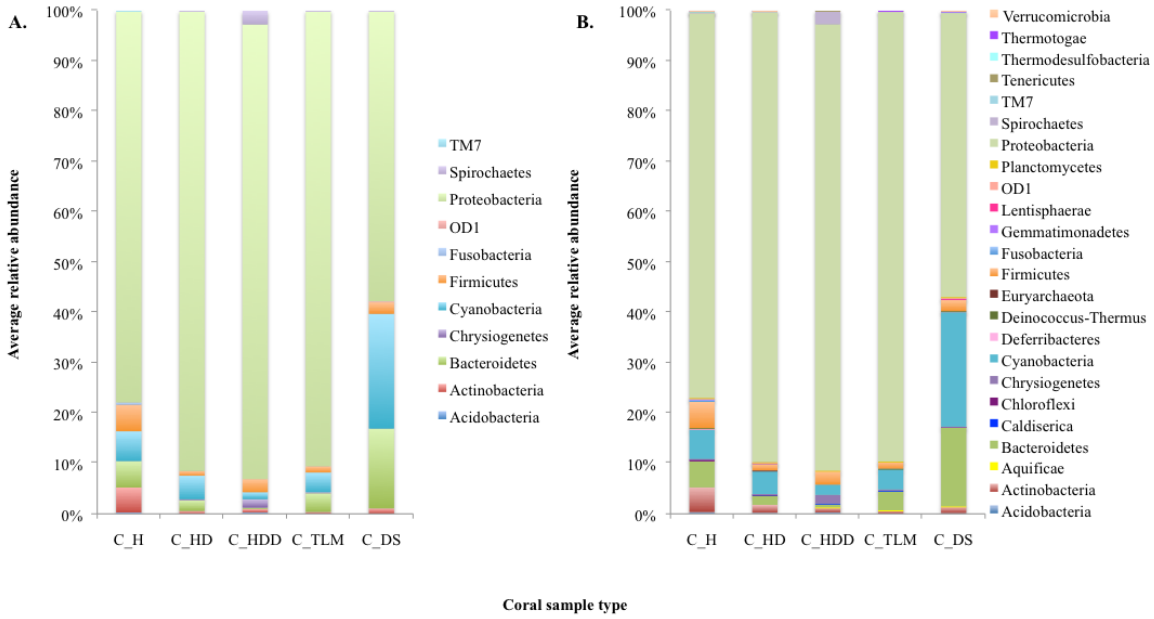

Figure 13. Comparison of the average relative abundance of bacteria within different phyla composing the microbial communities associated with each coral sample type with a (A) 1 percent abundance cut-off, and (B) 0.1 percent abundance cut-off (Bootstrap P = 0.80).

Taxonomic differences were examined between the two relative abundance cut-offs using a classification bootsrap confidence of 80 percent (Table 9). The resulting abundance tables were compared per sample at each cut-off level to quantify how much of the taxonomic diversty was lost using the 1 percent relative abunance parameter. As the associated bacterial-community composition was examined at a finer resolution, the number of rare taxa present increased while the dominant taxa present in each sample type remained the same (Table 10). At the genus level, 35 percent (n=16) of the taxa diversity was lost for 41 percent of the coral samples (n=46) using a 1 percent abundance cut-off (Table 9). Associated bacterial community composition were characterized at the class and family taxonomic levels using a 1 percent relative abundance level, since the same dominant taxa were present regardless of the relative abundance cut-off level used.

Taxonomic characterization of bacterial communities associated with apparently healthy and diseased *A. cervicornis* samples

Proteobacteria was the dominant phylum found in all coral samples (Figure 14). Specifically, α-proteobacteria dominated the microbiota of AH, HDD, and TLM samples (67.98%, 85.68%, and 48.05%, respectively), whereas γ-proteobacteria dominated HD and DS samples (77.78% and 31.39%, respectively) (Table 11). The community composition of AH *A. cervicornis* was dominated by α-proteobacteria (67.98%), followed by γ-proteobacteria (8.00%), Cyanobacteria (6.07%), and Actinobacteria (5.09%). Bacteria from phylum Fusobacteria and candidate phylum TM7 were only found in AH samples, and AH samples also contained more sequences from classes Actinobacteria, Bacteroidia, Bacilli, Clostridia, β-proteobacteria, and candidate division TM7 than any other sample type.

Table 9. Comparison of the total relative abundance of bacteria associated with each sample using a 1 and 0.1 percent cut-off level at each taxonomic level (Bootstrap P = 0.80).

Sample ID	Average relative abundances at each taxonomic level and abundance cut-off									
	Phylum		Class		Order		Family		Genus	
	0.01	0.001	0.01	0.001	0.01	0.001	0.01	0.001	0.01	0.001
25_K2puck_C_H	0.978	0.991	0.954	0.988	0.871	0.983	0.751	0.960	0.350	0.937
53_UnkA_C_HD	0.976	0.996	0.937	0.993	0.866	0.990	0.725	0.975	0.391	0.960
133_C_DS	0.979	0.994	0.967	0.989	0.895	0.984	0.727	0.968	0.416	0.948
115_UnkF_C_DS	0.986	0.996	0.968	0.995	0.926	0.989	0.815	0.972	0.475	0.955
105_UnkC_C_HD	0.962	0.998	0.950	0.996	0.903	0.995	0.757	0.987	0.476	0.980
151_UnkE_C_DS	0.987	0.994	0.971	0.992	0.904	0.984	0.817	0.968	0.489	0.946
139_176_C_DS	0.987	0.997	0.972	0.995	0.930	0.991	0.839	0.980	0.502	0.964
17_B2_C_DS	0.976	0.996	0.969	0.992	0.898	0.987	0.790	0.968	0.506	0.954
5_Y2_C_DS	0.987	0.996	0.967	0.995	0.921	0.988	0.831	0.971	0.523	0.947
147_UnkE_C_HD	0.966	0.996	0.961	0.990	0.903	0.987	0.735	0.975	0.531	0.964
107_UnkC_C_HDD	0.984	0.997	0.954	0.995	0.893	0.993	0.765	0.984	0.560	0.974
126_K152_C_H	0.959	0.998	0.941	0.994	0.849	0.990	0.745	0.972	0.573	0.957
56_UnkA_C_DS	0.989	0.998	0.974	0.998	0.931	0.997	0.836	0.988	0.578	0.968
70_135_C_TLM_rpt	0.982	0.995	0.957	0.992	0.902	0.985	0.829	0.959	0.595	0.932
6_Y2_C_TLM	0.986	0.995	0.975	0.992	0.900	0.992	0.795	0.971	0.602	0.959
108_UnkC_C_TLM	0.989	0.997	0.971	0.997	0.942	0.991	0.828	0.972	0.606	0.956
95_159_C_DS	0.975	0.997	0.953	0.996	0.910	0.991	0.839	0.969	0.661	0.951
150_UnkE_C_TLM	0.983	0.997	0.955	0.997	0.902	0.990	0.795	0.974	0.665	0.963
55_UnkA_C_TLM	0.992	0.998	0.974	0.994	0.916	0.991	0.856	0.979	0.678	0.965
39_Y66_C_D	0.984	0.999	0.962	0.997	0.923	0.994	0.877	0.979	0.763	0.970
127_K151_C_H	0.984	0.996	0.955	0.996	0.889	0.990	0.813	0.969	0.768	0.958
109_UnkC_C_DS	0.985	0.997	0.974	0.996	0.940	0.990	0.888	0.973	0.768	0.962
62_129_C_TLM	0.994	0.998	0.964	0.998	0.927	0.992	0.903	0.981	0.789	0.974
142_K1353_C_TLM	0.987	0.997	0.954	0.996	0.920	0.995	0.861	0.983	0.807	0.973
72_Y39_C_TLM_rpt	0.994	0.997	0.992	0.996	0.950	0.991	0.917	0.977	0.816	0.965
141_K1353_C_HDD	0.998	0.999	0.985	0.999	0.956	0.995	0.875	0.986	0.817	0.979

143_K1353_C_DS	0.987	0.999	0.974	0.999	0.941	0.995	0.884	0.987	0.824	0.983
125_K2_C_H	0.988	1.000	0.956	0.998	0.923	0.997	0.852	0.995	0.827	0.986
119_UnkG_C_H	0.998	0.998	0.979	0.997	0.957	0.992	0.913	0.987	0.844	0.979
94_159_C_TLM	0.981	0.997	0.974	0.996	0.942	0.990	0.914	0.983	0.849	0.978
47_Y39_C_DS	0.986	1.000	0.963	0.999	0.940	0.996	0.930	0.985	0.869	0.981
20_B2_C_D	0.988	0.999	0.969	0.999	0.951	0.998	0.921	0.997	0.891	0.995
132_C_TLM	0.995	0.999	0.985	0.997	0.956	0.992	0.941	0.987	0.893	0.979
138_176_C_TLM	0.978	0.997	0.972	0.996	0.960	0.992	0.919	0.987	0.902	0.984
100_172_C_HDD	0.985	0.999	0.971	0.998	0.954	0.998	0.937	0.995	0.924	0.992
88_172_C_TLM	0.993	0.999	0.987	0.998	0.967	0.995	0.949	0.990	0.934	0.986
113_UnkF_C_HDD	0.968	0.998	0.956	0.998	0.934	0.993	0.934	0.987	0.934	0.983
45_129_C_DS	0.992	1.000	0.982	1.000	0.967	1.000	0.958	1.000	0.939	1.000
101_172_C_TLM	0.986	0.999	0.980	0.998	0.975	0.996	0.948	0.992	0.939	0.989
129_87_C_HD	0.982	0.998	0.974	0.996	0.957	0.991	0.944	0.988	0.944	0.984
137_176_C_HDD	0.980	0.997	0.967	0.994	0.962	0.988	0.955	0.980	0.953	0.976
89_172_C_DS	0.977	0.999	0.971	0.998	0.961	0.993	0.955	0.986	0.955	0.982
114_UnkF_C_TLM	0.979	0.999	0.968	0.997	0.966	0.993	0.966	0.987	0.966	0.985
91_159_C_HD	0.986	1.000	0.985	0.997	0.984	0.995	0.984	0.992	0.970	0.991
83_UnkB_C_HDD_rpt	0.981	0.999	0.974	0.997	0.973	0.996	0.973	0.993	0.973	0.991
37_K2Puck_C_H	0.995	0.999	0.985	0.998	0.980	0.995	0.978	0.991	0.978	0.990

Table 10. Comparison of the average relative abundance of bacterial communities associated with each coral sample type at the class level with a (A) 1 percent abundance cut-off, and (B) 0.1 percent abundance cut-off (Bootstrap P = 0.80). Dominant taxa present in each sample type remain the same regardless of cut-off level.

A.

Phylum	Class	C_H	C_HD	C_HDD	C_TLM	C_DS
Acidobacteria	Holophagae	0.00	0.00	0.21	0.00	0.00
Actinobacteria	Actinobacteria	5.09	0.93	0.64	0.39	1.06
Bacteroidetes	Bacteroidia	1.01	0.20	0.12	0.17	0.08
	Flavobacteria	1.24	0.60	0.06	2.21	10.49
	Sphingobacteria	2.26	0.97	0.06	1.14	5.10
Chrysiogenetes	Chrysiogenetes	0.00	0.00	1.72	0.14	0.00
Cyanobacteria	Cyanobacteria	6.07	4.79	1.41	4.10	23.58
Firmicutes	Bacilli	1.37	0.00	0.11	0.08	0.03
	Clostridia	3.74	1.02	2.38	0.79	1.60
	Erysipelotrichi	0.00	0.00	0.00	0.17	0.14
Fusobacteria	Fusobacteria	0.45	0.00	0.00	0.00	0.00
OD1	OD1_	0.00	0.00	0.00	0.00	0.18
Proteobacteria	Alphaproteobacteria	**67.98**	12.28	**85.68**	**48.05**	23.79
	Betaproteobacteria	1.15	0.11	0.30	0.05	0.07
	Deltaproteobacteria	1.53	1.17	0.30	1.64	2.41
	Epsilonproteobacteria	0.00	0.00	0.00	0.32	0.00
	Gammaproteobacteria	8.00	**77.78**	4.25	40.64	**31.39**
Spirochaetes	Spirochaetes	0.00	0.14	2.76	0.12	0.08
TM7	TM7_	0.10	0.00	0.00	0.00	0.00
	Total reads	**68,917**	**42,899**	**89,830**	**238,727**	**337,925**

B.

Phylum	Class	C_H	C_HD	C_HDD	C_TLM	C_DS
Acidobacteria	Acidobacteria_Gp10	0.04	0.05	0.03	0.00	0.00
	Acidobacteria_Gp16	0.06	0.07	0.00	0.00	0.00
	Acidobacteria_Gp2	0.00	0.00	0.00	0.00	0.00
	Acidobacteria_Gp22	0.11	0.06	0.00	0.00	0.05
	Acidobacteria_Gp4	0.05	0.00	0.02	0.00	0.00
	Acidobacteria_Gp9	0.01	0.01	0.00	0.00	0.00
	Holophagae	0.02	0.00	0.23	0.01	0.01
Actinobacteria	Actinobacteria	4.91	1.57	0.99	0.63	1.33
Aquificae	Aquificae	0.00	0.00	0.02	0.05	0.04
Bacteroidetes	Bacteroidetes_	0.02	0.00	0.00	0.03	0.03
	Bacteroidia	1.31	0.34	0.41	0.33	0.49
	Flavobacteria	1.61	0.59	0.08	2.25	10.21
	Sphingobacteria	2.22	0.96	0.06	1.26	5.00
Caldiserica	Caldisericia	0.00	0.02	0.12	0.01	0.00
Chloroflexi	Anaerolineae	0.20	0.01	0.00	0.00	0.03
	Caldilineae	0.20	0.01	0.00	0.00	0.03
	Dehalococcoidetes	0.00	0.01	0.00	0.00	0.00
Chrysiogenetes	Chrysiogenetes	0.04	0.09	1.72	0.22	0.03
Cyanobacteria	Cyanobacteria	5.92	4.70	2.04	4.13	22.99
Deferribacteres	Deferribacteres	0.05	0.00	0.00	0.00	0.00
Deinococcus-Thermus	Deinococci	0.16	0.00	0.00	0.01	0.03
Euryarchaeota	Halobacteria	0.00	0.00	0.00	0.00	0.00
Firmicutes	Bacilli	1.56	0.27	0.18	0.20	0.11
	Clostridia	3.60	1.00	2.53	0.99	1.85
	Erysipelotrichi	0.03	0.00	0.01	0.20	0.28
Fusobacteria	Fusobacteria	0.52	0.13	0.00	0.02	0.16
Gemmatimonadetes	Gemmatimonadetes	0.02	0.00	0.00	0.00	0.00
Lentisphaerae	Lentisphaeria	0.00	0.01	0.00	0.00	0.00
OD1_	OD1_	0.18	0.08	0.00	0.00	0.26
Planctomycetes	Planctomycetacia	0.08	0.10	0.01	0.00	0.10
Proteobacteria	Alphaproteobacteria	**65.43**	12.04	**83.20**	**47.05**	23.18
	Betaproteobacteria	1.37	0.24	0.59	0.22	0.21
	Deltaproteobacteria	1.95	1.15	0.47	1.69	2.49
	Epsilonproteobacteria	0.20	0.03	0.01	0.53	0.13
	Gammaproteobacteria	7.75	**76.23**	4.59	39.92	**30.55**
Spirochaetes	Spirochaetes	0.04	0.14	2.68	0.24	0.17
TM7_	TM7_	0.15	0.06	0.00	0.00	0.01
Tenericutes	Mollicutes	0.02	0.00	0.02	0.00	0.00
Thermodesulfobacteria	Thermodesulfobacteria	0.04	0.00	0.00	0.00	0.00
Thermotogae	Thermotogae	0.10	0.01	0.00	0.02	0.11
Verrucomicrobi	Opitutae	0.02	0.01	0.00	0.00	0.12
	Verrucomicrobiae	0.00	0.01	0.00	0.00	0.01
	Total reads	**71,645**	**43,769**	**92,508**	**243,841**	**347,196**

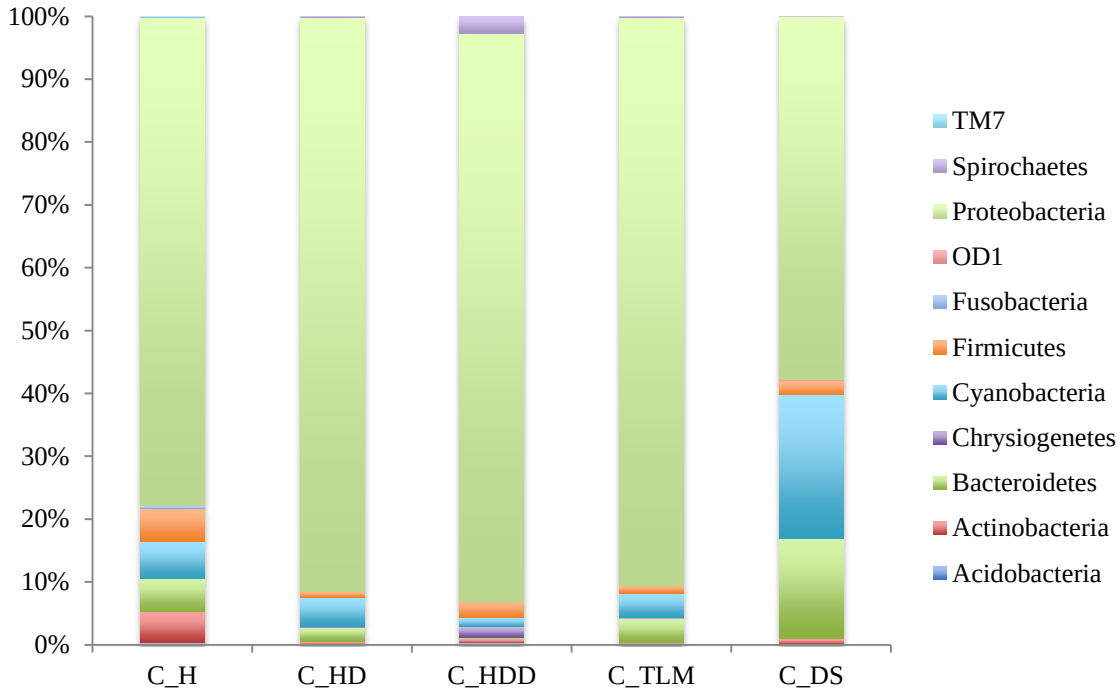

Figure 14. Comparison of the average relative abundance of bacteria within different phyla composing the microbial communities associated with each coral sample type (Bootstrap P = 0.80, cutoff = 0.01).

Table 11. Comparison of the percent abundance (%) of bacteria bacteria within different classes composing the microbial communities associated with each coral sample type (Bootstrap P = 0.80, cutoff = 0.01).

Phylum	Class	C_H	C_HD	C_HDD	C_TLM	C_DS
Acidobacteria	Holophagae	0.00	0.00	0.21	0.00	0.00
Actinobacteria	Actinobacteria	5.09	0.93	0.64	0.39	1.06
Bacteroidetes	Bacteroidia	1.01	0.20	0.12	0.17	0.08
	Flavobacteria	1.24	0.60	0.06	2.21	10.49
	Sphingobacteria	2.26	0.97	0.06	1.14	5.10
Chrysiogenetes	Chrysiogenetes	0.00	0.00	1.72	0.14	0.00
Cyanobacteria	Cyanobacteria	6.07	4.79	1.41	4.10	23.58
Firmicutes	Bacilli	1.37	0.00	0.11	0.08	0.03
	Clostridia	3.74	1.02	2.38	0.79	1.60
	Erysipelotrichi	0.00	0.00	0.00	0.17	0.14
Fusobacteria	Fusobacteria	0.45	0.00	0.00	0.00	0.00
OD1	OD1_	0.00	0.00	0.00	0.00	0.18
Proteobacteria	Alphaproteobacteria	**67.98**	12.28	**85.68**	**48.05**	23.79
	Betaproteobacteria	1.15	0.11	0.30	0.05	0.07
	Deltaproteobacteria	1.53	1.17	0.30	1.64	2.41
	Epsilonproteobacteria	0.00	0.00	0.00	0.32	0.00
	Gammaproteobacteria	8.00	**77.78**	4.25	40.64	**31.39**
Spirochaetes	Spirochaetes	0.00	0.14	2.76	0.12	0.08
TM7	TM7_	0.10	0.00	0.00	0.00	0.00
	Total reads:	**68,917**	**42,899**	**89,830**	**238,727**	**337,925**

Only three bacterial classes were abundant in HD samples with γ-proteobacteria comprising the majority of the community (77.78%), followed by α-proteobacteria (12.28%), and Cyanobacteria (4.79%) (Table 11). The associated bacterial communities in HDD samples were dominated by α-proteobacteria, which accounted for 85.68% of the community. All other bacterial classes found in HDD samples accounted for less than 5 percent of the community's total composition. HDD samples were the only samples that contained more than a trace amount of Chrysiogenetes and Spirochaetes, and HDD samples also contained the most bacteria from class Holophagae.

Approximately 89 percent of the bacterial community found in TLM samples was composed of Proteobacteria comprised of 48.05 and 40.64 percent α- and γ-proteobacteria, respectively. Similar to HDD samples, TLM-associated bacterial compositions were not taxonomically diverse. TLM samples were the only samples that contained ε-proteobacteria and contained more Erysipelotrichi than any other sample type.

Bacterial communities associated with the DS area of a diseased coral branch were the most diverse. Alpha- and γ-proteobacteria were the most abundant (31.39 and 23.79%, respectively) bacteria classes found in DS samples, followed by Cyanobacteria (23.58%), Flavobacteria (10.49%) and Sphingobacteria (5.10%) (Table 11). DS samples contained the most Bacteroidetes (both Flavobacteria and Sphingobacteria), Cyanobacteria, δ-proteobacteria compared to all other sample types. Finally, DS samples were the only sample type to contain candidate division OD1 bacteria.

Bray-Curtis dissimilarity clustering

Analysis of the average relative abundance of associated coral bacterial communities using multivariate ordination methods and analysis of similarity revealed clustering with respect to coral tissue-type (Figure 15). The bacterial communities associated with DS samples were more similar to each other than the other sample types (Figure 15). The majority of the TLM samples clustered closely with the DS samples, showing that the most diseased sections of the coral branch were more similar to each other than those associated with healthier disease states. A second cluster of mostly TLM samples was also found (Figure 15B). In this cluster, two of the TLM samples came from the same outplanted coral colony at FR, one sample was collected from an outplanted colony in CS, and the final sample was collected from a wild colony at LC all within the year 2012. The HDD sample that was a part of this cluster came from the same outplanted colony as the TLM sample from CS (Figure 15B). It is interesting to note that HD samples clustered more closely with DS and TLM samples than HDD samples. This observation is important as it serves as evidentiary support that what are perceived to be apparently healthy corals or non-diseased areas of the diseased coral colonies, actually are in a state of declining health when examined histologically (Chapter 1) and molecularly (Figure 15).

Conditions were collapsed into more general health states as follows: AH, HD and HDD samples were combined to create the " healthy-on-diseased" category, while TLM and DS samples were combined to create a general "diseased" category. Analysis of the average relative abundance of associated coral bacterial communities using

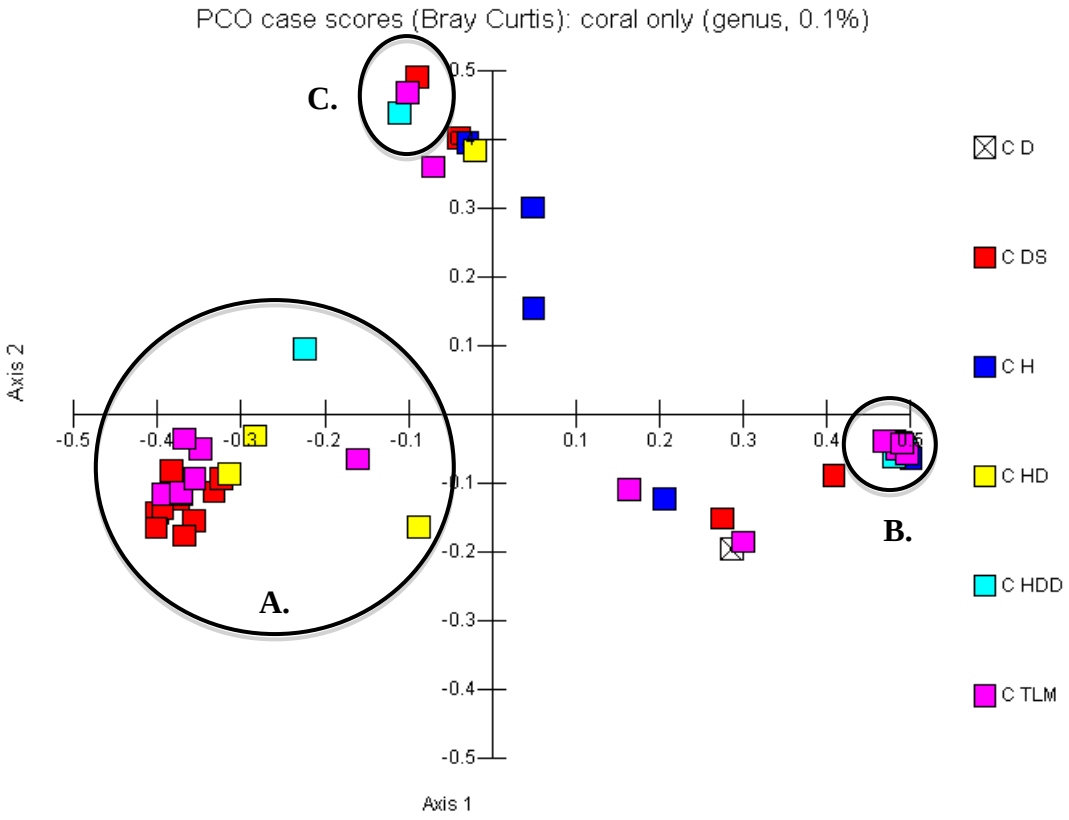

Figure 15. Bray-Curtis ordination of the bacterial communities associated with coral samples of varying health states. Clusters of interest have been encircled.

multivariate ordination methods and analysis of similarity revealed clustering with respect to coral health states (Figure 16).

Bacterial groups with statistical differences

While the previous PCO analysis successfully detected relatedness among samples, PCOs are unable to identify the biological features responsible for these relationships. Therefore, LEfSe was used was used to test for statistical differences between microbial communities, and detect specific taxa that explained most of the effect and were differentially abundant (Segata et al. 2011). Bacterial communities associated with AH samples were first compared with HD and HDD samples. No discriminative features were found using the default (LDA) value of log 2.0 (a=0.01). Three bacterial families were detected as significantly distinct features when comparing AH and TLM microbial communities (Figure 17). Family Vibrionaceae was the only differentially enriched family associated with TLM samples while Lachnospriaceae and an unknown family of Thiotrichales were the most depleted families associated with TLM samples. No significant features were identified from AH communities when compared with the microbial community associated with DS (Figure 18). Conversely, families Chrysiogenaceae, Cyanobacteria Family II, and an unknown family of Thiotrichales enriched DS associated microbial communities.

Since there were no LDA significant differences among AH, HD, and HDD microbial communities, these three sample types were collapsed into one class of "healthy." Because DS microbial communities primarily reflected successional overgrowth of the skeleton, DS samples were not used the final analysis. The results for

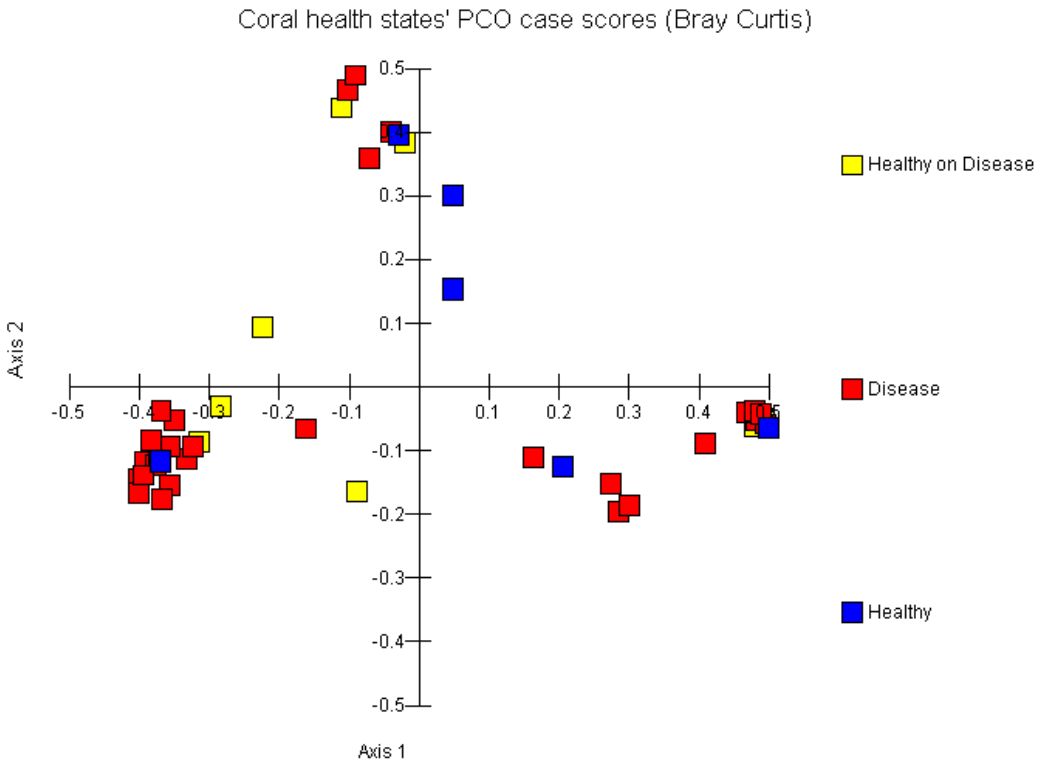

Figure 16. Bray-Curtis ordination of the bacterial communities associated with coral samples of varying health states. Clusters of interest have been encircled.

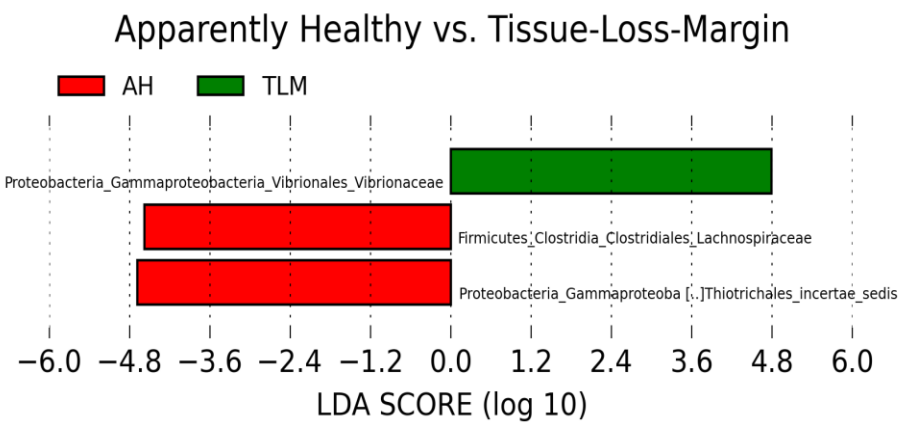

Figure 17. Bacterial families most depleted or enriched in AH and TLM coral samples as identified by LEfSe. Bacterial taxa enriched in TLM are indicated with positive LDA scores (green), and taxa depleted in TLM are indicated with negative scores (red). Only taxa that met the significant LDA threshold of 3.6 are shown (a=0.01).

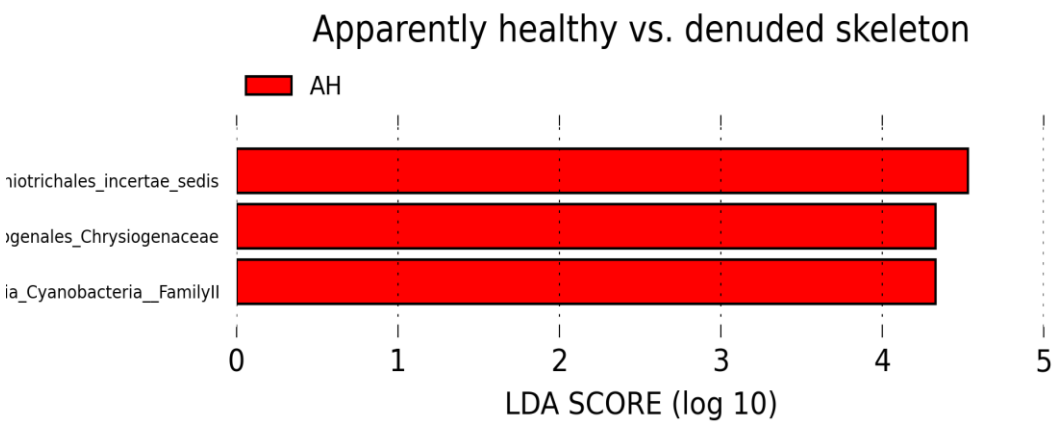

Figure 18. Bacterial families most depleted in AH and DS coral samples as identified by LEfSe. Bacterial taxa enriched in DS are indicated with positive LDA scores (red). Only taxa that met the significant LDA threshold of 3.6 are shown (a=0.01).

this comparison were similar to the significant features identified when comparing AH and TLM communities, but some differences did exist. TLM samples were selected to represent the disease category as these samples represent the site of disease progression. Once again family Vibrionaceae was shown to be enriched in the TLM microbial communities (Figure 19). A second family, Phaselicystidaceae, was also found to be enriched TLM samples when all healthy states were collapsed into one class. While Lachnospriaceae once again one of the most depleted families associated with TLM samples, the unknown family of Thiotrichales previously detected when comparing AH and TLM communities no longer was identified as a distinct feature. Instead, Cyanobacteria Family X was identified as the second most-depleted family associated with TLM samples when compared with the collapsed healthy class.

Key taxa

Vibrios have been associated with coral bacterial bleaching (*Vibrio shiloi* (Kushmaro et al. 2001)) and WBD-II (Ritchie and Smith 1998). The significant presence of Vibrionaceae in microbial communities associated with the coral disease margin in this study confirmed previous culture-based and culture-independent results reported in the coral disease literature. Looking at this family specifically, vibrios from four genera were identified using RDP 10 (Table 12). The majority of sequence reads 63%, n=45,647) belonged to the genus *Vibrio*, while 27% of the sequences could not be identified to the genus level. Vibrios were only detected in large abundances in TLM and DS samples (Figure 20). Although DS samples contained more sequence reads than TLM samples, only the vibrios within the TLM microbiota were found to be statistically significant

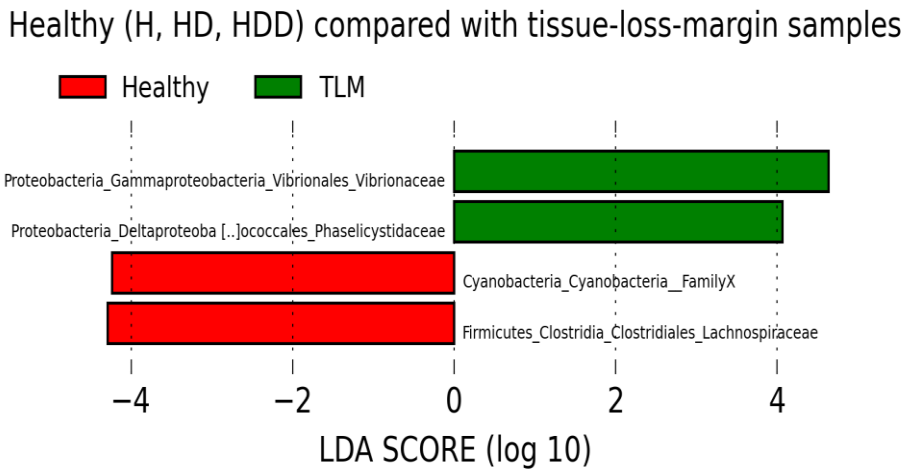

Figure 19. Bacterial families most depleted or enriched in collapsed healthy and diseased coral health states as identified by LEfSe. Bacterial taxa enriched in healthy samples are indicated with positive LDA scores (green), and taxa enriched in diseased samples are indicated with negative scores (red). Only taxa that met the significant LDA threshold of 3.6 are shown (a=0.01).

Table 12. Identified genera of family Vibrionaceae using RDP 10 (Bootstrap P = 0.80, cutoff = 0.01).

Vibrios	**Reads**
Proteobacteria_Gammaproteobacteria_Vibrionales_Vibrionaceae_Enterovibrio	148
Proteobacteria_Gammaproteobacteria_Vibrionales_Vibrionaceae_Listonella	1,636
Proteobacteria_Gammaproteobacteria_Vibrionales_Vibrionaceae_Photobacterium	5,090
Proteobacteria_Gammaproteobacteria_Vibrionales_Vibrionaceae_Vibrio	45,647
Proteobacteria_Gammaproteobacteria_Vibrionales_Vibrionaceae_other	19,497

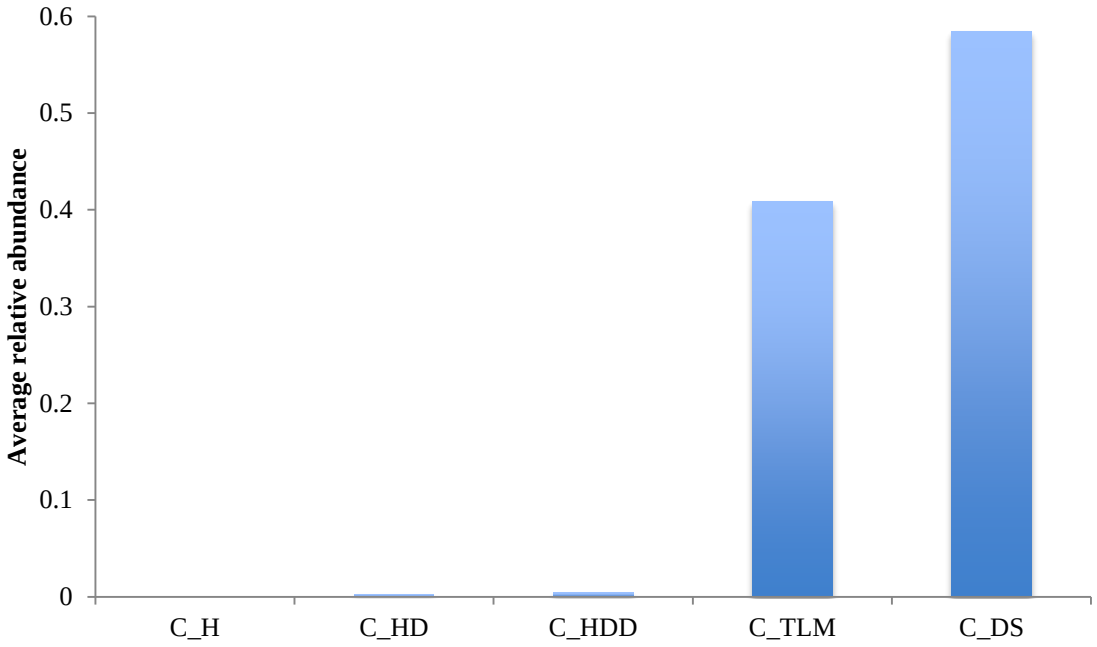

Figure 20. Relative abundance of bacteria from family Vibrionaceae found in each coral sample type (Bootstrap P = 0.80, cutoff = 0.01).

with LEfSe.

Another key bacterial taxon of interest was Rickettsiales. RDP 10 analysis of apparently healthy and diseased *A. cervicornis*, identified bacteria from three families of the order Rickettsiales (Table 13). Bacteria from family Rickettsiaceae were most prevalent in HDD and TLM samples (Figure 21), which confirms the histological observations reported in Chapter 1. Although there was a difference in the abundance of Rickettsiales per sample type, these differences were not significant.

Table 13. Identified genera of family Rickettsiales using RDP 10 (Bootstrap P = 0.80, cutoff = 0.01).

Rickettsia	**Reads**
Proteobacteria_Alphaproteobacteria_Rickettsiales_Anaplasmataceae_other	132
Proteobacteria_Alphaproteobacteria_Rickettsiales_Rickettsiaceae_other	8,302
Proteobacteria_Alphaproteobacteria_Rickettsiales_SAR11_Pelagibacter	79
Proteobacteria_Alphaproteobacteria_Rickettsiales_SAR11_other	130

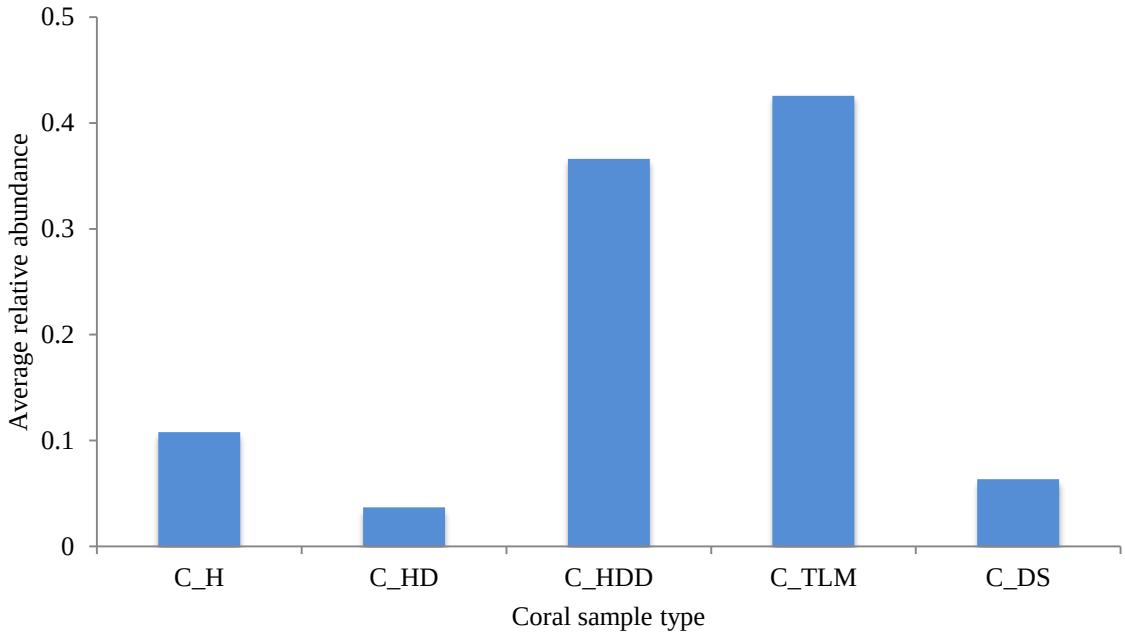

Figure 21. Relative abundance of bacteria from family Rickettsiales found in each coral sample type (Bootstrap P = 0.80, cutoff = 0.01).

Discussion

The microbial communities of tissue-loss diseased Caribbean acroporids are not well studied. Few culture-independent studies have used molecular techniques to examine the bacterial community structure associated with AH and WBD affected acroporids, and RTL has not yet been analyzed molecularly. (Casas et al. 2004) and (Pantos and Bythell 2006) were the most comprehensive studies that had characterized the bacterial community structure associated with WBD using culture-independent techniques, but the results of these studies were contradictory. (Casas et al. 2004) did not find any bacterial species exclusively on WBD-I affected corals and suggested that a non-pathogenic cause of disease existed, whereas (Pantos and Bythell 2006) did find distinct differences between AH and WBD affected *A. palmata* microbial communities.

The present work analyzed the microbial community composition associated with tissue-loss diseases on a comparative basis targeting a single host species, *A. cervicornis.* The composition of bacterial communities between AH and diseased *A. cervicornis* samples was different. Significant changes were observed in bacterial community richness between AH coral fragments and the TLM of diseased fragments specifically, and AH and DS communities. The predominant bacterial phylum found in all coral sample types was Proteobacteria, which is consistent with previous observations based on culture-independent methods on WBD (Pantos and Bythell 2006), as well as culture-based (Rohwer et al. 2001; Cooney et al. 2002; Frias-Lopez et al. 2002; Beleneva et al. 2005; Kvennefors et al. 2010) and culture-independent methods of other white syndromes and coral diseases.

Changes in *A. cervicornis*-associated microbial communities were consistent across sample types when the more inclusive, or higher, taxonomic levels were considered. However, this consistency disappeared at lower taxonomic levels. For example, no dominant γ-proteobacteria were found at the genus-level. *Vibrio* was the most abundant genus found at 2 percent abundance, while the other 46 bacterial genera each accounted for less than 1% of the total abundance. Similar observations have also been found in gut microbiome studies (Spor et al. 2011). This latter study identified numerous unknown genera that were related to known genera but with low bootstrap values. The only consistent taxonomic grouping was at the family level.

Most marine bacteria have not been sequenced further increasing the challenges of this study. While there is the potential for a unique genus or species of bacteria to have a special metabolic pathway that is relevant to tissue-loss diseases, there are no empirical data to support this. Therefore, this study analyzed microbial differences at the class and family level, as organisms from the same family tend to have the same functionality.

Over 35 percent of the samples lost between 40–65 percent of their relative abundance at the genus level using the 1% abundance cut off, meaning rare taxa accounted for a large portion to the majority of these communities. More sequences were retained and there was more consistency across all phylogenetic levels using a 0.1 abundance cut-off; however, these genera were too sparse and the lower coverage presented a statistical issue due to the presence of many zeros within the data. Although two depths of coverage were obtained, the data using the 1 percent cut off was favored because the analysis is more biologically relevant due to the aforementioned reasons.

This study found that AH *A. cervicornis* bacterial communities were dominantly composed of 68% α-proteobacteria, 8% γ-proteobacteria, 6% Cyanobacteria and 5% Actinobacteria. These results were somewhat similar to (Pantos and Bythell 2006) who characterized the bacterial communities associated with AH and WBD-affected *A. palmata*. (Pantos and Bythell 2006) found similar results in the abundance of α-proteobacteria (63%) and Actinobacteria (6%) in AH *A. palmata* bacterial communities using 16S rDNA cloning and sequencing techniques. However, (Pantos and Bythell 2006) found a greater abundance of Firmicutes (14%), δ-proteobacteria (9%), β-proteobacteria (9%) than the current study which only found 5% Firmicutes (total percentage of a combined three classes), 2% δ-proteobacteria, and 1% β-proteobacteria. (Pantos and Bythell 2006) also determined that the AH communities were composed of 5% Actinomycetes, however this study found less than 1% of this bacterial order present in AH *A. cervicornis* associated bacterial communities. The difference in AH acroporid bacterial communities could indicate the presence of species-specific communities found in each acroporid host (Beleneva et al. 2005). Therefore, future studies should analyze both species using the same molecular techniques.

The Cyanobacteria identified by the RDP 10 Bayesian Classifier need to be investigated further at a finer resolution. This analysis identified some of the cyanobacteria OTUs as relatives of family Bacillariophyceae, which are diatoms. However, this analysis was not detecting this eukaryotic organism. Instead, these sequences most likely represent different members of the photobiont, which is also why the diatom-like organisms were identified as Cyanobacteria, when they are not in fact

Eubacteria. Members of the dinoflagellate photobiont were not detected because the primers used in this study did not overlap with the organisms' sequences.

The bacterial communities associated with diseased coral tissue sections used in (Pantos and Bythell 2006) were defined as samples taken from the lesion boundary at the interface between healthy tissue and bare skeleton, and are comparable to the TLM samples used in the present study. This study showed that TLM-associated bacterial compositions were not taxonomically diverse. Approximately 89 percent of the bacterial community found in TLM samples was composed of Proteobacteria comprised of 48.05 and 40.64 percent α- and γ-proteobacteria, respectively. Alphaproteobacteria decreased from 68 percent abundance in AH associated communities to 48 percent in TLM microbial communities, whereas γ-proteobacteria abundance increased from 8 percent to 41 percent, respectively. This increase in γ-proteobacteria was largely driven by a significant increase in bacteria from family Vibrionaceae. Additionally, a decrease in the abundance of Actinobacteria was observed when AH and TLM communities were compared (5 to <1%, respectively). Once again, Firmicutes, Betaproteobacteria and Deltaproteobacteria abundance in this study (2%, 0.07%, and 2%, respectively), were much lower than what was reported in (Pantos and Bythell 2006) (10%, 2.5%, and 7.5%, respectively). Although the relative abundances of each of these classes were different, the same trends were observed in both studies.

Bray-Curtis PCO analysis of the collapsed disease states revealed more than one disease cluster (Figure 16). It is apparent that there were two distinct clusters of diseased samples, however, these clusters may not represent the presence of different diseases.

Almost all of the DS samples clustered together, which is most likely due to the abundance of cyanobacteria from successional overgrowth of the coral skeleton. The difference between the two clusters of the collapsed disease states was most likely driven by the overwhelming presence of TLM samples in cluster B when comparing both ordinations (Figure 15 and Figure 16). Analysis of all coral sample types showed that the majority of the DS samples were found in cluster A, while TLM samples were found within both clusters (Figure 15). The multi-clustering of TLM bacterial communities could be due to differences in the amount of tissue that was present within the normally pigmented section of the disease margin. This differentiation could also be due to differences in the disease progression, where perhaps the disease was more active or microorganisms were more infective in some margins than others. Overall, this PCO suggests that all but the central two coral samples are in some state of decline.

It was interesting to see that the HD samples clustered more closely with the diseased tissues of cluster A (Figure 15) than the HDD samples. This confirmed what was observed with the histological data (Chapter 1) and provides molecular evidence to support the hypothesis that HD coral branches are not in fact healthy. Thus, the HD branches may already be in the process of being infected or dying.

The composition of DS microbial communities are more likely related to the colonization of the skeleton itself, but probably do not represent the actual tissue-loss disease pathogens apart from the remnants of some remaining tissues. The TLM can be most accurately characterized as the site of necrosis or tissue death. The HDD area of the diseased branch is where the infective process or true causal effect most likely exists,

following what is observed histologically. However, the microbial communities associated among the three healthy states (AH, HD, HDD) were not found to be significantly different.

Changes or differences between the microbial communities associated with AH and diseased coral colonies have rarely resulted in the gain or elimination of bacterial orders. Yet, a shift in the relative sequence abundance (dysbiosis) of the γ-proteobacteria, specifically Vibrionaceae, was solely associated with TLM areas of diseased branches. Vibrios have often been associated with marine diseases. *Vibrio harveyi (carchariae)* has been identified as the putative pathogen of WBD-II in *A. cervicornis* (Ritchie and Smith 1998) and *Vibrio coralliilyticus* YB was suggested as the WBD causing agent in *Pocillopora damicornis* (Ben-Haim and Rosenberg 2002). Ritchie (2006) observed an environmental shift from beneficial bacteria to *Vibrio*-dominated *A. palmata* mucus, which was proposed to cause losses in antibiotic protective qualities of the mucus. An increase in vibrios has also been reported using culture-dependent techniques in yellow-band disease (YBD) affecting *Montipora aequituberculata,* and WS-affected *A. hyacinthus* (Kvennefors et al. 2010), but this has not always been the case. (Cárdenas et al. 2012) found that Vibrionales actually decreased in WPD-affected *Diploria strigosa* and *Siderastrea siderea,* which suggests that vibrios may play more of a role in some coral diseases such as WBD or RTL, but may not represent biomarkers for other diseases (WPD).

(Ritchie and Smith 1995) suggested that coral secreted mucus was attractive to microorganisms closely associated with the superficial mucus of hydrobionts, particularly

bacteria from genus *Vibrio*. Family Vibrionaceae was found to be both more abundant as well as biologically consistent within TLM microbial communities. This study provided molecular evidence that the presence of vibrios can be considered a biomarker of tissue-loss diseases affecting *A. cervicornis* colonies, although no causality explanations could be derived from this observation.

Another key taxon of interest was Rickettsiales. There is some debate regarding the association of *Rickettsia* bacterium and WBD-I. Casas et al. (2004) indicated that a marine Rickettsiales-like bacterium, particularly in the SML, was associated with WBD-I (Casas et al. 2004); however, (Kline and Vollmer 2011) argued that *Rickettsia* were not likely involved in causing WBD-I. (Casas et al. 2004) found that both AH and WBD affected acroporid bacterial communities were dominated by a coral-associated Rickettsiales 1 (CAR1) bacterium using cloning and sequencing methods. In the last decade, sequencing databases have become more comprehensive, sequencing technology has become more advanced, and the depth of coverage of the data has increased. The present study used a more advanced sequencing techniques to characterize the microbiota associated with AH and diseased *A. cervicornis* at a much deeper depth of coverage. Few sequences from SAR11, ubiquitous marine bacteria, were found suggesting little contamination from the water column. Bacteria from family Rickettsiaceae were most prevalent in HDD and TLM samples, which confirmed the histological observations reported in Chapter 1. Although there is a difference in the abundance of Rickettsiales per sample type, these differences were not significant.

Little is understood about the etiology, pathogenesis, and transmission dynamics of infection in tissue-loss diseases affecting *A. cervicornis* (Sutherland et al. 2004; Williams and Miller 2005). Additional factors such as environmental conditions and coral immunity need to be examined in order to understand the full etiology and pathogenesis of tissue-loss diseases. Additionally, the role of viruses cannot be excluded in the pathogenicity of these tissue-loss diseases. While it has been confirmed that BBD is associated with a community of bacteria (Cooney et al. 2002), this has not been confirmed for WBD. Distinct differences between the bacterial communities associated with healthy and diseased acroporid tissues has led to the suggestion that bacteria are more than opportunistic invaders (Casas et al. 2004; Pantos and Bythell 2006; Vollmer and Kline 2008). Imbalance resulting from disease is likely due to an alteration in the community-based mechanisms controlling population growth (Beleneva et al. 2005; Cárdenas et al. 2012). Determining which components of the coral holobiont are involved in disease has challenged and limited coral disease studies (Rosenberg et al. 2007a). This work supports the notion that coral tissue-loss diseases are polymicrobial diseases associated with an imbalance or dysbiosis of residential bacterial populations and proposes that the increase in bacteria from family Vibrionaceae as a biomarker of tissue-loss disease-affected *A. cervicornis* colonies. Now that the microbial communities associated with apparently healthy and diseased *A. cervicornis* have been characterized, future studies should compare the microbiota of each tissue-loss disease (WBD-I, WBD-II, and RTL), as there were not enough samples of each disease type for comparison.

CHAPTER 4: MICROBIAL COMMUNITIES ASSOCIATED WITH REEF SEDIMENT DO NOT APPEAR TO BE CORRELATED WITH CORAL DISEASE

Introduction

Increases in human population rates in coastal areas have led to large-scale land development projects since more than 40 percent of the world's population (~2.5 billion people) live within 100 km of the coast (Burke et al. 2011). As a result, coral-reef ecosystems are facing an intensifying array of anthropogenic threats (Harvell et al. 1999; Cesar 2000; Knowlton 2001; Hoegh-Guldberg et al. 2007; Burke et al. 2011). Development of coastal areas directly causes physical damage to coral reefs from dredging, and indirectly degrades the reefs due to increased sedimentation, eutrophication, and turbidity rates (Rogers 1990).

It was last estimated that 32 percent of Caribbean coral reefs are threatened by coastal development (Cesar et al. 2003). The construction of new infrastructure requires large areas of land to be cleared leading to increased rates of terrestrial deforestation, soil erosion, clearing of coastal mangroves, and dredging of sea grass beds (Burke et al. 2011). These activities release large quantities of sediments into coastal waters leading to increased turbidity levels and sedimentation on coral reefs (Cesar et al. 2003; Burke et al. 2011). Both increases in turbidity and sedimentation can create a shading effect reducing

the amount and quality of ambient light that reaches corals' endosymbiotic zooxanthellae. This effect causes zooxanthellae densities and photochemical efficiency to decrease, which prevents the proper functioning of cellular processes, such as photosynthesis and metabolism, and stresses the coral's energy budget (Rogers 1990; Philipp and Fabricius 2003). High levels of sedimentation have also been found to inhibit the heterotrophic feeding efficiency of corals, further compromising a coral's energy intake (Richmond 1993). Sediment stress impacts coral physiology and reproduction by slowing coral growth and affecting colony morphology (Risk 2014). Both increased sedimentation and turbidity levels can inhibit the settling of new larval recruits due to loss of habitat from algal overgrowth trapping sediment (Aronson et al. 2008). Hodgson (1990) showed that only moderate levels of sediment stress were required to prevent coral larval settlement, especially where fine sediment particles were of concern.

Chronic sediment resuspension is also a threat to coral reefs. Coastal runoff and dredging projects for beach nourishment and port construction further exacerbate sediment influx by resuspending benthic sediment particles (Nearing et al. 2005). (Storlazzi et al. 2004) found that a small amount of continually resuspended sediment had the same impact on a reef as an area with high sedimentation rates or an area where a large sediment plume existed. Research has also shown that sediments composed of mostly fine particles are more harmful to reefs because they block light and create localized anoxic zones (Weber et al. 2006).

Corals exhibit species-specific and inter-colony tolerance limits to sediment stress and increased turbidity levels (Vargas-Ángel et al. 2007). Corals are capable of removing

sediment by secreting mucus, moving epidermal cell cilia and tentacles, and distending their polyps with seawater, but some species are better at ridding themselves of sediment than others (Rogers 1990; Philipp and Fabricius 2003). These sediment-clearing mechanisms are energetically costly to an already compromised coral. Therefore, a coral may not be able to get rid of the sediment during periods of chronic or high sedimentation (Peters and Pilson 1985). Colonies with lower stress tolerance thresholds, those that have been previously injured, and those that have experienced or are experiencing disease may be less resistant to the effects of increased sediment loading, resulting in an increased rate of tissue alterations or necrosis (Vargas-Ángel et al. 2007).

The level of impact from sediment stress depends on whether the deteriorating environmental conditions are short-term or chronic, both of which can lead to sublethal and lethal impacts. Coral reefs within close proximity to a point-source of high sedimentation and found within areas with high resuspension rates generally exhibit lower live coral cover (Acevedo et al. 1989). Regardless of proximity or duration, both an increase in sediment stress and turbidity levels greatly tax a coral's energy budget and results in damage or death of the coral from bleaching and necrosis, affecting the overall health of the reef.

Poor environmental conditions metabolically depress a coral's ability to fight infections, which has led to the suggestion of a host/pathogen component associated with sediment stress (Harvell et al. 2002; Ben-Haim et al. 2003; Vargas-Ángel et al. 2007). (Harvell et al. 2007) showed that increases in sedimentation rates associated with weather events and anthropogenic activities were contributors to increased disease prevalence.

Later studies further associated declining coral health to an increase in sediment loading from deforestation (Ryan et al. 2008) and correlated coral disease prevalence with seasonal coastal run off and increased sediment loads (Haapkylä et al. 2011).

Ample circumstantial evidence suggests that sediment stress is a likely an environmental driver of coral disease (Sutherland et al. 2004; Fabricius 2005; Haapkylä et al. 2011), but there is uncertainty as to whether sedimentation simply compromises coral disease resistance to potential pathogens or increases pathogen virulence (Bruno et al. 2003; Harvell et al. 2007). Hodgson (1990) suggested that silt-associated bacteria were the cause of coral-tissue necrosis after finding that treating seawater with antibiotics reduced tissue damage. These findings demonstrated that sedimentation might serve as a mechanism for bacterial pathogen transmission from marine or terrestrial substrates to coral polyps. However, (Kavousi et al. 2013) found that white mat bacterial infections found on Persian Gulf *Porites* spp. were a result of a secondary microbial effect of sediment stress and were not thought to be primary pathogens that attack coral tissues directly. (Pollock et al. 2014) were the first to state that sediment plume exposure was a main driver of coral white syndrome (WS) on the Great Barrier Reef. These researchers found that WS disease prevalence was 2.5-fold higher where sediment plumes were present due to dredging activities.

Although sedimentation effects on coral health have been well-documented both experimentally *ex situ* and *in situ* (Rogers 1983, 1990; Cortés and Risk 1985; Peters and Pilson 1985; Hodgson 1990; Riegl 1995; Riegl and Branch 1995; Philipp and Fabricius 2003; Weber et al. 2006, 2012; Vargas-Ángel et al. 2007; Flores et al. 2012; Risk 2014),

few studies to date have directly linked reef sediment as an environmental driver of coral diseases. Coral Restoration Foundation (CRF) nursery manager, Ken Nedimyer, questioned whether a microorganism in the sediment triggered the uncharacteristic upward progression of WBD disease (pers. comm. 2011). This phenomenon was observed on *A. cervicornis* branches that were touching sediment in both the CRF nursery and outplanted colonies on reefs in the Upper Florida Keys during the summer of 2011 and 2012 (Figure 22).

This study was the first to use Ion Torrent's PGM technology to sequence 16S rDNA amplicons from coral tissue and reef-sediment samples to characterize the composition of these microbial communities. This study directly compared the bacterial communities extracted from samples of apparently healthy and diseased *A. cervicornis* with those associated with adjacent sediment samples in order to test for whether sediment-associated bacterial communities were a source of potential pathogens that might be causing coral tissue-loss diseases.

Methods

Sample information

Fifty-eight coral samples from seven coral reefs across the Upper Florida Keys (see Chapter 1, Table 1 and Figure 1), USA, were collected from a single host species, *A. cervicornis*. Eight apparently healthy (C_AH) samples, eight healthy-on-diseased (C_HD) samples (HD samples were collected from normally pigmented branches of a diseased colony), 11 healthy-on-diseased sections from the diseased branch (C_HDD) samples (HDD samples refer to the normally pigmented section of tissue located on a

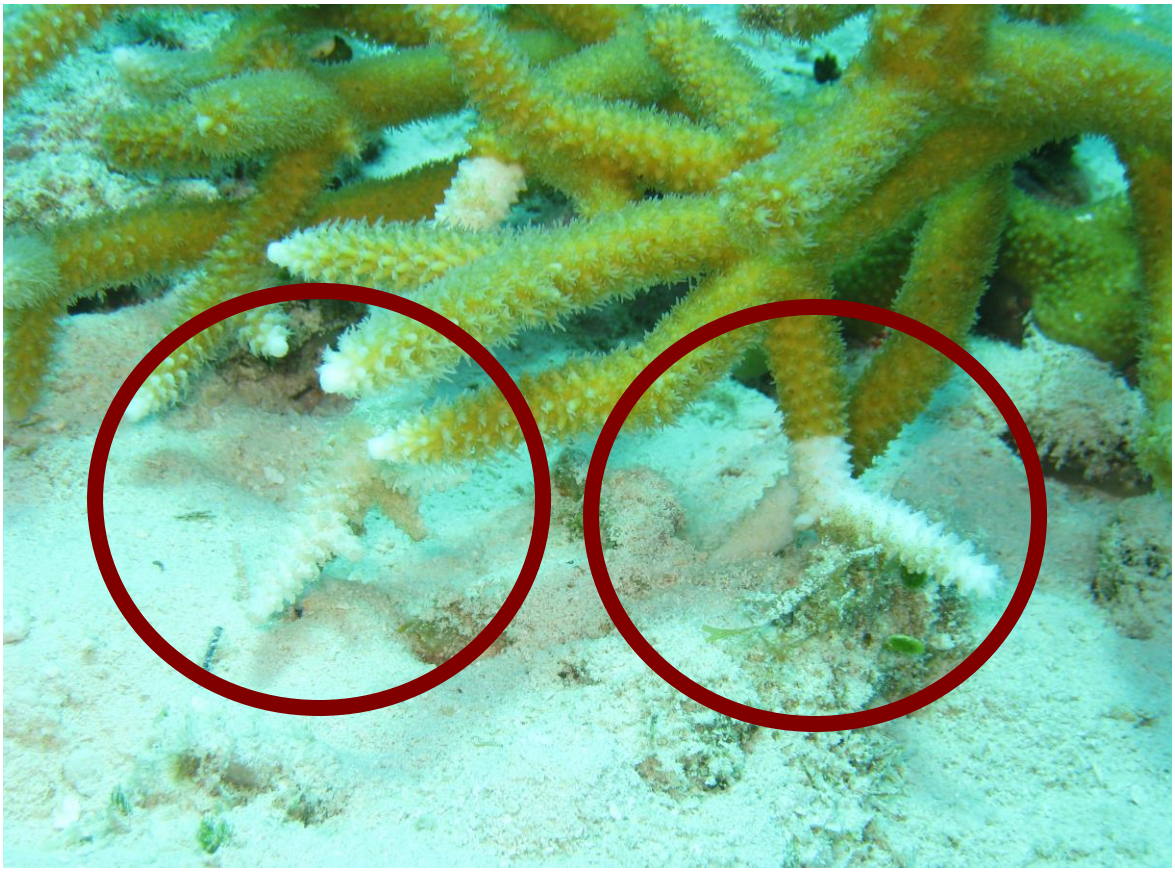

Figure 22. Uncharacteristic disease progression of white-band disease type I in the Upper Florida Keys. Photo courtesy of E. Peters.

coral branch that contains a disease lesion), 16 tissue-loss-margin (C_TLM) samples, and 15 denuded skeleton (C_DS) samples were analyzed using next-generation sequencing (NGS). Additionally, corresponding sediment samples were sampled from either the base of each coral colony or under the specific branch of interest. A total of 32 sediment samples were collected: 13 diseased (S_D) samples were collected from either directly under the area of a coral colony exhibiting signs of disease or from areas where a coral branch exhibiting signs of disease were touching the sediment; 10 healthy-on-diseased (S_HD) sediment samples were collected directly under the normally pigmented branches of a diseased colony; and 9 apparently healthy (S_AH) sediment samples were collected from the base of a coral colony that exhibited no signs of disease (see appendices II and III). Field site descriptions, coral-tissue sample collection, and sample fixation for molecular analysis were discussed in Chapter 1, and all molecular techniques used were described in Chapter 2.

RDP 10 and principal coordinate analysis

De-multiplexed sequences from multitag pyrosequencing (MTPS) and Ion Torrent™ were assigned taxonomic identifications using the RDP 10 Bayesian Classifier (Version 1.2) available on MBAC's Galaxy portal. Taxonomic classifications were examined using a relative abundance cut-off of 1 percent, and with a classification bootstrap confidence of 0.80, and the average relative abundances of the bacteria associated with coral-tissue and reef-sediment samples were examined at all taxonomic levels (phylum to genus).

Principal coordinate analyses (PCOs) were conducted on the RDP 10 data using the MultiVariate Statistical Package (MVSP) (Version 3.1). Bray-Curtis ordination was used to determine whether significant differences were found:

(1) among sediment samples (S_H, S_HD, S_D).

(2) between sample types (coral (C) and sediment (S),

(3) among all sample types (C_H, C_HD, C_HDD, C_TLM, C_DS, S_H, S_HD, S_D),

(4) among collapsed health categories by sample type (C_H, C_HD, C_D, S_H, S_HD, S_D), and

(5) among collapsed health categories (AH, HD, and D) for all samples (combined C and S),

Linear discriminant analysis effective size estimation

Linear Discriminant Analysis (LDA) Effective Size (LEfSe) estimation was used to identify indicator bacterial taxa that were differentially abundant or depleted through pairwise comparisons of (1) sediment sample types, and (2) between coral-tissue and reef-sediment samples.

Results

A total of 1,616,397 sequences were obtained from 90 samples processed using MTPS (n=85,197 sequences) and Ion Torrent™ (n=1,531,200 sequences) sequencing methods. . Sample reads ranged from 122 to 126,570 with an average of 17,960 reads per sample. Thirteen samples had less than 1,500 reads and were dropped from the study, retaining a total of 1,609,791 sequences for this analysis. The sequences for 6 C_AH, five

C_HD, 6 C_HDD, 14 C_TLM, 15 C_DS, 12 S_D, 10 S_HD and 9 S_AH samples were examined for this study (n=77).

De-multiplexed sequences from both MTPS and Ion Torrent™ were entered into the RDP 10 Bayesian Classifier to obtain taxonomic identification. The RDP 10 Classifier provided a hierarchical description and average relative abundances of the coral tissue- and sediment-associated bacteria that spanned from phylum to genus. In total, the bacterial communities associated with all sediment samples from the Upper Florida Key were composed of 11 phyla comprised of 20 classes, 44 orders, 100 families, and 196 genera, when examined using a 1 percent relative abundance cut-off. Twenty-eight bacterial phyla comprised of 54 classes, 99 orders, 213 families, and 406 genera were identified when examined using a 0.1 percent relative abundance cut-off. Microbial communities associated with healthy and diseased coral tissues were characterized in Chapter 3.

Bacterial taxa found in both coral-tissue and sediment communities overlapped the most at the phylum level (82% overlap in taxa) (Table 14) but no sequences were found for phylum Chrysiogenetes and candidate phylum TM7 in sediment samples. The amount of overlapping taxa decreased from 82% at the phylum level to only 23% at the genus level. Similar to the associated coral bacterial communities, bacteria from phylum Proteobacteria were most abundant in the microbiota of the sediment samples (49%) (Figure 23). The community composition for each sediment sample type varied very little, and sediment community diversity was also similar among samples, despite the condition of the coral colony where the sediment sample was collected.

Table 14. Comparison of taxonomic groups found in bacteria associated with coral tissue, reef sediment, and taxonomic units found in both sample types.

	Coral tissue		Reef sediment		Taxa found in both coral tissue and reef sediment	
Taxonomic level	Taxonomic units	Reads	Taxonomic units	Reads	Taxonomic units	Total reads
Phylum	11	795,195	9	780,848	9	1,576,043
Class	19	778,298	14	773,642	13	1,551,940
Order	43	747,484	31	720,737	30	1,468,221
Family	89	698,617	59	609,740	48	1,308,357
Genera	153	586,184	88	348,565	45	934,749

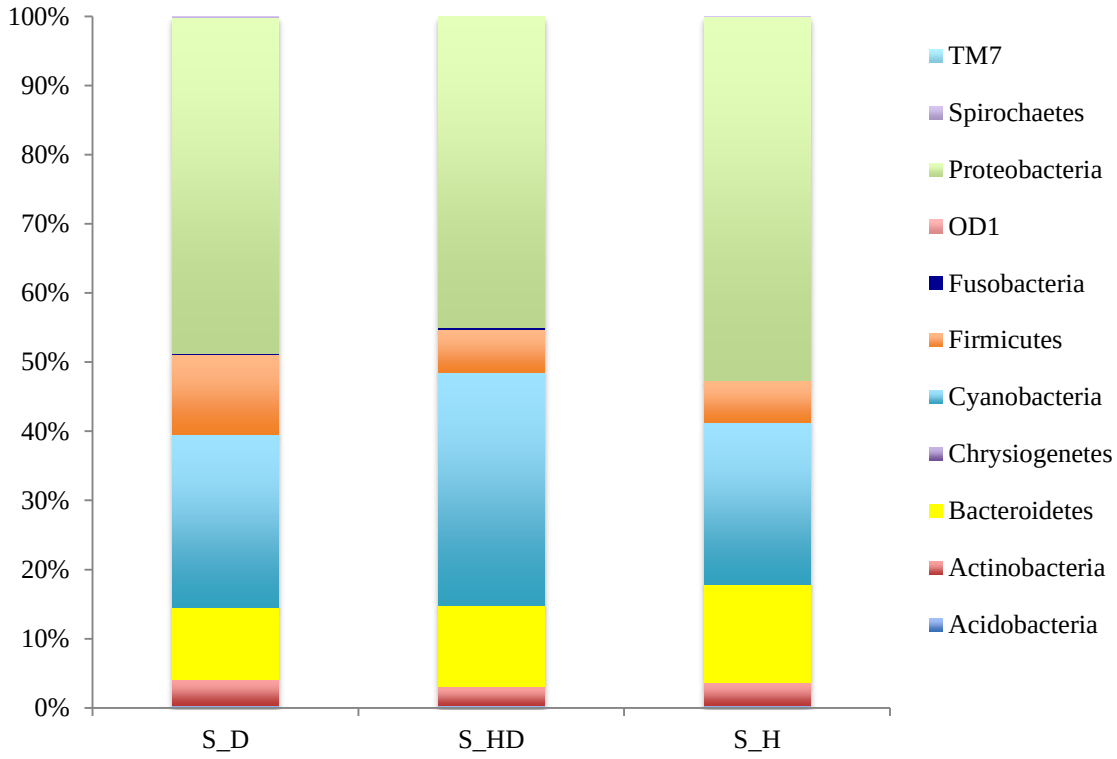

Figure 23. Comparison of the average relative abundance of bacteria within different phyla composing the microbial communities associated with each sediment sample type at the phylum level (Bootstrap P = 0.80, cutoff = 0.01).

Cyanobacteria was the most abundant microbial class found in AH and HD sediment samples (24 and 35%, respectively), whereas α-proteobacteria were the most abundant class in D samples (26%) (Table 15). The presence of Cyanobacteria identified by the RDP 10 Bayesian Classifier once again reflects the detection of members from the photobiont (see Chapter 3's Discussion). The relative abundance of each bacterial class within the community was similar among sample types. Only slight changes in relative abundance were observed for each class among sample types, with the exception of an increase in Cyanobacteria in S_HD samples and an increase in Firmicutes in S_D samples. However, these increases were not significantly different than the abundances in other sample-associated microbial communities.

Analysis of the average relative abundance of sediment-associated bacterial communities using multivariate ordination methods and analysis of similarity revealed no clustering among sediment sample types (Figure 24). Despite this fact, LEfSe analysis of the sediment communities revealed one discriminant feature that was significantly more abundant in S_HD-associated communities than AH-sediment communities (Figure 25). The Sphingobacteria family, Saprospiraceae, was the only differentially enriched family associated with HD samples when compared to AH-sediment communities. No discriminative features were found between S_AH and S_D or S_HD and S_D-associated communities using the default logarithmic (LDA) value of 2.0 (a=0.01).

PCO analysis of coral and sediment samples revealed distinct clustering of the samples by sample type (Figure 26). Sediment samples clustered separately from coral-tissue samples (all sample types included) indicating that the bacterial communities

Table 15. Comparison of the percent abundance (%) of bacterial communities associated with each coral sample type at the class level (Bootstrap P = 0.80, cutoff = 0.01). The five most dominant classes are highlighted for each sample type with the most abundant class in bold.

Phylum	Class	S_H	S_HD	S_D
Acidobacteria	Acidobacteria_Gp22	0.00	0.00	0.08
Actinobacteria	Actinobacteria	3.26	2.62	3.85
Bacteroidetes	Bacteroidia	1.14	1.02	0.92
	Flavobacteria	5.66	4.63	4.12
	Sphingobacteria	7.18	5.60	5.38
Cyanobacteria	Cyanobacteria	**23.94**	**34.91**	24.83
Firmicutes	Clostridia	5.66	6.38	11.01
Fusobacteria	Fusobacteria	0.05	0.36	0.27
OD1	OD1_	0.03	0.00	0.00
Proteobacteria	Alphaproteobacteria	22.28	21.56	**26.12**
	Betaproteobacteria	0.04	0.00	0.00
	Deltaproteobacteria	7.78	5.01	5.82
	Gammaproteobacteria	22.97	17.93	17.41
Spirochaetes	Spirochaetes	0.00	0.00	0.18
	Total reads:	**265,508**	**245,196**	**262,938**

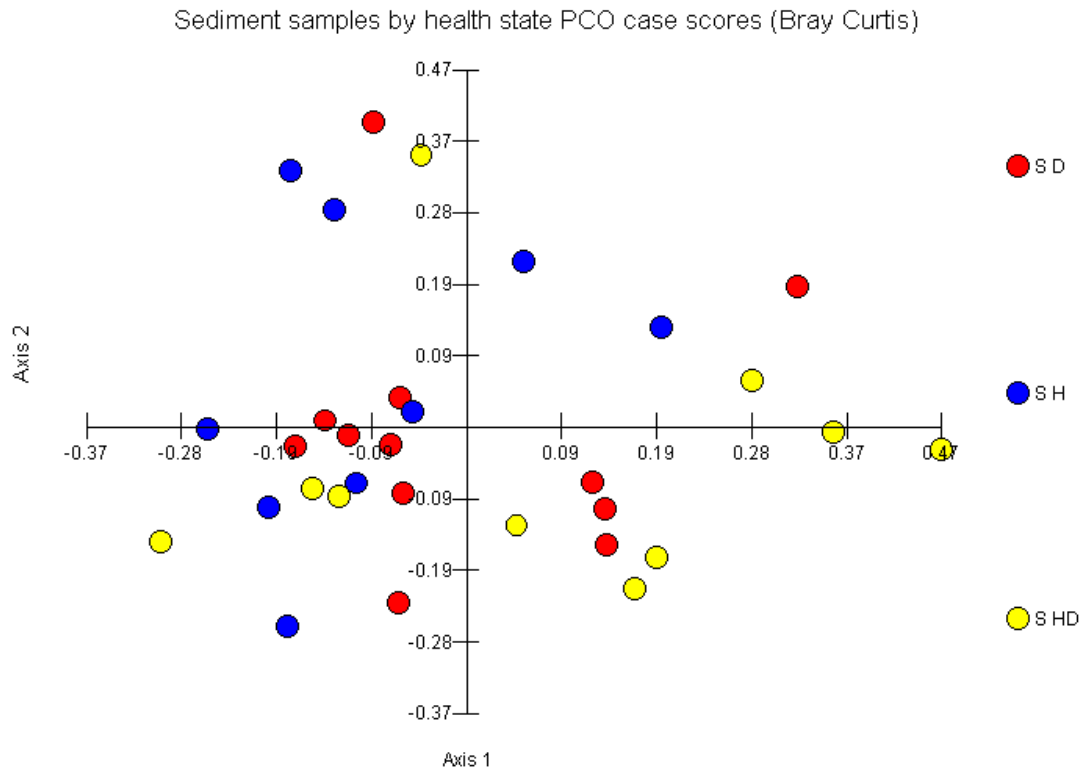

Figure 24. Bray-Curtis ordination of the bacterial communities associated with sediment samples collected from corresponding apparently healthy, healthy-on-diseased, and diseased-coral colonies.

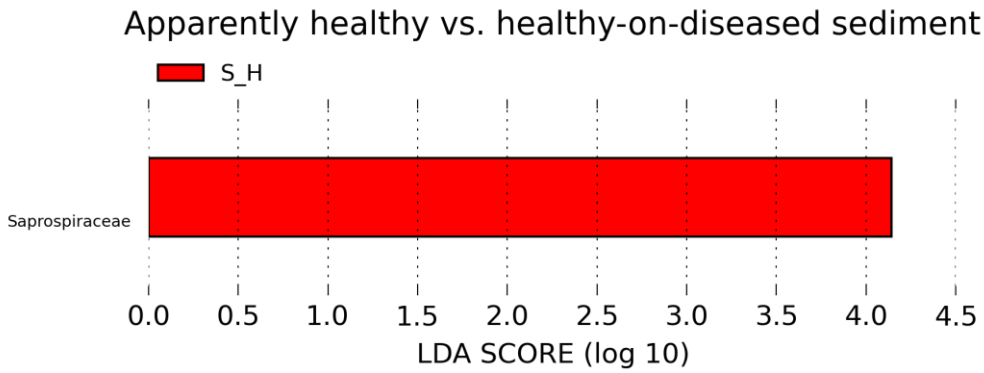

Figure 25. Bacteria families most depleted in S_AH and S_HD sediment samples as identified by LEfSe. The bacterial family that enriched HD communities is indicated with a positive LDA score (red). Only one family met the significant LDA threshold of 3.6 (a=0.01).

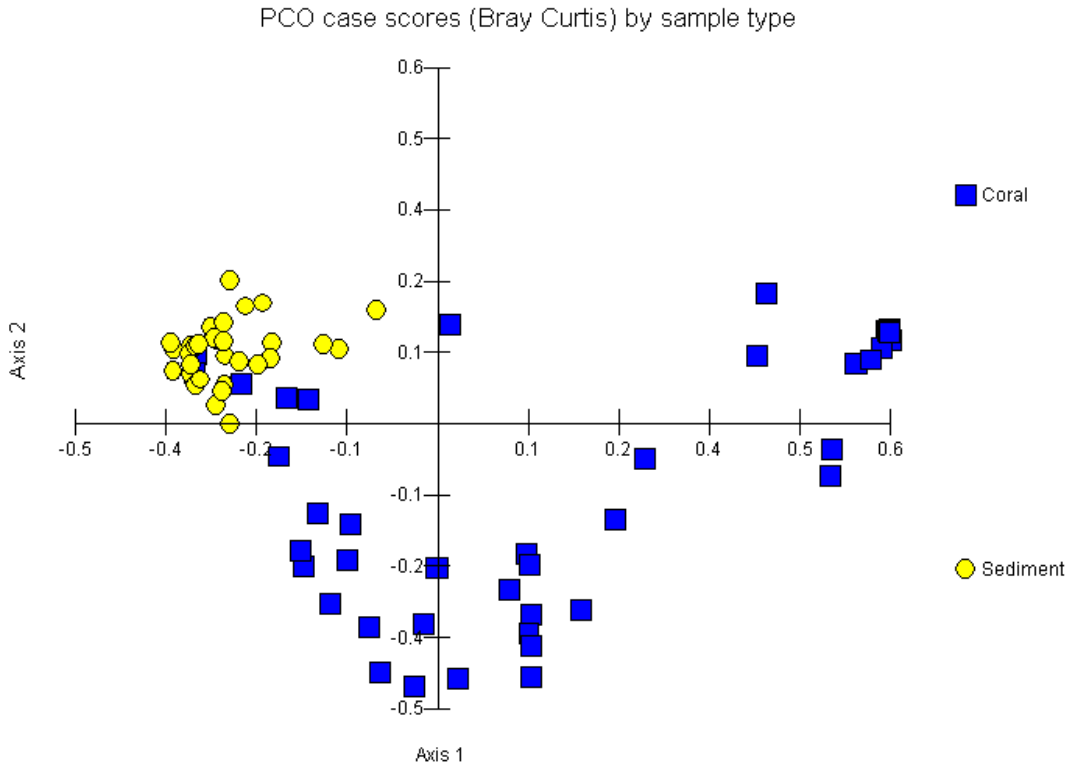

Figure 26. Bray-Curtis ordination of the bacterial communities associated with all sediment and all coral sample types.

associated with coral tissue and sediment were different. The microbial communities of C_DS were most similar to the communities associated with the sediment samples (Figure 27). Actinobacteria were more consistently abundant in all sediment sample types, whereas these bacteria were only observed in AH coral-associated communities. Sediment samples contained a higher abundance of Bacteroidetes, particularly Flavobacteria and Sphingobacteria, than all coral sample types except C_DS. Overall, Cyanobacteria and Firmicutes (Clostridia) were more abundant in sediment microbial communities than found in the coral microbiota. Although Proteobacteria were still the most abundant phylum of bacteria found within the sediment microbiota, these bacteria were found in lower abundances overall compared to coral samples. More specifically, there were less α- and γ-proteobacteria present in sediment microbial communities, and an increase in δ-proteobacteria was observed.

LEfSe analysis detected 37 discriminant features between coral and sediment microbial communities. Thirty-two bacterial families differentially enriched sediment samples, and five bacterial families were found to enrich coral-associated bacterial communities (Propionibacteriaceae, Rickettsiaceae, Colwelliaceae, Oceanospirillaceae, and Enterobacteriaceae) (Figure 28). One Actinobacteria family (Acidimicrobiaceae), five Bacteroidetes (Flammeovirgaceae, Flavobacteriaceae, Cryomorphaceae, Saprospiraceae, and Rikenellaceae), three Firmicutes (Clostridiaceae, Peptococcaceae, and Lachnospiraceae), one Fusobacteria (Fusobacteriaceae), eight Cyanobacteria families (Chloroplast, Family I, Family II, Family III, Family IV, Family VIII, Family X, and Family XIII), four α-proteobacteria (Rhodobacteraceae, Hyphomonadaceae,

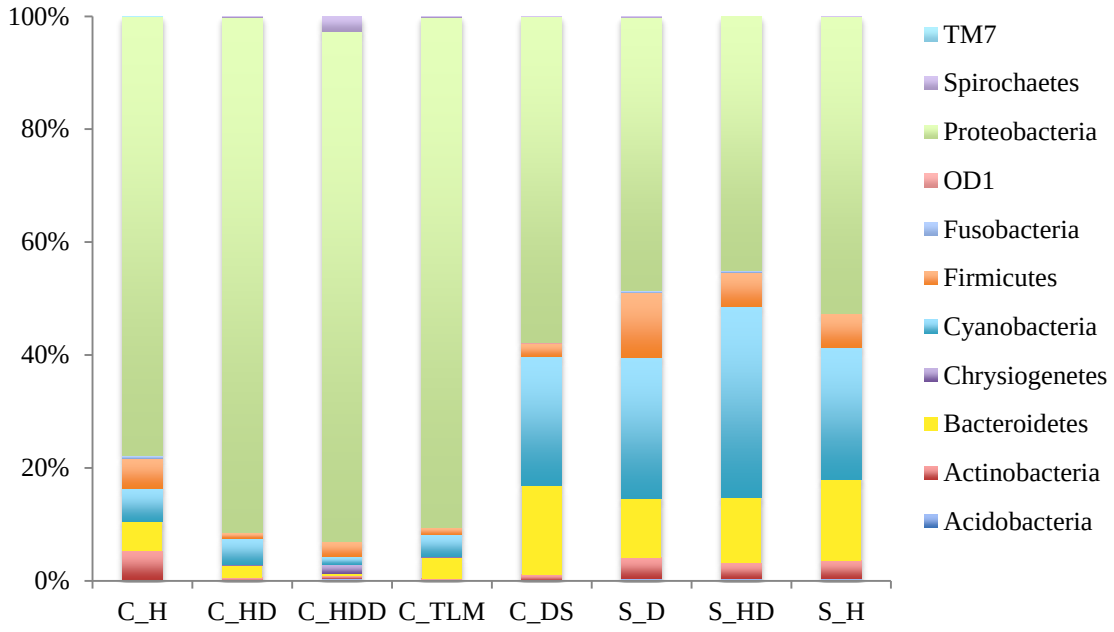

Figure 27. Comparison of the average relative abundance of bacterial communities associated with all coral and all sediment sample types at the phylum level (Bootstrap P = 0.80, cutoff = 0.01).

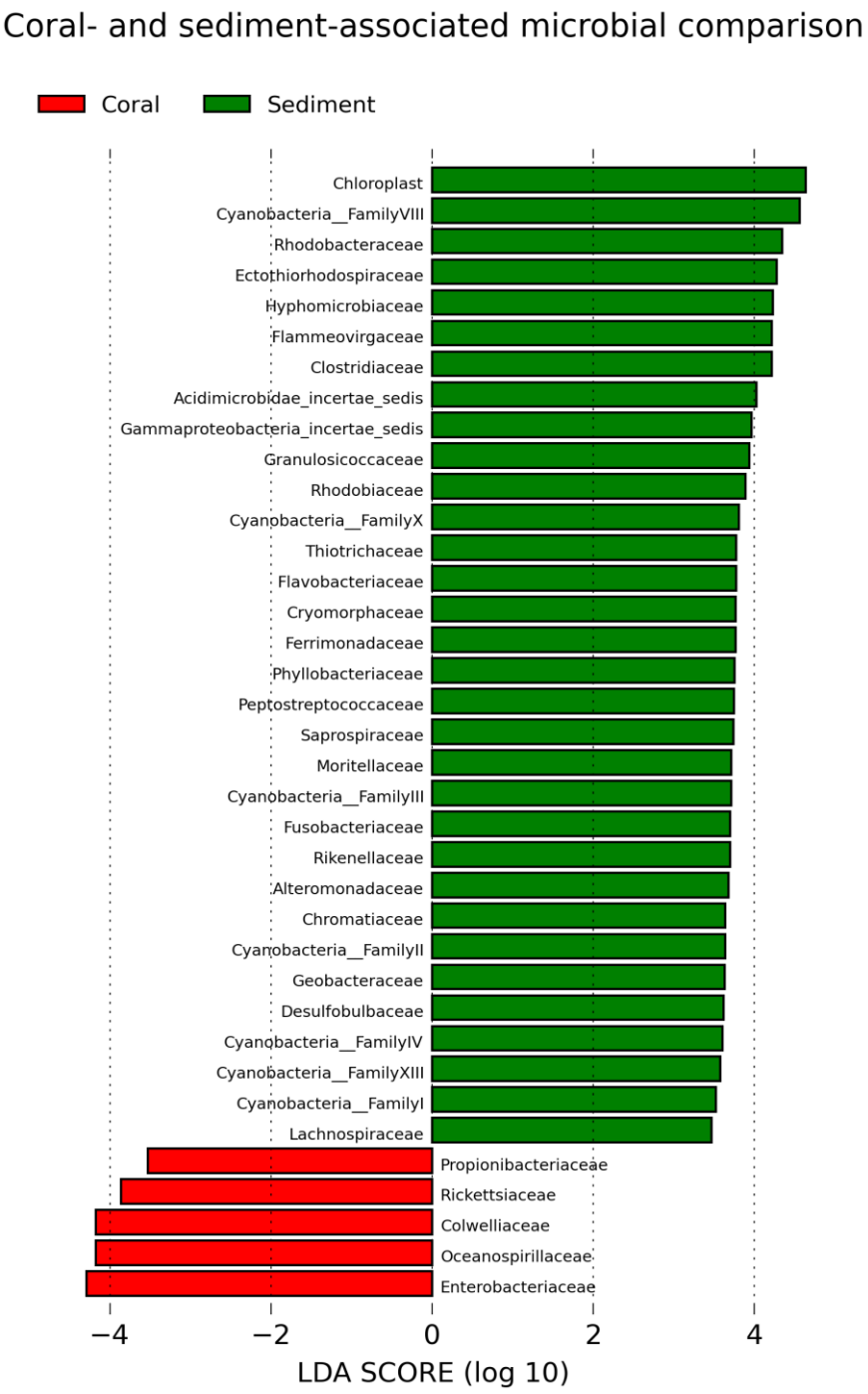

Figure 28. Bacterial families most depleted in coral and sediment samples as identified by LEfSe. The bacterial families that enriched sediment communities are indicated with a positive LDA score (green), and taxa depleted in sediment are indicated with negative scores (red). Only taxa that met the significant LDA threshold of 3.6 are shown (a=0.01).

Rhodobiaceae, and Phyllobacteriaceae), two δ-proteobacteria (Geobacteraceae and Desulfobulbaceae), and eight γ-proteobacteria (Ectothiorhodospiraceae, Granulosicoccaceae, Thiotrichaceae, Ferrimonadaceae, Moritellaceae, Alteromonadaceae, Chromatiaceae, and one family Incertae_sedis) were significantly more abundant in sediment microbial communities than coral communities. The LEfSe results showed that sediment-associated microbial communities were significantly more diverse than the coral microbiota.

A PCO analysis of sediment samples and collapsed coral health categories, where the coral healthy-on-diseased class includes both C_HD and C_HDD samples and the coral diseased category contains both C_TLM and C_DS samples, showed that sediment samples once again clustered separately from the coral samples (Figure 29). Healthy-on-diseased coral samples clustered closest to the sediment samples, and the coral-diseased samples appeared to form two clusters similar to what was found in Chapter 3 (Figure 16). On examining all coral and sediment types, the sediment samples still clustered together regardless of sample type and it appeared that the C_TLM samples were again driving the two separate clusters of diseased samples (Figure 30).

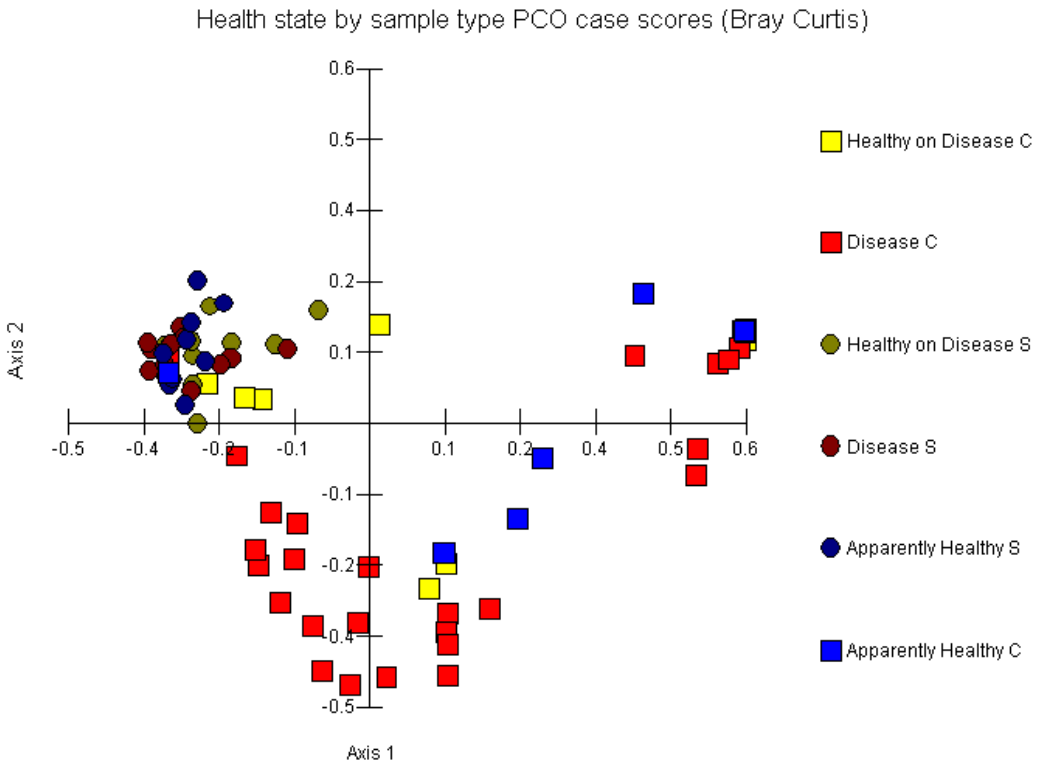

Figure 29. Bray-Curtis ordination of the bacterial communities associated with sediment and coral samples of varying health states.

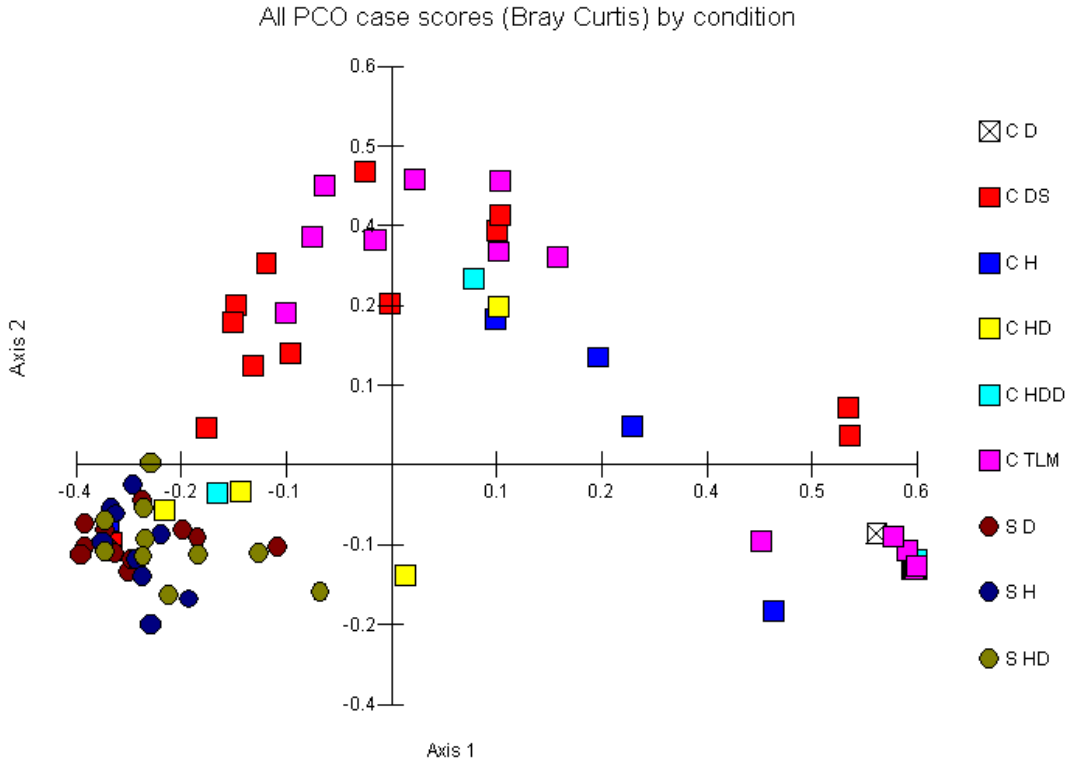

Figure 30. Bray-Curtis ordination of the bacterial communities associated with all sediment and coral sample types.

Discussion

Little is understood about the etiology, pathogenesis, and transmission dynamics of infection in tissue-loss diseases (Sutherland et al. 2004; Williams and Miller 2005). Additional factors, such as environmental conditions, need to be examined to understand the full etiology and pathogenesis of tissue-loss diseases. There has been much speculation that anthropogenic stressors such as sedimentation are directly associated with coral diseases (Aronson and Precht 2001b; Precht et al. 2002; Gardner et al. 2003), and only recently has sediment plume exposure been defined as a main driver of coral disease ((Pollock et al. 2014). Most of the coral disease literature refers to abiotic factors as drivers of coral disease or environmental stressors that exacerbate coral disease. However, these abiotic factors are not being identified as pathogens despite the fact that they could play a role in causing disease. This study was the first study to look at reef sediment as a potential pathogen of coral disease, as gross observations of coral branches touching the sediment have shown the uncharacteristic upward progression of WBD-I.

No differences in microbial communities associated with reef-sediment samples were observed, regardless of the condition of the coral colony from which the sediment was collected. The microbial communities associated with coral DS were most similar to sediment bacterial assemblages. Almost all of the DS samples clustered together, which is most likely due to the abundance of cyanobacteria from successional overgrowth of the skeleton. LEfSe analysis showed that bacteria from family Saprospiraceae enriched healthy-on-diseased sediment samples. Family Saprospiraceae is comprised of three common environmental bacteria genera. Since less than one percent of Saprospiraceae were found in the coral tissue-loss margin, it is likely that healthy-on-diseased sediment

samples simply had a higher abundance of these bacteria and were not correlated with coral disease.

PCO analysis revealed that the sediment microbiota was distinct from coral samples. LEfSe analysis showed that sediment-associated bacterial communities were significantly more diverse, as they were enriched with 32 bacterial families, whereas only five families enriched the coral microbiota compared to the sediment microbiota. Bacteria from orders Vibrionales and Rickettsiales have previously been associated with coral diseases. Vibrionales were detected in both coral- and sediment-associated bacterial communities, but were not shown to be statistically more abundant in one sample type. Rickettsiales bacteria are obligate intracellular parasites, and were not detected in the reef sediment. Therefore, it was expected that LEfSe analysis would show that Rickettsiales bacteria enriched coral microbial communities,

In this case, PCO analysis showed that healthy-on-diseased coral samples clustered closest to the sediment samples. This most likely represents the presence of more ubiquitous taxa associated with HD coral samples and may indicate that disease-causing bacteria are not included in these communities, since diseased samples were found at a greater spatial distance from the sediment samples in the analysis. The diseased coral samples appear to be clustering together, with the possibility of two clusters of diseased samples. The difference between the two clusters of the diseased samples is most likely driven by the overwhelming presence of TLM samples in one of the clusters as was observed in Chapter 3. This separation of TLM samples could once

again represent a difference between active and dormant disease and/or differences in the timing of the disease progression.

Unfortunately, no correlations between reef sediment and coral tissue loss could be observed using PCO analyses. The manifestation of declining coral health due to increased stress exacerbated by sediment may more accurately describe what the data are reflecting. Future analysis of the sediment microbiota at a finer scale may reveal the presence of a specific pathogen(s) found living within the sediment, but it should emphasized that both small and moderate increases in multiple stressors, such as sediment stress, could serve as abiotic pathogens of disease. Conservative approaches should be taken in coral reef restoration efforts worldwide. Until reef sediment can be examined at a finer scale to rule out pathogenic agents, restoration practices should implement the utmost care when handling coral fragments, and contact with sediment should be minimized.

CHAPTER 5: PHYLOGENETIC ANLAYSIS OF BACTERIAL COMMUNITIES ASSOCIATED WITH APPARENTLY HEALTHY AND DISEASE-AFFECTED *ACROPORA CERVICORNIS* CONFIRMS TAXONOMIC COMPARISONS

Introduction

Corals harbor an important endosymbiotic holobiont comprised of a diverse array of microorganisms (Knowlton and Rohwer 2003; Ritchie and Smith 2004; Reshef et al. 2006; Rosenberg et al. 2007b). These microbial associates have been shown to aid in nutrient and carbon cycling (Williams et al. 1987; Shashar et al. 1994; Ritchie and Smith 1995; Lesser et al. 2004) and enhance coral defense through antibiotic and antimicrobial properties (Koh 1997; Castillo et al. 2001; Ritchie and Smith 2004; Geffen and Rosenberg 2005; Kelman et al. 2006; Ritchie 2006; Nissimov et al. 2009; Kvennefors et al. 2010). Conversely, bacterial infections have been suggested as causative agents in many coral diseases worldwide (Richardson 1998; Harvell et al. 1999; Green and Bruckner 2000; Hughes et al. 2003; Pandolfi et al. 2003; Rosenberg and Loya 2004; Sutherland et al. 2004; Weil 2004; Williams and Miller 2005; Vollmer and Kline 2008).

The coral holobiont has been studied intensively with regards to coral disease (Rosenberg et al. 2007b; Vega Thurber et al. 2009), as these diseases are attributed to being one of the greatest causes for reef decline globally (Harvell et al. 2007; Hoegh-

Guldberg et al. 2007). Coral-disease investigations have predominately focused on identifying a causative pathogen typically through the identification of potential pathogenic bacteria using culture-dependent and/or culture-independent techniques with varying results (Ritchie and Smith 1997; Rohwer et al. 2001, 2002; Pantos et al. 2003; Bourne and Munn 2005; Pantos and Bythell 2006; Ritchie 2006; Lampert et al. 2008; Daniels et al. 2011). Culture-based methods underestimate the true diversity of bacteria and are biased towards a very small percentage (less than 1%) of microbial associates that readily grow on culture media (Amann et al. 1995; Suzuki et al. 1997; Rohwer et al. 2001). Culture-independent techniques overcome these limitations but previously only the complexity and diversity of the most dominant taxa found in microbial communities were described (Sunagawa et al. 2009, 2010).

The development of high-throughput sequencing methodologies has allowed for the detection of diverse rare taxa, providing novel insights about the underestimated polymicrobial communities associated with coral tissues (Sogin et al. 2006; Sunagawa et al. 2010). Next-generation sequencing (NGS) technologies have led to better sample diversity representation (Lim et al. 2014) and have increased our understanding of microbial diversity, population structure, functional potential, and geographic distribution considerably (Pedrós-Alió 2006; Sogin et al. 2006). This study used multitag pyrosequencing (MTPS) and Ion Torrent™ NGS to study bacterial communities associated with coral diseases, and conducted a phylogenetic analysis using the quantitative insights into microbial ecology (Qiime) open-source bioinformatics pipeline to examine the whole microbial community overall at a finer resolution. Using Qiime,

this study (1) characterized and compared the bacterial communities associated with apparently healthy *A. cervicornis*, diseased *A. cervicornis*, and the adjacent reef sediment, (2) examined Rickettsiales and Vibrionales abundance (3) compared the results of the phylogenetic analysis with the results of the taxonomic analysis reported in Chapter 3.

Methods

Sample information

Fifty-eight coral samples from seven coral reefs across the Upper Florida Keys, USA (see Chapter 1, Table 1 and Figure 1), were collected from a single host species, *A. cervicornis*. Eight apparently healthy (C_AH) samples, 8 healthy-on-diseased (C_HD) samples (HD samples were collected from normally pigmented branches of a diseased colony), 11 healthy-on-diseased section of the diseased branch (C_HDD) samples (HDD samples refer to the normally pigmented section of tissue located on a coral branch that contains a disease lesion), 16 tissue-loss-margin (C_TLM) samples, and 15 denuded skeleton (C_DS) samples were analyzed using NGS. Additionally, corresponding sediment samples were sampled at each coral colony. A total of 32 sediment samples were collected: 13 diseased (S_D) samples were collected from either directly under the area of a coral colony exhibiting signs of disease or from areas where a coral branch exhibiting signs of disease was touching the sediment; 10 healthy-on-diseased (S_HD) sediment samples were collected directly under the normally pigmented branches of a diseased colony; and 9 apparently healthy (S_AH) sediment samples were collected from the base of a coral colony that exhibited no signs of disease. Field site descriptions, coral-

tissue sample collection, and sample fixation for molecular analysis were discussed in Chapter 1 and all molecular techniques used were described in Chapter 2.

Quantitative insights into microbial ecology

Sequence data were examined using Qiime and the unique fraction metric (UniFrac). Qiime is an open-source software pipeline that is designed specifically for comparing and analyzing microbial communities from raw high-throughput sequencing data (Caporaso et al. 2010b). Qiime clustered reads into operational taxonomic units (OTUs), which were identified using a 16S rRNA gene database, Greengenes (http://greengenes.lbl.gov) (DeSantis et al. 2006) as a reference database and the OTU sequences were aligned to create a phylogenetic tree. Qiime uses the UCLUST consensus taxonomy assigner to taxonomically identify the representative sequence of a cluster (OTU) of similar sequences identified using a similarity threshold of 0.97 (Edgar 2010). Representative sequences were aligned in Qiime using the python nearest alignment space termination tool (PyNAST) (Caporaso et al. 2010a). PyNAST is a reimplementation of the nearest alignment space termination (NAST) sequence alignment algorithm. The NAST algorithm aligns a candidate sequence to the most similar sequence in a template alignment, resulting in multiple sequence alignments (MSAs) (Caporaso et al. 2010a). Sequence alignments were filtered using a 16S alignment Lane mask to remove columns containing mostly gaps from locations known to be excessively variable (Lane 1991). The resulting filtered alignments were then used to build a phylogenetic tree, which serves as the basis for UniFrac diversity measurements.

Unique fraction metric

UniFrac quantifies community similarity based on phylogenetic relatedness by measuring the phylogenetic distances between sets of taxa. UniFrac measures the fraction of the branch length of the tree that leads to descendants from either one environment or the other (Lozupone and Knight 2005). Alpha and beta diversities of the bacterial communities were analyzed in Qiime using the UniFrac to describe the diversity both within a sample (alpha diversity) and between samples (beta diversity). Chao1 alpha diversity metrics were calculated to describe the richness of taxa in a single sample. Rarefaction curves were then produced to depict the number of OTUs identified as a function of the number of reference sequences.

In this study, UniFrac was used to test for significant differences between microbial communities of all coral-tissue health states and reef-sediment sample types. UniFrac metric determined if two communities were different if the fraction of the tree length unique to one health state was greater than expected by chance using Monte Carlo simulations and randomizations (Lozupone and Knight 2005). Principal coordinate analysis (PCO) visualized distance matrices generated by UniFrac in three-dimensions using Emperor. Unweighted and weighted (weighted by sample abundance) Beta diversities (between-sample diversity) were also based on the UniFrac metric.

Results

A total of 1,616,397 sequences were obtained from 90 samples processed using MTPS (n=85,197 sequences) and Ion Torrent™ (n=1,531,200 sequences) sequencing methods. Sample reads ranged from 122 to 126,570, with an average of 17,960 reads per sample. Thirteen samples had less than 1,500 reads and were dropped from the study,

retaining a total of 1,609,791 sequences for this analysis. The sequences for 6 C_AH, five C_HD, 6 C_HDD, 14 C_TLM, 15 C_DS, 12 S_D, 10 S_HD and 9 S_AH samples were examined for this study (n=77).

We obtained 114,488 OTUs with Qiime using a 97 percent similarity threshold, but approximately 41 percent of the OTUs (n=48,000) were unknowns. The Qiime taxonomic identification of the sequence data revealed that bacterial communities associated with coral fragments collected from the Upper Florida Keys were composed of 50 phyla comprised of 151 classes, 300 orders, 524 families, and 947 genera (Table 16). All bacterial OTUs resulting from the Qiime and RDP 10 analyses with abundances greater than one percent were compared at the genus-level, as this level contains the most diversity. It is not surprising that the two RDP 10 analyses were the most similar (Table 17). The Qiime and RDP 10 (0.001 cut-off) results were the next most similar, sharing unidentified genera from families Flavobacteriaceae, Hyphomicrobiaceae, Rhodobacteraceae, and Enterobacteriaceae. Only genus *Vibrio* was identified consistently across all three analyses, although more overlap among analyses was found at the family level.

Similar to RDP 10, Qiime analysis also found Proteobacteria to be the dominant phylum found in all sample types (44%) (Figure 31). Specifically, α-proteobacteria was the most abundant bacterial class associated with all coral samples and S_HD and S_D samples (17%, 62%, 39%, 25%, 37%, 39%, and 41%, respectively), whereas γ-proteobacteria was the most abundant class in S_H communities (29%) (Table 18). The microbial composition of each sample type for known bacterial classes determined by

Table 16. Comparison of the number of OTUs identified at each taxonomic level using different analyses.

Taxonomic assignment method	Phylum	Class	Order	Family	Genus
RDP (1% abundance cut-off)	11	19	43	89	153
RDP (0.1% abundance cut-off)	24	42	86	192	352
UCLUST consensus taxonomy assigner	50	151	300	524	947

Table 17. All OTUs identified at the genus level that accounted for more than one percent of the total relative abundance using both RDP and Qiime analyses are shown. Red represents OTUs that were found in all three analyses; blue represents OTUs that were found in both RDP 10 analyses, and orange represents OTUs that were found in the RDP 10 (0.1 cut-off) and Qiime analyses.

TAXON	RELATIVE ABUNDANCE
RDP 10 (1 percent abundance cut-off)	
Proteobacteria_Gammaproteobacteria_Alteromonadales_Colwelliaceae_Thalassomonas	1.10%
Proteobacteria_Gammaproteobacteria_Chromatiales_Ectothiorhodospiraceae_unknown_Ectothiorhodosinus	1.23%
Proteobacteria_Alphaproteobacteria_Rhizobiales_Methylobacteriaceae_Methylobacterium	1.33%
Cyanobacteria_Cyanobacteria__Family VIII_GpVIII	1.81%
Cyanobacteria_Cyanobacteria__Family VIII_unknown_GpVIII	1.86%
Proteobacteria_Gammaproteobacteria_Vibrionales_Vibrionaceae_Vibrio	2.28%
Cyanobacteria_Cyanobacteria__Chloroplast_Bacillariophyta	7.51%
Proteobacteria_Alphaproteobacteria_Rhodospirillales_Rhodospirillaceae_unknown_Oceanibaculum	17.31%
RDP 10 (0.1 percent abundance cut-off)	
Proteobacteria_Gammaproteobacteria_Alteromonadales_Colwelliaceae_Thalassomonas	1.20%
Cyanobacteria_Cyanobacteria__Chloroplast_other	1.25%
Firmicutes_Clostridia_Clostridiales_Clostridiaceae_other	1.27%
Proteobacteria_Alphaproteobacteria_Rhizobiales_Methylobacteriaceae_Methylobacterium	1.34%
Proteobacteria_Alphaproteobacteria_Rhizobiales_Hyphomicrobiaceae_other	1.35%
Bacteroidetes_Sphingobacteria_Sphingobacteriales_Flammeovirgaceae_other	1.55%
Proteobacteria_Gammaproteobacteria_Enterobacteriales_Enterobacteriaceae_other	1.66%
Proteobacteria_Gammaproteobacteria_Chromatiales_Ectothiorhodospiraceae_other	1.86%
Cyanobacteria_Cyanobacteria__Family VIII_GpVIII	1.88%
Cyanobacteria_Cyanobacteria__Family VIII_other	1.94%
Proteobacteria_Gammaproteobacteria_Oceanospirillales_Oceanospirillaceae_other	2.07%
Proteobacteria_Gammaproteobacteria_Vibrionales_Vibrionaceae_Vibrio	2.44%
Bacteroidetes_Flavobacteria_Flavobacteriales_Flavobacteriaceae_other	2.48%
Proteobacteria_Gammaproteobacteria_Alteromonadales_Alteromonadaceae_other	2.93%
Proteobacteria_Alphaproteobacteria_Rhodobacterales_Rhodobacteraceae_other	7.47%
Cyanobacteria_Cyanobacteria__Chloroplast_Bacillariophyta	7.56%
Proteobacteria_Alphaproteobacteria_Rhodospirillales_Rhodospirillaceae_other	18.77%
Qiime (UCLUST consensus taxonomy assigner)	
k__Bacteria;p__Proteobacteria;c__Alphaproteobacteria;o__;f__;g__	1.02%
k__Bacteria;p__Proteobacteria;c__Gammaproteobacteria;o__;f__;g__	1.06%
k__Bacteria;p__Proteobacteria;c__Gammaproteobacteria;o__Alteromonadales;f__OM60;g__	1.10%
k__Bacteria;p__Spirochaetes;c__Spirochaetes;o__Spirochaetales;f__Spirochaetaceae;g__Spirochaeta	1.13%
k__Bacteria;p__Proteobacteria;c__Gammaproteobacteria;o__Alteromonadales;f__Colwelliaceae;Other	1.47%

k__Bacteria;p__Bacteroidetes;c__Flavobacteriia;o__Flavobacteriales;f__Flavobacteriaceae;g__	1.54%
k__Bacteria;p__Proteobacteria;c__Alphaproteobacteria;o__Rhizobiales;f__Hyphomicrobiaceae;g__	1.84%
k__Bacteria;p__Proteobacteria;c__Gammaproteobacteria;o__Thiotrichales;f__Piscirickettsiaceae;g__	1.99%
k__Bacteria;p__Proteobacteria;c__Gammaproteobacteria;o__Vibrionales;f__Vibrionaceae;g__Vibrio	2.35%
k__Bacteria;p__Proteobacteria;c__Gammaproteobacteria;o__Enterobacteriales;f__Enterobacteriaceae;g__	2.41%
k__Bacteria;p__Cyanobacteria;c__Oscillatoriophycideae;o__Chroococcales;f__Xenococcaceae;g__	3.54%
k__Bacteria;p__Proteobacteria;c__Alphaproteobacteria;o__Rhodobacterales;f__Rhodobacteraceae;g__	6.48%
k__Bacteria;p__Cyanobacteria;c__Chloroplast;o__Stramenopiles;f__;g__	7.82%
k__Bacteria;p__Proteobacteria;c__Alphaproteobacteria;o__Rickettsiales;f__;g__	18.13%

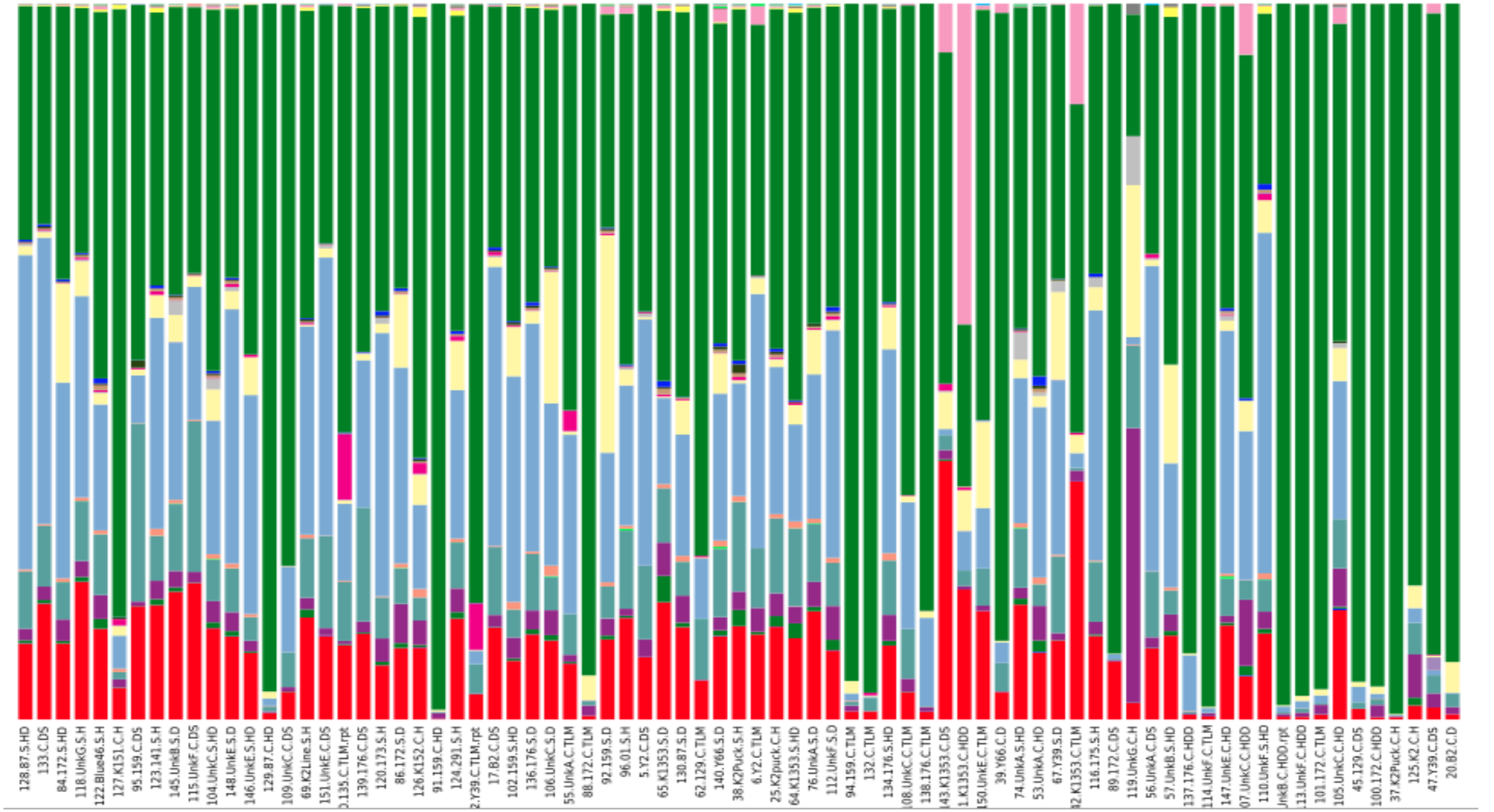

Figure 31. Comparison of the average relative abundance of bacteria by phyla in the microbial communities associated with each coral health state using Qiime.

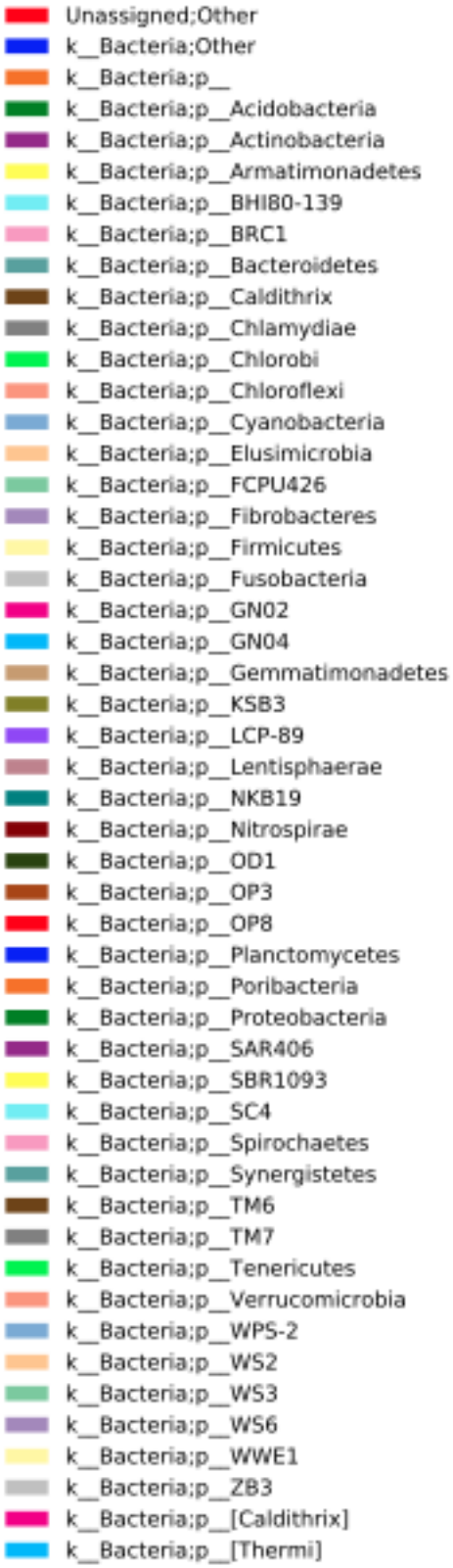

Legend for Figure 1.

Table 18. All OTUs that account for more than one percent of the total abundance are shown. The top five most abundant OTUs at the class level for each sample type is highlighted, with the most dominant in bold.

OTUs at the class level	C_H	C_HD	C_HDD	C_TLM	C_DS	S_H	S_HD	S_D
Unassigned;Other;Other	12.03%	5.63%	7.78%	15.68%	7.72%	11.54%	7.25%	7.76%
k__Bacteria;p__Actinobacteria;c__Acidimicrobiia	2.24%	0.74%	1.64%	1.01%	1.51%	1.54%	1.15%	1.37%
k__Bacteria;p__Actinobacteria;c__Actinobacteria	6.52%	1.71%	0.15%	0.38%	1.16%	0.12%	0.40%	0.51%
k__Bacteria;p__Bacteroidetes;c__[Saprospirae]	0.92%	0.47%	0.56%	0.79%	0.61%	1.15%	0.31%	1.13%
k__Bacteria;p__Bacteroidetes;c__Bacteroidia	1.89%	0.97%	0.22%	0.94%	0.49%	0.23%	0.44%	0.10%
k__Bacteria;p__Bacteroidetes;c__Cytophagia	2.14%	0.83%	1.65%	1.70%	1.24%	2.73%	1.42%	1.01%
k__Bacteria;p__Bacteroidetes;c__Flavobacteriia	2.30%	0.90%	1.65%	2.52%	2.48%	3.86%	2.83%	3.18%
k__Bacteria;p__Cyanobacteria;c__Chloroplast	7.53%	5.39%	7.93%	9.63%	9.55%	9.39%	5.81%	13.13%
k__Bacteria;p__Cyanobacteria;c__Oscillatoriophycideae	9.71%	4.95%	7.78%	5.20%	6.49%	3.52%	2.80%	2.07%
k__Bacteria;p__Cyanobacteria;c__Synechococcophycideae	2.92%	1.47%	2.82%	3.92%	1.87%	1.69%	1.27%	1.56%
k__Bacteria;p__Cyanobacteria;Other	1.90%	0.42%	0.82%	0.85%	0.54%	0.44%	0.20%	0.59%
k__Bacteria;p__Firmicutes;c__Bacilli	2.37%	0.51%	0.07%	0.52%	0.21%	0.10%	0.35%	0.19%
k__Bacteria;p__Firmicutes;c__Clostridia	4.04%	1.61%	1.98%	3.09%	3.29%	2.65%	5.90%	1.62%
k__Bacteria;p__Fusobacteria;c__Fusobacteriia	1.33%	0.11%	0.03%	0.36%	0.26%	0.62%	0.04%	0.15%
k__Bacteria;p__GN02;c__BD1-5	0.00%	0.00%	0.05%	0.13%	0.00%	1.74%	0.01%	0.30%
k__Bacteria;p__Proteobacteria;c__Alphaproteobacteria	**16.63%**	**62.36%**	**39.45%**	**25.26%**	**37.48%**	20.86%	**38.97%**	**40.58%**
k__Bacteria;p__Proteobacteria;c__Betaproteobacteria	2.00%	0.36%	0.20%	0.43%	0.47%	0.91%	0.17%	1.07%
k__Bacteria;p__Proteobacteria;c__Deltaproteobacteria	3.74%	1.10%	1.73%	2.25%	2.71%	3.78%	2.67%	3.04%
k__Bacteria;p__Proteobacteria;c__Epsilonproteobacteria	0.06%	0.02%	0.04%	0.11%	0.11%	0.37%	0.02%	0.13%
k__Bacteria;p__Proteobacteria;c__Gammaproteobacteria	15.33%	7.40%	21.11%	17.46%	18.83%	**29.11%**	26.30%	16.55%
k__Bacteria;p__Spirochaetes;c__Spirochaetes	0.14%	0.02%	0.02%	5.26%	0.74%	0.15%	0.21%	0.48%

Qiime was similar to the RDP 10 class abundances. However, Qiime separated out an unassigned category that included sequences that could not be taxonomically identified, and this classification accounted for one of the top five most abundant classes found in all sample types. Without including the unassigned category, the four most abundant bacterial classes found in C_AH, C_HD, C_HDD, and C_DS samples were α-proteobacteria (17%, 62%, 39%, 25%, 37%, respectively), γ-proteobacteria (15%, 7%, 21%, 17%, 19%, respectively), Oscillatoriophycideae, (10%, 5 %, 8%, 5%, 6%, respectively), and Chloroplast (8%, 5 %, 10%, 10%, 10%, respectively) (Table 18). Actinobacteria was the fifth most abundant class comprising C_AH and C_HD (7% and 2%, respectively), whereas the fifth most abundant class varied for C_HDD, C_TLM, and C_DS samples. A third Cyanobacteria class, Synechococcophycideae accounted for three percent of the total relative abundance for C_HDD samples, Spirochaetes were the fifth most abundant bacterial class in C_TLM samples (5%), and Clostridia accounted for three percent of C_DS samples. The presence of Cyanobacteria identified by Qiime results from the detection of members from the photobiont as was seen with RDP 10 (see Chapter 3's Discussion).

All reef-sediment sample types (S_H, S_HD, and S_D) shared three of the same most abundant bacterial classes with coral samples [α-proteobacteria (21%, 39%, and 41%, respectively), γ-proteobacteria (29%, 26%, and 17%, respectively), and Chloroplast (9%, 9%, and 13%, respectively)], but Flavobacteriia was the fourth most abundant class found in all reef-sediment communities (4%, 3%, and 3%, respectively). Unlike the composition of coral-associated bacterial communities, δ-proteobacteria were also one of

the most abundant classes found in S_H and S_D samples (4% and 3%, respectively), and Clostridia accounted for the fifth most abundant class found in S_HD communities (6%).

Out of the 947 OTUs identified by Qiime at the genus level, only fourteen of the genera had a relative abundance greater than one percent (Table 19). These 14 genera accounted for approximately 62 percent of the total relative abundance of the bacterial OTUs identified at this level. The remaining 38 percent of the total relative abundance was comprised of rare taxa composed of 933 OTUs with an abundance of less than one percent. For this reason, taxonomic comparisons of microbial communities among sample types were not analyzed at the genus level. However, it is noteworthy that Rickettsiales-like bacteria accounted for over half of the total community abundance in 18 percent of the samples (n-=14) (Figure 32). This was not found in the RDP analysis.

Alpha diversity

Results from the Chao1 alpha diversity analysis confirmed Linear Discriminant Analysis (LDA) Effective Size (LEfSe) estimation results from Chapter 4 and showed that sediment samples were significantly more diverse than coral samples (Chao1) (Figure 33). After examining sample types on a finer scale, the microbial communities of all three sediment types were more diverse than any of the associated coral bacterial communities (Chao1) (Figure 34). C_AH, C_HD, and C_DS contained the most diverse microbial communities, whereas C_HDD and C_D communities where the least diverse (Chao1).

Table 19. All OTUs identified at the genus level that accounted for more than one percent of the total relative abundance using Qiime are shown.

OTU	Total percent abundance
k__Bacteria;p__Proteobacteria;c__Alphaproteobacteria;o__;f__;g__	1.02%
k__Bacteria;p__Proteobacteria;c__Gammaproteobacteria;o__;f__;g__	1.06%
k__Bacteria;p__Proteobacteria;c__Gammaproteobacteria;o__Alteromonadales;f__OM60;g__	1.10%
k__Bacteria;p__Spirochaetes;c__Spirochaetes;o__Spirochaetales;f__Spirochaetaceae;g__Spirochaeta	1.13%
k__Bacteria;p__Proteobacteria;c__Gammaproteobacteria;o__Alteromonadales;f__Colwelliaceae;Other	1.47%
k__Bacteria;p__Bacteroidetes;c__Flavobacteriia;o__Flavobacteriales;f__Flavobacteriaceae;g__	1.54%
k__Bacteria;p__Proteobacteria;c__Alphaproteobacteria;o__Rhizobiales;f__Hyphomicrobiaceae;g__	1.84%
k__Bacteria;p__Proteobacteria;c__Gammaproteobacteria;o__Thiotrichales;f__Piscirickettsiaceae;g__	1.99%
k__Bacteria;p__Proteobacteria;c__Gammaproteobacteria;o__Vibrionales;f__Vibrionaceae;g__Vibrio	2.35%
k__Bacteria;p__Proteobacteria;c__Gammaproteobacteria;o__Enterobacteriales;f__Enterobacteriaceae;g__	2.41%
k__Bacteria;p__Cyanobacteria;c__Oscillatoriophycideae;o__Chroococcales;f__Xenococcaceae;g__	3.54%
k__Bacteria;p__Proteobacteria;c__Alphaproteobacteria;o__Rhodobacterales;f__Rhodobacteraceae;g__	6.48%
k__Bacteria;p__Cyanobacteria;c__Chloroplast;o__Stramenopiles;f__;g__	7.82%
k__Bacteria;p__Proteobacteria;c__Alphaproteobacteria;o__Rickettsiales;f__;g__	18.13%
Total	**61.55%**

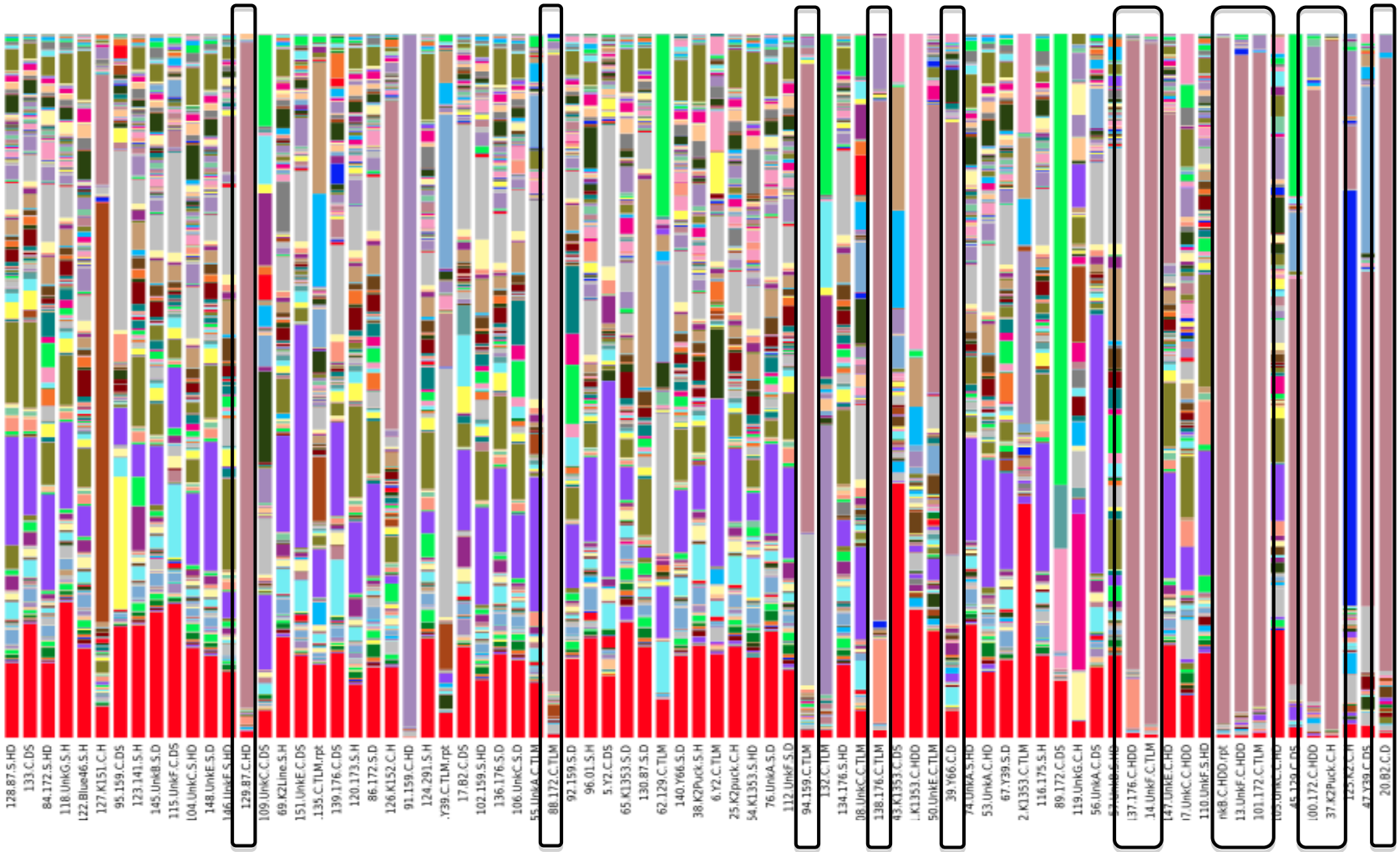

Figure 32. Comparison of the average relative abundance of genera of bacteria in microbial communities associated with each coral health state using Qiime. All samples where Rickettsiales-like bacteria comprise over half of the sample's total abundance are circled (n=14).

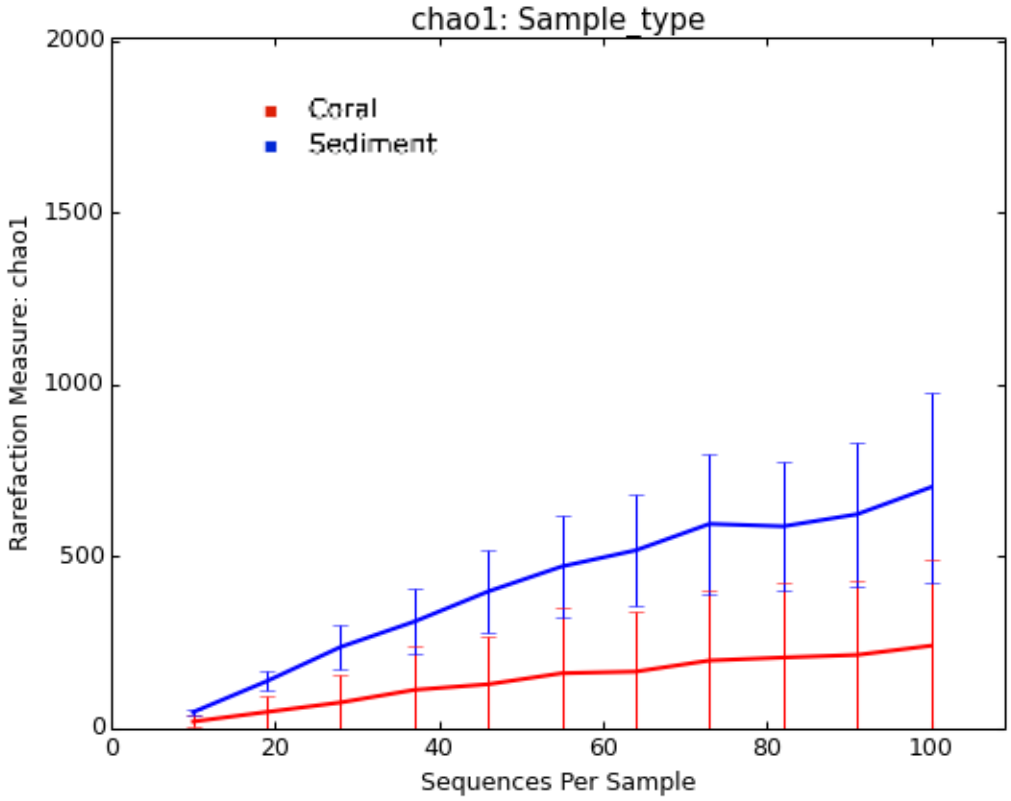

Figure 33. The vertical axis of the rarefaction plot displays the diversity of the community, while the horizontal axis displays the number of sequences considered in the diversity calculation. Each line on the figure represents the average of all microbial communities belonging to a group within coral and sediment samples.

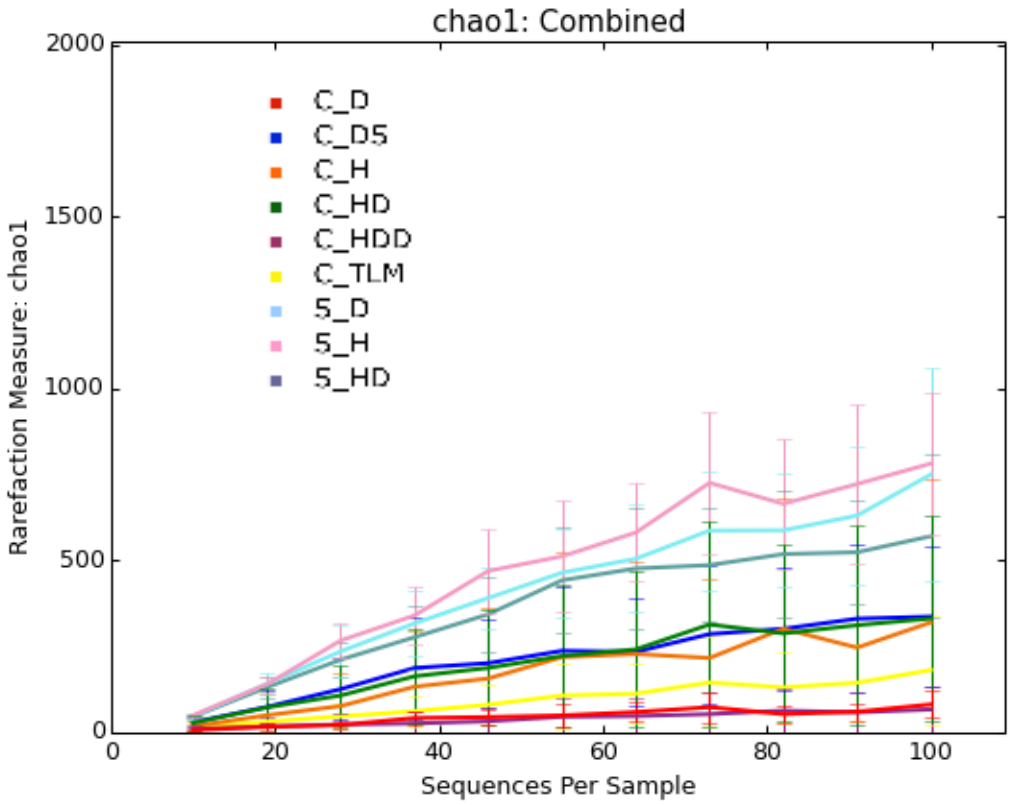

Figure 34. The vertical axis of the rarefaction plot displays the diversity of the community, where the horizontal axis displays the number of sequences considered in the diversity calculation. Each line on the figure represents the average of all microbial communities belonging to a group within each sample type.

Beta significance and diversity

Weighted UniFrac analysis revealed no significant differences between coral- and sediment-associated bacterial communities ($p = 0.74$). The microbial communities associated with S_H and S_HD samples were the only communities that were found to be statistically significant, according to the weighted UniFrac (Table 20). However, no communities were found to be significantly different when applying the Bonferroni corrected p-value. Weighted and unweighted UniFrac metrics analyzed the bacterial communities for all field sites, colonies of origin, colony type (nursery, outplant, or wild), depth, and sample year (2011 vs. 2012). The unweighted UniFracs for all comparisons were statistically different ($p<=0.005$). Out of all of the weighted comparisons, the only communities that were statistically different were the communities associated with two original coral colonies, Blue 46 and Unknown G ($p<=0.005$) (colony information presented in Appendix II). The beta-diversity of the bacterial communities was analyzed using weighted UniFrac distances to construct three-dimensional principal coordinate analysis (PCO) plots (Figure 35 and Figure 36). The results of the PCO analyses showed that the Qiime results were the same as what was observed in the PCO analyses presented in Chapter 4 (Figure 8).

Table 20. Comparison of unweighted and weighted UniFrac results for all sample conditions.

		Weighted UniFrac		Unweighted UniFrac	
sample 1	sample 2	p value	p value (Bonferroni corrected)	p value	p value (Bonferroni corrected)
C_D	C_HDD	0.935	1	0	<=5.0e-03
C_D	C_H	0.955	1	0	<=5.0e-03
C_D	S_D	0.975	1	0	<=5.0e-03
C_D	C_HD	0.98	1	0	<=5.0e-03
C_D	S_H	0.985	1	0	<=5.0e-03
C_D	S_HD	0.985	1	0	<=5.0e-03
C_D	C_DS	0.995	1	0	<=5.0e-03
C_D	C_TLM	1	1	0	<=5.0e-03
C_DS	S_D	0.065	1	0	<=5.0e-03
C_DS	S_H	0.075	1	0	<=5.0e-03
C_DS	S_HD	0.34	1	0	<=5.0e-03
C_DS	C_H	0.805	1	0	<=5.0e-03
C_DS	C_HDD	0.98	1	0	<=5.0e-03
C_DS	C_HD	0.985	1	0	<=5.0e-03
C_DS	C_TLM	0.99	1	0	<=5.0e-03
C_H	C_TLM	0.645	1	0	<=5.0e-03
C_H	S_H	0.825	1	0	<=5.0e-03
C_H	S_HD	0.84	1	0	<=5.0e-03
C_H	S_D	0.88	1	0	<=5.0e-03
C_H	C_HDD	0.985	1	0	<=5.0e-03
C_H	C_HD	1	1	0	<=5.0e-03
C_HD	S_H	0.98	1	0	<=5.0e-03
C_HD	C_HDD	0.99	1	0	<=5.0e-03
C_HD	S_D	0.99	1	0	<=5.0e-03
C_HD	S_HD	0.995	1	0	<=5.0e-03
C_HD	C_TLM	1	1	0	<=5.0e-03
C_HDD	S_H	0.965	1	0	<=5.0e-03
C_HDD	S_D	0.98	1	0	<=5.0e-03
C_HDD	S_HD	0.98	1	0	<=5.0e-03
C_HDD	C_TLM	0.99	1	0	<=5.0e-03
C_TLM	S_H	0.53	1	0	<=5.0e-03
C_TLM	S_D	0.58	1	0	<=5.0e-03
C_TLM	S_HD	0.615	1	0	<=5.0e-03
S_D	S_HD	0.765	1	0	<=5.0e-03
S_D	S_H	0.955	1	0	<=5.0e-03
S_H	S_HD	0.05*	1	0	<=5.0e-03

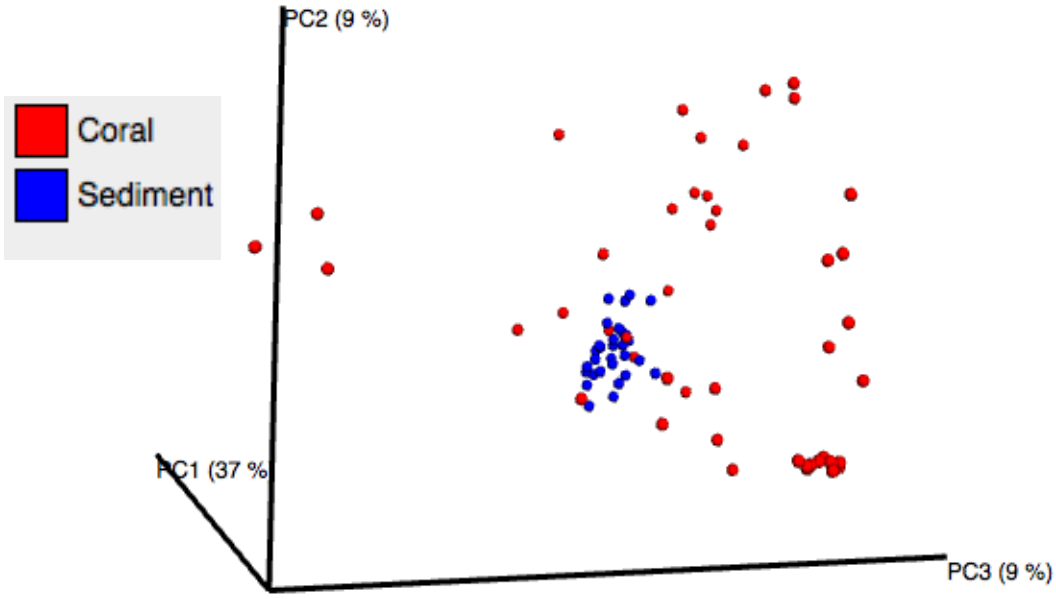

Figure 35. Three-dimensional PCO visualization for a weighted UniFrac comparing coral and sediment samples.

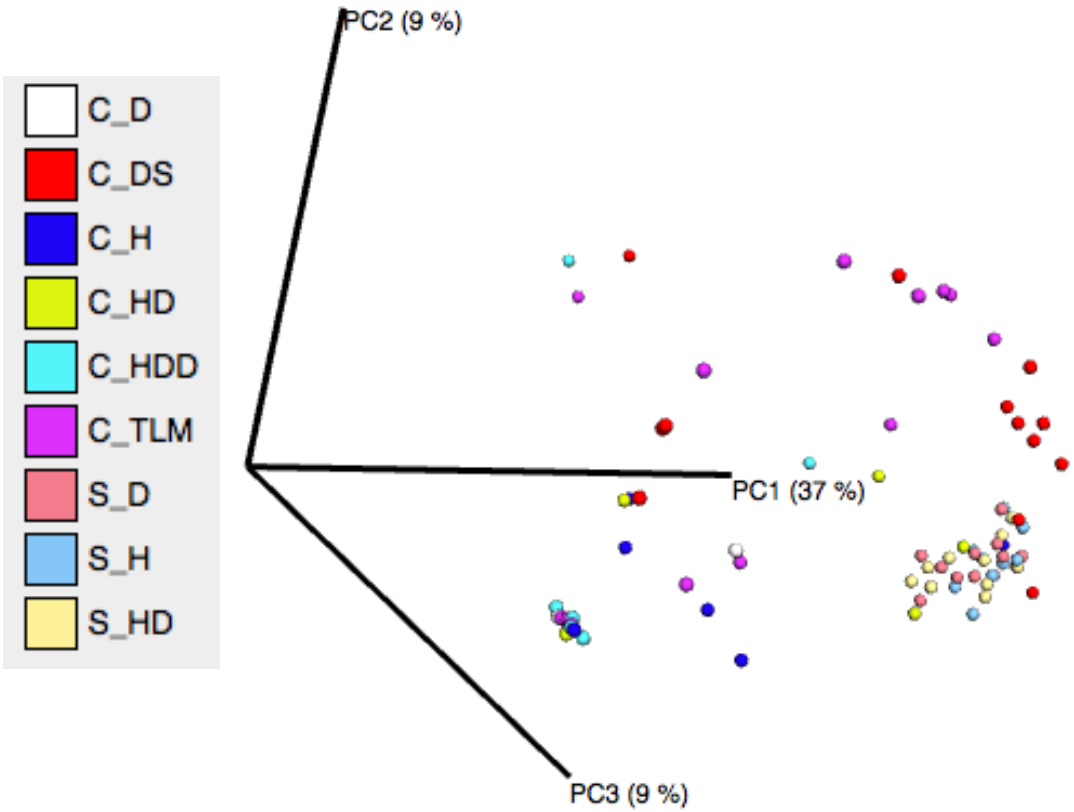

Figure 36. Three-dimensional PCO visualization for a weighted UniFrac comparing all sediment and coral sample types.

Discussion

Culture-independent methods were used to characterize the composition and diversity of bacterial communities associated with reef sediment, apparently healthy and disease-affected *A. cervicornis* tissue. While Qiime identified many more taxa than RDP 10, almost half of the OTUs detected could not be taxonomically identified. The development of high-throughput sequencing techniques have exponentially increased the amount of data produced and have provided a wealth of new insights regarding microbial community studies. However, these studies are still challenged by the fact that taxonomic identification of OTUs still relies heavily on the information available from previously described species (Handelsman 2004).

Qiime analysis confirmed the presence of both Vibrionales and Rickettsiales in coral tissue. Taxonomic comparisons between Qiime and both RDP 10 analyses detected the same total relative abundance of *Vibrio* bacteria, but the large abundance of Rickettsiales-like bacteria found in the Qiime analysis was not expected. Rickettsiales bacteria accounted for 18% of the total relative abundance when analyzed by Qiime, but only accounted for 4% of the total relative abundance analyzed by RDP 10. The difference in Rickettsiales abundance between analyses may be due to differences in the clustering of OTUs. Misidentifications in Qiime may have been possible, as Qiime only selects a representative sequence for each cluster, which is by default the first sequence in a cluster. The greater abundance detected in the Qiime analysis does represent what is observed in histological examinations of the coral tissue more accurately.

Both alpha diversity analysis (Chao1) and LEfSe showed that sediment samples were more significantly diverse than coral samples. Although the number of samples

present for each sample type differed, the rarefaction curves illustrated that overall sampling was carried out at the appropriate depth. Apparently-healthy sediment, S_D, and C_H coral samples were the only sample types that did not appear to reach their saturation point. The rarefaction curve for C_H samples specifically, shows that not enough samples were included for this community to be accurately characterized. These samples were the most difficult to extract genomic DNA from due to their high mucus content, and the number of AH samples collected in 2012 was limited so that the health of these colonies would not be compromised by our study. Future studies should include more AH samples so that the microbiota of apparently health *A. cervicornis* can be accurately described, but as this is a threatened (ESA) and endangered (IUCN) species, much consideration and appropriate caution should be taken while determining sample needs.

Most other studies have found the microbial communities of diseased coral colonies to be more diverse than apparently healthy communities (Sunagawa et al. 2009; Roder et al. 2014). However, this study showed an increase in diversity in the apparently healthy coral microbiota. Qiime is a phylogenetic approach that examines the whole microbial community overall by determining whether the branches of the phylogenetic trees are different. All pairwise comparisons analyzed using unweighted UniFrac showed that the microbial communities were statistically different. These results confirmed that the composition and diversity of the microbial communities among all sample types were different. However, the unweighted UniFrac only examines the tree topology. Weighted UniFrac places weight on the phylogenetic tree branches based on relative abundance.

Only one of the weighted UniFrac comparisons between two coral colonies (Blue 46 and Unknown G) was statistically significant. No other comparisons were significant. Therefore, from a diversity perspective, the composition or diversity of the microbial community associated with each sample type was different, but there were no phylogenetic differences when weighted.

Qiime is one of the standard bioinformatic pipelines for conducting microbial community analysis from raw DNA sequencing data. However, our results were comparable to what was found for RDP 10. Although Qiime identified more OTUs. the PCOs were the same for both analyses. The next step for this research will be to select all Vibrionales and Rickettsiales sequences and run these sequences through the National Center for Biotechnology Information's basic local alignment search tool (BLAST) for identification at a finer resolution, especially since the Rickettsiales-like bacteria could only be identified to the order level. Furthermore, now that the microbial communities associated with apparently healthy and diseased *A. cervicornis* have been defined at the finest resolution to date, future studies should examine OTU physiology and metabolism. There is still a need for improvements for effective metagenomic data analysis, as determining a starting place for determining importance of the rare taxa remains a daunting and cumbersome task.

CONCLUSIONS

The data generated in this project provided evidence to reject null hypotheses 1 and 4, and failed to reject null hypotheses 2 and 3. Taxonomic and phylogenetic comparisons of the composition of bacterial communities associated with *A. cervicornis* revealed significant difference between apparently healthy and diseased tissue samples. Specifically, significant changes were observed in bacterial community richness between apparently healthy coral samples and the tissue-loss margin and denuded skeleton portions of diseased fragments.

Principle coordinate analysis showed that the reef-sediment microbiota was distinct from communities harbored by coral tissues. Furthermore, linear discrimant analysis showed that sediment-associated bacterial communities were significantly more diverse than coral communities. However, no correlations between reef sediment and tissue-loss diseases affecting *A. cervicornis* were observed.

Comparisons between taxonomic and phylogenetic analyses yielded different results regarding the relative abundance of Rickettsiales bacteria and need to be investigated further. Differences in the abundance of Rickettsiales found in each coral sample type were observed by both analyses, but these differences were not found to be

significant. It is noteworthy that Rickettsiales-like bacteria accounted for over half of the total community abundance in 18 percent of the samples (n-=14) according to the phylogenetic analysis. Rickettsiales-like bacteria appear to be a potential putative pathogen of tissue-loss diseases affecting *A. cervicornis,* but cannot be conclusively defined as such. Therefore the null hypothesis, which states: Rickettsiales abundance does not differ in apparently healthy and diseased *A. cervicornis* tissue, could not be definitively rejected.

Comparisons between taxonomic and phylogenetic analyses detected the same total relative abundance of *Vibrio* bacteria. Vibrionales were detected in both coral- and sediment-associated bacterial communities, but were not shown to be statistically more abundant in *A. cervicornis* tissues or reef sediment. Bacteria from family Vibrionaceae were found to be both more abundant and biologically consistent within microbial communities associated with the tissue-loss margin of diseased coral tissues when compared to all other coral sample types. These data provided molecular evidence to support the idea that the presence of vibrios can be considered a biomarker of tissue-loss diseases affecting *A. cervicornis* colonies, although no causality explanations could be derived from this observation. This work supports the notion that coral tissue-loss diseases are polymicrobial diseases associated with an imbalance or dysbiosis of residential bacterial populations and proposes that the increase in bacteria from family Vibrionaceae is a biomarker of tissue-loss disease-affected *A. cervicornis* colonies.

APPENDIX I

This appendix contains a list of samples that were collected during summer 2011. Sample types are defined as: apparently healthy (AH), healthy-on-diseased (HD), healthy-on-diseased section of diseased branch (HDD), tissue-loss margin (TLM), denuded skeleton (DS), and diseased (D).

Collection Date	Colony No.	Field Site	Sample Type	Lesion Description	Condition	Sample Name
6/22/11	Y66	Aquarius	Coral	RTL	D	39_Y66_C_D
6/25/11	Y66	Aquarius	Sediment	RTL	D	140_Y66_S_D
6/29/11	Y39	Aquarius	Coral	WBD	TLM	72_Y39_C_TLM
6/29/11	Y39	Aquarius	Coral	WBD	DS	47_Y39_C_DS
6/29/11	Y39	Aquarius	Sediment	WBD	D	67_Y39_S_D
6/29/11	O1	Aquarius	Sediment	Apparently Healthy	AH	96_01_S_H
	Blue 46	Conch Shallow	Sediment	Apparently Healthy	AH	122_Blue46_S_H
	141	Conch Shallow	Sediment	Apparently Healthy	AH	123_141_S_H
	291	Conch Shallow	Sediment	Apparently Healthy	AH	124_291_S_H
6/27/11	Big Rock Acer	CRF Nursery	Coral	WBD	TLM	70_135_C_TLM
6/24/11	K1 353	CRF Nursery	Coral	WBD	HDD	141_K1353_C_HDD
6/24/11	K1 353	CRF Nursery	Coral	WBD	TLM	142_K1353_C_TLM
6/24/11	K1 353	CRF Nursery	Coral	WBD	DS	143_K1353_C_DS
6/22/11	K1 353	CRF Nursery	Sediment	WBD	HD	64_K1353_S_HD
6/22/11	K1 353	CRF Nursery	Sediment	WBD	D	65_K1353_S_D
6/29/11	K2puck	CRF Nursery	Coral	Apparently Healthy	AH	25_K2puck_C_H
6/29/11	K2puck	CRF Nursery	Coral	Apparently Healthy	AH	37_K2Puck_C_H

6/29/11	K2puck	CRF Nursery	Sediment	Apparently Healthy	AH	38_K2Puck_S_H
6/29/11	K2-Line	CRF Nursery	Sediment	Apparently Healthy	AH	69_K2Line_S_H
6/23/11	K2(a)	CRF Nursery	Coral	Apparently Healthy	AH	125_K2_C_H
6/27/11	K1 152	CRF Nursery	Coral	Apparently Healthy	AH	126_K152_C_H
6/27/11	K1 152	CRF Nursery	Coral	Apparently Healthy	AH	127_K151_C_H
6/3/11	B2	KLDR	Coral	WBD	TLM	20_B2_C_TLM
6/3/11	B2	KLDR	Coral	WBD	DS	17_B2_C_DS
6/3/11	Y2	KLDR	Coral	WBD	TLM	6_Y2_C_TLM
6/3/11	Y2	KLDR	Coral	WBD	DS	5_Y2_C_DS
6/29/11	#129	Molasses	Coral	RTL	TLM	62_129_C_TLM
6/29/11	#129	Molasses	Coral	RTL	DS	45_129_C_DS

APPENDIX II

This appendix contains a list of samples that were collected during summer 2012. Sample types are defined as: apparently healthy (AH), healthy-on-diseased (HD), healthy-on-diseased section of diseased branch (HDD), tissue-loss margin (TLM), and denuded skeleton (DS), and diseased (D).

Collection Date	Colony No.	Field Site	Sample Type	Condition	Sample Name
6/24/12	#173	Conch Shallow	Sediment	AH	120_173_S_H
6/24/12	#176	Conch Shallow	Coral	HDD	137_176_C_HDD
6/24/12	#176	Conch Shallow	Coral	TLM	138_176_C_TLM
6/24/12	#176	Conch Shallow	Coral	DS	139_176_C_DS
6/24/12	#176	Conch Shallow	Sediment	HD	134_176_S_HD
6/24/12	#176	Conch Shallow	Sediment	D	136_176_S_D
6/23/12	#172	French	Coral	HDD	100_172_C_HDD
6/23/12	#172	French	Coral	TLM	101_172_C_TLM
6/23/12	#172	French	Coral	DS	89_172_C_DS
6/23/12	#172	French	Sediment	HD	84_172_S_HD
6/23/12	#172	French	Sediment	D	86_172_S_D
6/23/12	#159	French	Coral	HD	91_159_C_HD
6/23/12	#159	French	Coral	TLM	94_159_C_TLM
6/23/12	#159	French	Coral	DS	95_159_C_DS
6/23/12	#159	French	Sediment	HD	102_159_S_HD
6/23/12	#159	French	Sediment	D	92_159_S_D
6/23/12	Unknown A, top R of #158	KLDR	Coral	HD	53_UnkA_C_HD
6/23/12	Unknown A, top R of #158	KLDR	Coral	TLM	55_UnkA_C_TLM
6/23/12	Unknown A, top R of #158	KLDR	Coral	DS	56_UnkA_C_DS
6/23/12	Unknown A, top R of #158	KLDR	Sediment	HD	74_UnkA_S_HD

6/23/12	Unknown A, top R of #158	KLDR	Sediment	D	76_UnkA_S_D
6/23/12	Unknown B, in b/t #146 & #147	KLDR	Coral	HDD	83_UnkB_C_HDD
6/23/12	Unknown B, in b/t #146 & #147	KLDR	Sediment	HD	57_UnkB_S_HD
6/23/12	Unknown B, in b/t #146 & #147	KLDR	Sediment	D	145_UnkB_S_D
6/24/12	Unknown G, 150 degrees from #89	Little Conch	Coral	AH	119_UnkG_C_H
6/24/12	Unknown G, 150 degrees from #89	Little Conch	Sediment	AH	118_UnkG_S_H
6/24/12	Unknown F in bt #82 & #98	Little Conch	Coral	HDD	113_UnkF_C_HDD
6/24/12	Unknown F in bt #82 & #98	Little Conch	Coral	TLM	114_UnkF_C_TLM
6/24/12	Unknown F in bt #82 & #98	Little Conch	Coral	DS	115_UnkF_C_DS
6/24/12	Unknown F in bt #82 & #98	Little Conch	Sediment	HD	110_UnkF_S_HD
6/24/12	Unknown F in bt #82 & #98	Little Conch	Sediment	D	112_UnkF_S_D
6/24/12	#87	Little Conch	Coral	HD	129_87_C_HD
6/24/12	#87	Little Conch	Coral	TLM	132_C_TLM
6/24/12	#87	Little Conch	Coral	DS	133_C_DS
6/24/12	#87	Little Conch	Sediment	HD	128_87_S_HD
6/24/12	#87	Little Conch	Sediment	D	130_87_S_D
6/24/12	Unknown E	Little Conch	Coral	HD	147_UnkE_C_HD
6/24/12	Unknown E	Little Conch	Coral	TLM	150_UnkE_C_TLM
6/24/12	Unknown E	Little Conch	Coral	DS	151_UnkE_C_DS
6/24/12	Unknown E	Little Conch	Sediment	HD	146_UnkE_S_HD
6/24/12	Unknown E	Little Conch	Sediment	D	148_UnkE_S_D
6/24/12	#175	Molasses Reef	Sediment	AH	116_175_S_H
6/23/12	Unknown C, R of #167	Molasses	Coral	HD	105_UnkC_C_HD
6/23/12	Unknown C, R of #167	Molasses	Coral	HDD	107_UnkC_C_HDD
6/23/12	Unknown C, R of #167	Molasses	Coral	TLM	108_UnkC_C_TLM
6/23/12	Unknown C, R of #167	Molasses	Coral	DS	109_UnkC_C_DS
6/23/12	Unknown C, R of #167	Molasses	Sediment	HD	104_UnkC_S_HD
6/23/12	Unknown C, R of #167	Molasses	Sediment	D	106_UnkC_S_D

REFERENCES

Acevedo R, Morelock J, Olivieri RA (1989) Modification of coral reef zonation by terrigenous sediment stress. PALAIOS 4:92–100

Adey WH (1978) Coral reef morphogenesis: A multidimensional model. Science 202:831–837

Ainsworth TD, Fine M, Blackall LL, Hoegh-Guldberg O (2006) Fluorescence in situ hybridization and spectral imaging of coral-associated bacterial communities. Appl. Environ. Microbiol. 72:3016–3020

Amann RI, Ludwig W, Schleifer KH (1995) Phylogenetic identification and in situ detection of individual microbial cells without cultivation. Microbiol. Rev. 59:143–169

Antonius A (1973) New observations on coral destruction in reefs. Tenth Meeting of the Association of Island Marine Laboratories of the Caribbean 10:3

Antonius A (1977) Coral mortality in reefs: a problem for science and management. Proceedings of the 3rd International Coral Reef Symposium 2:617–623

Aronson RB, Precht WF (2001a) Evolutionary paleoecology of Caribbean coral reefs. In: Allmon W.D., Bottjer D.J. (eds) Evolutionary Paleoecology: The Ecological Context of Macroevolutionary Change. Columbia University Press, New York, NY, pp 228

Aronson RB, Precht WF (2001b) White-band disease and the changing face of Caribbean coral reefs. In: Porter J.W. (eds) The Ecology and Etiology of Newly Emerging Marine Diseases. Springer Netherlands, pp 25–38

Aronson RB, Precht WF, Macintyre IG (1998) Extrinsic control of species replacement on a Holocene reef in Belize: The role of coral disease. Coral Reefs 17:223–230

Aronson R, Bruckner A, Moore J, Precht B, Weil E (2008) *Acropora cervicornis*. The IUCN Red List of Threatened Species. Version 2014.3. http://www.iucnredlist.org/details/summary/133381/0

Bayer T, Neave MJ, Alsheikh-Hussain A, Aranda M, Yum LK, Mincer T, Hughen K, Apprill A, Voolstra CR (2013) The microbiome of the Red Sea coral *Stylophora pistillata* is dominated by tissue-associated Endozoicomonas bacteria. Appl. Environ. Microbiol. 79:4759–4762

Beleneva IA, Dautova TI, Zhukova NV (2005) Characterization of communities of heterotrophic bacteria associated with healthy and diseased corals in Nha Trang Bay (Vietnam). Mikrobiologiia 74:667–676

Ben-Haim Y, Rosenberg E (2002) A novel *Vibrio* sp. pathogen of the coral *Pocillopora damicornis*. Marine Biology 141:47–55

Ben-Haim Y, Thompson FL, Thompson CC, Cnockaert MC, Hoste B, Swings J, Rosenberg E (2003) *Vibrio coralliilyticus* sp. nov., a temperature-dependent pathogen of the coral *Pocillopora damicornis*. Int J Syst Evol Microbiol 53:309–315

Benson AA, Muscatine L (1974) Wax in coral mucus: Energy transfer from corals to reef fishes. Limnol. Oceanogr. 19:810–814

Bentis CJ, Kaufman L, Golubic S (2000) Endolithic fungi in reef-building corals (order: Scleractinia) are common, cosmopolitan, and potentially pathogenic. Biol. Bull. 198:254–260

Boulon R, Chiappone M, Halley R, Jaap W, Keller B, Kruczynski B, Miller M, Rogers C (2005) Biological Review Team.

Bourne DG, Garren M, Work TM, Rosenberg E, Smith GW, Harvell CD (2009) Microbial disease and the coral holobiont. Trends Microbiol. 17:554–562

Bourne DG, Munn CB (2005) Diversity of bacteria associated with the coral *Pocillopora damicornis* from the Great Barrier Reef. Environ. Microbiol. 7:1162–1174

Bruckner A (2002) Proceedings of the Caribbean Acropora workshop--potential application of the U.S. Endangered Species Act as a conservation strategy. U.S. Department of Commerce, National Oceanic and Atmospheric Administration, National Marine Fisheries Service. Silver Springs, MD

Bruno JF, Petes LE, Drew Harvell C, Hettinger A (2003) Nutrient enrichment can increase the severity of coral diseases. Ecol. Lett. 6:1056–1061

Burke LM (2004) Reefs at Risk in the Caribbean. World Resources Institute, Washington, D.C

Burke L, Reytar K, Spalding M, Perry A (2011) Reefs at Risk Revisited. World Resources Institute, Washington, DC

Bythell JC, Barer MR, Cooney RP, Guest JR, O'Donnell AG, Pantos O, Le Tissier MDA (2002) Histopathological methods for the investigation of microbial communities associated with disease lesions in reef corals. Lett. Appl. Microbiol. 34:359–364

Caporaso JG, Bittinger K, Bushman FD, DeSantis TZ, Andersen GL, Knight R (2010a) PyNAST: A flexible tool for aligning sequences to a template alignment. Bioinformatics 26:266–267

Caporaso JG, Kuczynski J, Stombaugh J, Bittinger K, Bushman FD, Costello EK, Fierer N, Peña AG, Goodrich JK, Gordon JI, Huttley GA, Kelley ST, Knights D, Koenig JE, Ley RE, Lozupone CA, McDonald D, Muegge BD, Pirrung M, Reeder J, Sevinsky JR, Turnbaugh PJ, Walters WA, Widmann J, Yatsunenko T, Zaneveld J, Knight R (2010b) QIIME allows analysis of high-throughput community sequencing data. Nat. Methods 7:335–336

Cárdenas A, Rodriguez-R LM, Pizarro V, Cadavid LF, Arévalo-Ferro C (2012) Shifts in bacterial communities of two Caribbean reef-building coral species affected by white plague disease. ISME J. 6:502–512

Carpenter KE, Abrar M, Aeby G, Aronson RB, Banks S, Bruckner A, Chiriboga A, Cortés J, Delbeek JC, DeVantier L, Edgar GJ, Edwards AJ, Fenner D, Guzmán HM, Hoeksema BW, Hodgson G, Johan O, Licuanan WY, Livingstone SR, Lovell ER, Moore JA, Obura DO, Ochavillo D, Polidoro BA, Precht WF, Quibilan MC, Reboton C, Richards ZT, Rogers AD, Sanciangco J, Sheppard A, Sheppard C, Smith J, Stuart S, Turak E, Veron JEN, Wallace C, Weil E, Wood E (2008) One-third of reef-building corals face elevated extinction risk from climate change and local impacts. Science 321:560–563

Carson FL, Hladik C (2009) Histotechnology: A Self-Instructional Text. American Society for Clinical Pathology, Hong Kong, China

Casas V, Kline DI, Wegley L, Yu Y, Breitbart M, Rohwer F (2004) Widespread association of a Rickettsiales-like bacterium with reef-building corals. Environ. Microbiol. 6:1137–1148

Castillo I, Lodeiros C, Núñez M, Campos I (2001) In vitro evaluation of antibacterial substances produced by bacteria isolated from different marine organisms. Rev. Biol. Trop. 49:1213–1222

Carson FL, Hladik C (2009) Histotechnology: A Self-Instructional Text. American Society for Clinical Pathology, Hong Kong, China

Cesar H, Burke L, Pet-Soede L (2003) The economics of worldwide coral reef degradation. Cesar Environmental Economic Consulting, Arnhem, and WWF-Netherlands, Zeist, The Netherlands.

Cesar HSJ (2000) Coral reefs: Their functions, threats and economic value. Collected Essays on the Economics of Coral Reefs. Kalmar University, Kalmar, Sweden, pp 14–39

Clarke R, Ressom HW, Wang A, Xuan J, Liu MC, Gehan EA, Wang Y (2008) The properties of high-dimensional data spaces: Implications for exploring gene and protein expression data. Nat Rev Cancer 8:37–49

Coles SL, Strathmann R (1973) Observations on coral mucus "flocs" and their potential trophic significance. Limnol. Oceanogr. 18:673–678

Connell JH (1978) Diversity in tropical rain forests and coral reefs. Science 199:1302–1310

Conservation International (2008) Economic values of coral reefs, mangroves and seagrasses: A global compilation. Center for Applied Biodiversity Science, Conservation International, Arlington, VA, USA

Cook G (2009) A Comparative Analysis of Bacterial Communities Associated with Apparently Healthy and Diseased Corals Inhabiting the Wider Caribbean Region. Dissertation, George Mason University

Cooney RP, Pantos O, Tissier MDAL, Barer MR, O´Donnell AG, Bythell JC (2002) Characterization of the bacterial consortium associated with black band disease in coral using molecular microbiological techniques. Environ. Microbiol. 4:401–413

Cortés JN, Risk MJ (1985) A reef under siltation stress: Cahuita, Costa Rica. Bull. Mar. Sci. 36:339–356

Costanza R, Arge R d', de Groot R, Farber S, Grasso M, Hannon B, Limburg K, Naeem S, O'Neill RV, Paruelo J, Raskin RG, Sutton P, van den Belt M (1997) The value of the world's ecosystem services and natural capital. Nature 387:253–260

Côté IM, Gill JA, Gardner TA, Watkinson AR (2005) Measuring coral reef decline through meta-analyses. Philos. Trans. R. Soc. Lond. B. Biol. Sci. 360:385–395

Daniels C, Zeifman A, Heym K, Ritchie K, Watson C, Berzins I, Breitbart M (2011) Spatial heterogeneity of bacterial communities in the mucus of *Montastraea annularis*. Mar. Ecol. Prog. Ser. 426:29–40

Denner EBM, Smith GW, Busse H-J, Schumann P, Narzt T, Polson SW, Lubitz W, Richardson LL (2003) *Aurantimonas coralicida* gen. nov., sp. nov., the causative agent of white plague type II on Caribbean scleractinian corals. Int. J. Syst. Evol. Microbiol. 53:1115–1122

DeSantis TZ, Hugenholtz P, Larsen N, Rojas M, Brodie EL, Keller K, Huber T, Dalevi D, Hu P, Andersen GL (2006) Greengenes, a chimera-checked 16S rRNA gene database and workbench compatible with ARB. Appl. Environ. Microbiol. 72:5069–5072

DiSalvo L, Gundersen K (1971) Regenerative functions and microbial ecology of coral reefs. I. Assays for microbial population. Can. J. Microbiol. 17:1081–1089

DiSalvo LH (1971a) Regenerative functions and microbial ecology of coral reefs: Labelled bacteria in a coral reef microcosm. J. Exp. Mar. Biol. Ecol. 7:123–136

DiSalvo LH (1971b) Regenerative functions and microbial ecology of coral reefs. II. Oxygen metabolism in the regenerative system. Can. J. Microbiol. 17:1091–1100

Domart-Coulon IJ, Traylor-Knowles N, Peters E, Elbert D, Downs CA, Price K, Stubbs J, McLaughlin S, Cox E, Aeby G, Brown PR, Ostrander GK (2006) Comprehensive characterization of skeletal tissue growth anomalies of the finger coral *Porites compressa*. Coral Reefs 25:531–543

Ducklow HW, Mitchell R (1979) Bacterial populations and adaptations in the mucus layers on living corals. Limnol. Oceanogr. 24:715–725

Dustan P (1977) Vitality of reef coral populations off Key Largo, Florida: Recruitment and mortality. Environ. Geol. 2:51–58

Dustan P (1999) Coral reefs under stress: Sources of mortality in the Florida Keys. Nat. Resour. Forum 23:147–155

Edgar RC (2010) Search and clustering orders of magnitude faster than BLAST. Bioinformatics 26:2460–2461

Fabricius KE (2005) Effects of terrestrial runoff on the ecology of corals and coral reefs: Review and synthesis. Mar. Pollut. Bull. 50:125–146

Fisher RA (1936) The use of multiple measurements in taxonomic problems. Annals of Eugenics 7:179–188

Flores F, Hoogenboom MO, Smith LD, Cooper TF, Abrego D, Negri AP (2012) Chronic exposure of corals to fine sediments: Lethal and sub-lethal impacts. PLoS ONE 7:e37795

Frias-Lopez J, Klaus JS, Bonheyo GT, Fouke BW (2004) Bacterial community associated with black band disease in corals. Appl. Environ. Microbiol. 70:5955–5962

Frias-Lopez J, Zerkle AL, Bonheyo GT, Fouke BW (2002) Partitioning of bacterial communities between seawater and healthy, black band diseased, and dead coral surfaces. Appl. Environ. Microbiol. 68:2214–2228

Fuhrman JA, Campbell L (1998) Marine ecology: Microbial microdiversity. Nature 393:410–411

Futch JC, Griffin DW, Banks K, Lipp EK (2011) Evaluation of sewage source and fate on southeast Florida coastal reefs. Mar. Pollut. Bull. 62:2308–2316

Galloway SB, Woodley CM, Bruckner AW (2009) Coral health and disease in the Pacific: Vision for action. US Department of Commerce, National Oceanic and Atmospheric Administration, National Ocean Service, National Centers for Coastal Ocean Science,

Galloway S, Work T, Bochsler V, Harley R, Kramarsky-Winters E, McLaughlin S, Meteyer C, Morado J, Nicholson J, Parnell P, Peters E, Reynolds T, Rotstein D, Sileo L, Woodley C (2007) Coral Disease and Health Workshop: Coral Histopathology II.

Gardner TA, Côté IM, Gill JA, Grant A, Watkinson AR (2003) Long-term region-wide declines in Caribbean corals. Science 301:958–960

Garrison VH, Shinn EA, Foreman WT, Griffin DW, Holmes CW, Kellogg CA, Majewski MS, Richardson LL, Ritchie KB, Smith GW (2003) African and Asian dust: From desert soils to coral reefs. BioScience 53:469–480

Geffen Y, Rosenberg E (2005) Stress-induced rapid release of antibacterials by scleractinian corals. Mar. Biol. 146:931–935

Gignoux-Wolfsohn SA, Marks CJ, Vollmer SV (2012) White band disease transmission in the threatened coral, *Acropora cervicorni*s. Sci. Rep. 2:

Gil-Agudelo DL, Smith GW, Weil E (2006) The white band disease type II pathogen in Puerto Rico. Rev. Biol. Trop. 54:59–67

Gladfelter WB (1982) White-band disease in *Acropora palmata*: Implications for the structure and growth of shallow reefs. Bull. Mar. Sci. 32:639–643

Gladfelter WB, Gladfelter EH, Monahan RK, Ogden JC, Dill RF (1977) Environmental studies of Buck Island Reef National Monument, St. Croix, U.S.V.I.

Glaser KB, Mayer AMS (2009) A renaissance in marine pharmacology: From preclinical curiosity to clinical reality. Biochem. Pharmacol. 78:440–448

Goldberg WM (1973) The ecology of the coral-octocoral communities off the southeast Florida coast: Geomorphology, species composition, and zonation. Bull. Mar. Sci. 23:465–488

Goreau TF, Goreau NI, Goreau TJ (1979) Corals and Coral Reefs. Sci. Am. 241:124–136

Goreau TJ, Cervino J, Goreau M, Hayes R, Hayes M, Richardson L, Smith GW, DeMeyer K, Nagelkerken I, Garzon-Ferrera J, Gil D, Garrison G, Williams EH, Bunkley-Williams L, Quirolo C, Patterson K, Porter JW, Porter K (1998) Rapid spread of disease in Caribbean coral reefs. Rev. Biol. Trop. 46:157–171

Graham NAJ, Wilson SK, Jennings S, Polunin NVC, Bijoux JP, Robinson J (2006) Dynamic fragility of oceanic coral reef ecosystems. Proc. Natl. Acad. Sci. 103:8425–8429

Gray MA, Pratte ZA, Kellogg CA (2013) Comparison of DNA preservation methods for environmental bacterial community samples. FEMS Microbiol. Ecol. 83:468–477

Green EP, Bruckner AW (2000) The significance of coral disease epizootiology for coral reef conservation. Biol. Conserv. 96:347–361

Green EP, Short FT (2003) World Atlas of Seagrasses. University of California Press, Los Angeles, CA

Haapkylä J, Unsworth RKF, Flavell M, Bourne DG, Schaffelke B, Willis BL (2011) Seasonal rainfall and runoff promote coral disease on an inshore reef. PLoS ONE 6:e16893

Hajibabaei M, Shokralla S, Zhou X, Singer GAC, Baird DJ (2011) Environmental barcoding: A next-generation sequencing approach for biomonitoring applications using river benthos. PLoS ONE 6:e17497

Hakim HI, Radj OK, Khoe MM, Pratam GA, Nasima D, Ambariyanto, Sarjito, Sudoyo H (2012) Causative agents of white band disease from culturable bacterial community associated with healthy and diseased corals *Acropora humilis* and *Acropora tortuosa* from Karimunjawa Islands, Indonesia. Ecologia 2:52–59

Handelsman J (2004) Metagenomics: Application of Genomics to Uncultured Microorganisms. Microbiol. Mol. Biol. Rev. 68:669–685

Harvell CD, Kim K, Burkholder JM, Colwell RR, Epstein PR, Grimes DJ, Hofmann EE, Lipp EK, Osterhaus ADME, Overstreet RM, Porter JW, Smith GW, Vasta GR (1999) Emerging marine diseases--climate links and anthropogenic factors. Science 285:1505–1510

Harvell CD, Mitchell CE, Ward JR, Altizer S, Dobson AP, Ostfeld RS, Samuel MD (2002) Climate warming and disease risks for terrestrial and marine biota. Science 296:2158–2162

Harvell D, Jordán-Dahlgren E, Merkel S, Rosenberg E, Raymundo L, Smith G, Weil E, Willis B (2007) Coral disease, environmental drivers, and the balance between coral and microbial associates. Oceanography 20:172–195

Hatcher BG (1988) Coral reef primary productivity: A beggar's banquet. Trends Ecol. Evol. 3:106–111

Highsmith RC (1982) Reproduction by fragmentation in corals. Mar. Ecol. Prog. Ser. Oldendorf 7:207–226

Hodgson G (1990) Tetracycline reduces sedimentation damage to corals. Mar. Biol. 104:493–496

Hoegh-Guldberg O, Mumby PJ, Hooten AJ, Steneck RS, Greenfield P, Gomez E, Harvell CD, Sale PF, Edwards AJ, Caldeira K, Knowlton N, Eakin CM, Iglesias-Prieto R, Muthiga N, Bradbury RH, Dubi A, Hatziolos ME (2007) Coral reefs under rapid climate change and ocean acidification. Science 318:1737–1742

Hogarth WT (2006) Endangered and threatened species: Final listing determinations for the elkhorn coral and staghorn coral. Fed. Regist. 7126852–26861

Holden C (1996) Coral disease hot spot in Florida Keys. Science 274:2017–2017

Hughes TP (1994) Catastrophes, phase shifts, and large-scale degradation of a Caribbean coral reef. Sci.-AAAS-Wkly. Pap. Ed. 265:1547–1551

Hughes TP, Baird AH, Bellwood DR, Card M, Connolly SR, Folke C, Grosberg R, Hoegh-Guldberg O, Jackson JBC, Kleypas J, Lough JM, Marshall P, Nyström M, Palumbi SR, Pandolfi JM, Rosen B, Roughgarden J (2003) Climate change, human impacts, and the resilience of coral reefs. Science 301:929–933

Jaap WC, Lyons WG, Dustan P, Halas JC (1989) Stony coral (Scleractinia and Milleporina) community structure at Bird Key Reef, Ft. Jefferson National Monument, Dry Tortugas, Florida. State of Florida, Department of Natural Resources, Florida Marine Research Institute 46: 1-31, St. Petersburg, FL

Kaczmarsky LT, Draud M, Williams EH (2005) Is there a relationship between proximity to sewage effluent and the prevalence of coral disease. Caribb J Sci 41:124–137

Kavousi J, Tavakoli-Kolour P, Barkhordari A, Bahrami A (2013) Mass mortality of Porites corals on Northern Persian Gulf Reefs due to sediment-microbial interactions. Int. J. Mar. Sci. 3:306–310

Kellogg C (2004) Tropical Archaea: Diversity associated with the surface microlayer of corals. Mar. Ecol. Prog. Ser. 273:81–88

Kelman D, Kashman Y, Rosenberg E, Kushmaro A, Loya Y (2006) Antimicrobial activity of Red Sea corals. Mar. Biol. 149:357–363

Kline DI, Vollmer SV (2011) White band disease (type I) of endangered Caribbean acroporid corals is caused by pathogenic bacteria. Sci. Rep. 1:

Knowlton N (2001) The future of coral reefs. Proc. Natl. Acad. Sci. 98:5419–5425

Knowlton N, Rohwer F (2003) Multispecies microbial mutualisms on coral reefs: The host as a habitat. Am. Nat. 162:S51–62

Koch, R (1882) Die aetiologie der tuberculose. Berl Klinische Wochenschrift 19 :221–230

Koh EGL (1997) Do scleractinian corals engage in chemical warfare against microbes? J. Chem. Ecol. 23:379–398

Kruskal WH, Wallis WA (1952) Use of ranks in one-criterion variance analysis. J. Am. Stat. Assoc. 47:583–621

Kushmaro A, Banin E, Loya Y, Stackebrandt E, Rosenberg E (2001) *Vibrio shiloi* sp. nov., the causative agent of bleaching of the coral *Oculina patagonica*. Int. J. Syst. Evol. Microbiol. 51:1383–1388

Kvennefors ECE, Sampayo E, Ridgway T, Barnes AC, Hoegh-Guldberg O (2010) Bacterial communities of two ubiquitous Great Barrier Reef corals reveals both site- and species-specificity of common bacterial associates. PLoS ONE 5:e10401

Lajeunesse TC (2005) "Species" radiations of symbiotic dinoflagellates in the Atlantic and Indo-Pacific since the Miocene-Pliocene transition. Mol. Biol. Evol. 22:570–581

Lamb JB, Willis BL (2011) Using coral disease prevalence to assess the effects of concentrating tourism activities on offshore reefs in a tropical marine park. Conserv. Biol. J. Soc. Conserv. Biol. 25:1044–1052

Lampert Y, Kelman D, Nitzan Y, Dubinsky Z, Behar A, Hill RT (2008) Phylogenetic diversity of bacteria associated with the mucus of Red Sea corals. FEMS Microbiol. Ecol. 64:187–198

Lane DJ (1991) 16S/23S rRNA sequencing. In: Stackebrandt E., Goodfellow M. (eds) Nucleic Acid Techniques in Bacterial Systematics. John Wiley and Sons, Chichester, pp 115–175

Lecuit M, Abachin E, Martin A, Poyart C, Pochart P, Suarez F, Bengoufa D, Feuillard J, Lavergne A, Gordon JI, Berche P, Guillevin L, Lortholary O (2004) Immunoproliferative small intestinal disease associated with *Campylobacter jejuni*. N. Engl. J. Med. 350:239–248

Lema KA, Willis BL, Bourne DG (2012) Corals form characteristic associations with symbiotic nitrogen-fixing bacteria. Appl. Environ. Microbiol. 78:3136–3144

Lesser MP, Bythell JC, Gates RD, Johnstone RW, Hoegh-Guldberg O (2007) Are infectious diseases really killing corals? Alternative interpretations of the experimental and ecological data. J. Exp. Mar. Biol. Ecol. 346:36–44

Lesser MP, Mazel CH, Gorbunov MY, Falkowski PG (2004) Discovery of symbiotic nitrogen-fixing cyanobacteria in corals. Science 305:997–1000

Lewis JB, Price WS (1975) Feeding mechanisms and feeding strategies of Atlantic reef corals. J. Zool. 176:527–544

Li J, Chen Q, Long L-J, Dong J-D, Yang J, Zhang S (2014) Bacterial dynamics within the mucus, tissue and skeleton of the coral *Porites lutea* during different seasons. Sci. Rep. 4:

Lim YW, Cuevas DA, Silva GGZ, Aguinaldo K, Dinsdale EA, Haas AF, Hatay M, Sanchez SE, Wegley-Kelly L, Dutilh BE, Harkins TT, Lee CC, Tom W, Sandin SA, Smith JE, Zgliczynski B, Vermeij MJA, Rohwer F, Edwards RA (2014) Sequencing at sea: Challenges and experiences in Ion Torrent PGM sequencing during the 2013 Southern Line Islands Research Expedition. PeerJ 2:

Lozupone C, Knight R (2005) UniFrac: A new phylogenetic method for comparing microbial communities. Appl. Environ. Microbiol. 71:8228–8235

Luckhurst BE, Luckhurst K (1978) Analysis of the influence of substrate variables on coral reef fish communities. Mar. Biol. 49:317–323

McAllister DE (1995) Status of the World Ocean and Its Biodiversity: Conservation of Marine & Coastal Biodiversity: Sustainable Use of Its Components: Fair and

Equitable Sharing of Benefits from Utilization of Genetic Resources. Ocean Voice International, Ottawa, ON

Merriman B, Ion Torrent R&D Team, Rothberg JM (2012) Progress in ion torrent semiconductor chip based sequencing. Electrophoresis 33:3397–3417

Miller J, Waara R, Muller E, Rogers C (2006) Coral bleaching and disease combine to cause extensive mortality on reefs in US Virgin Islands. Coral Reefs 25:418–418

Miller M, Bourque A, Bohnsack J (2002) An analysis of the loss of acroporid corals at Looe Key, Florida, USA: 1983–2000. Coral Reefs 21:179–182

Miller MW, Jaap WC, Chiappone M, Vargas-Angel B, Keller B, Aronson RB, Shinn EA (2003) *Acropora* corals in Florida: Status, trends, conservation, and prospects for recovery. Potential application of the U.S. Endangered Species Act as a conservation strategy. NOAA Techinal Memorandum NMFS-OPR-24, Silver Spring, MD

Miller MW, Lohr KE, Cameron CM, Williams DE, Peters EC (2014) Disease dynamics and potential mitigation among restored and wild staghorn coral, *Acropora cervicornis*. PeerJ 2:e541

Mills DK, Fitzgerald K, Litchfield CD, Gillevet PM (2003) A comparison of DNA profiling techniques for monitoring nutrient impact on microbial community composition during bioremediation of petroleum-contaminated soils. J. Microbiol. Methods 54:57–74

Mitchell R, Chet I (1975) Bacterial attack of corals in polluted seawater. Microb. Ecol. 2:227–233

Moberg F, Folke C (1999) Ecological goods and services of coral reef ecosystems. Ecol. Econ. 29:215–233

Moore GE (1965) Cramming more components onto integrated circuits. Electronics 38:114–117

Myers JL, Sekar R, Richardson LL (2007) Molecular detection and ecological significance of the cyanobacterial genera *Geitlerinema* and *Leptolyngbya* in black band disease of corals. Appl. Environ. Microbiol. 73:5173–5182

Nearing MA, Jetten V, Baffaut C, Cerdan O, Couturier A, Hernandez M, Le Bissonnais Y, Nichols MH, Nunes JP, Renschler CS, Souchère V, van Oost K (2005) Modeling response of soil erosion and runoff to changes in precipitation and cover. CATENA 61:131–154

Nissimov J, Rosenberg E, Munn CB (2009) Antimicrobial properties of resident coral mucus bacteria of *Oculina patagonica*. FEMS Microbiol. Lett. 292:210–215

NOAA (2015) Florida Keys National Marine Sanctuary Map Library. http://floridakeys.noaa.gov/fknms_map/maplibrary.html

Pandolfi JM, Bradbury RH, Sala E, Hughes TP, Bjorndal KA, Cooke RG, McArdle D, McClenachan L, Newman MJH, Paredes G, Warner RR, Jackson JBC (2003) Global trajectories of the long-term decline of coral reef ecosystems. Science 301:955–958

Pantos O, Bythell JC (2006) Bacterial community structure associated with white band disease in the elkhorn coral *Acropora palmata* determined using culture-independent 16S rRNA techniques. Dis. Aquat. Org. 69:79–88

Pantos O, Cooney RP, Le Tissier MDA, Barer MR, O'Donnell AG, Bythell JC (2003) The bacterial ecology of a plague-like disease affecting the Caribbean coral *Montastrea annularis*. Environ. Microbiol. 5:370–382

Patterson KL, Porter JW, Ritchie KB, Polson SW, Mueller E, Peters EC, Santavy DL, Smith GW (2002) The etiology of white pox, a lethal disease of the Caribbean elkhorn coral, *Acropora palmata*. PNAS 99:8725–8730

Pedrós-Alió C (2006) Marine microbial diversity: can it be determined? Trends Microbiol. 14:257–263

Peters EC (1984) A survey of cellular reactions to environmental stress and disease in Caribbean scleractinian corals. Helgoländer Meeresunters. 37:113–137

Peters EC (1997) Diseases of coral-reef organisms. In: Birkeland C. (eds) Life and Death of Coral Reefs. Springer, New York, pp 114–136

Peters EC, Halas JC, McCarty HB (1986) Calicoblastic neoplasms in Acropora palmata, with a review of reports on anomalies of growth and form in corals. J. Natl. Cancer Inst. 76:895–912

Peters EC, Oprandy JJ, Yevich PP (1983) Possible causal agent of "white band disease" in Caribbean acroporid corals. J. Invertebr. Pathol. 41:394–396

Peters EC, Pilson MEQ (1985) A comparative study of the effects of sedimentation on symbiotic and asymbiotic colonies of the coral Astrangiadanae Milne Edwards and Haime 1849. J. Exp. Mar. Biol. Ecol. 92:215–230

Peters EC, Price KL, Horowitz DJB (2005) Histological preparation of invertebrates for evaluating contaminant effects. In: Ostrander G.K. (eds) Techniques in Aquatic Toxicology. Taylor & Francis, Boca Raton, FL, pp 653–686

Philipp E, Fabricius K (2003) Photophysiological stress in scleractinian corals in response to short-term sedimentation. J. Exp. Mar. Biol. Ecol. 287:57–78

Pollock FJ, Lamb JB, Field SN, Heron SF, Schaffelke B, Shedrawi G, Bourne DG, Willis BL (2014) Sediment and turbidity associated with offshore dredging increase coral disease prevalence on nearby reefs. PLoS ONE 9:e102498

Pollock FJ, Morris PJ, Willis BL, Bourne DG (2011) The urgent need for robust coral disease diagnostics. PLoS Pathog 7:e1002183

Polson SW, Higgins J, Woodley C (2008) PCR-based assay for detection of four coral pathogens. Proceedings of the 11th International Coral Reef Symposium, Ft. Lauderdale, FL. pp. 247–251

Porter JW, Dustan P, Jaap WC, Patterson KL, Kosmynin V, Meier OW, Patterson ME, Parsons M (2001) Patterns of spread of coral disease in the Florida Keys. Hydrobiologia 460:1–24

Precht W, Bruckner A, Aronson R, Bruckner R (2002) Endangered acroporid corals of the Caribbean. Coral Reefs 21:41–42

Prophet EB, Mills B, Arrington JB, Sobin LH (1992) Laboratory Methods in Histotechnology. American Registry of Pathology, Washington, D.C

Rappé MS, Giovannoni SJ (2003) The uncultured microbial majority. Annu. Rev. Microbiol. 57:369–394

Reaka-Kudla ML (1997) The global biodiversity of coral reefs: A comparison with rain forests. Joseph Henry Press, Washington, D.C.

Reshef L, Koren O, Loya Y, Zilber-Rosenberg I, Rosenberg E (2006) The coral probiotic hypothesis. Environ. Microbiol. 8:2068–2073

Richardson LL (1998) Coral diseases: What is really known? Trends Ecol. Evol. 13:438–443

Richardson LL, Goldberg WM, Carlton RG, Halas JC (1998) Coral disease outbreak in the Florida Keys: Plague type II. Rev. Biol. Trop. 46:187–198

Richardson LL, Sekar R, Myers JL, Gantar M, Voss JD, Kaczmarsky L, Remily ER, Boyer GL, Zimba PV (2007) The presence of the cyanobacterial toxin microcystin in black band disease of corals. FEMS Microbiol. Lett. 272:182–187

Richardson LL, Smith GW, Ritchie KB, Carlton RG (2001) Integrating microbiological, microsensor, molecular, and physiologic techniques in the study of coral disease pathogenesis. Hydrobiologia 460:71–89

Richman S, Loya Y, Sloboclkin LB (1975) The rate of mucus production by corals and its assimilation by the coral reef copepod *Acartia negligens*. Limnol. Oceanogr. 20:918–923

Richmond RH (1993) Coral reefs: Present problems and future concerns resulting from anthropogenic disturbance. Am. Zool. 33:524–536

Riegl B (1995) Effects of sand deposition on scleractinian and alcyonacean corals. Mar. Biol. 121:517–526

Riegl B, Branch GM (1995) Effects of sediment on the energy budgets of four scleractinian (Bourne 1900) and five alcyonacean (Lamouroux 1816) corals. J. Exp. Mar. Biol. Ecol. 186:259–275

Risk MJ (1972) Fish diversity on a coral reef in the Virgin Islands. Atoll Research Bulletin 153:1–4

Risk MJ (2014) Assessing the effects of sediments and nutrients on coral reefs. Curr. Opin. Environ. Sustain. 7:108–117

Ritchie KB (2006) Regulation of microbial populations by coral surface mucus and mucus-associated bacteria. Mar. Ecol. Prog. Ser. 322:1–14

Ritchie KB, Smith GW (1995) Preferential carbon utilization by surface bacterial communities from water mass, normal, and white-band diseased *Acropora cervicornis*. Mol. Mar. Biol. Biotech. 4:345–352

Ritchie KB, Smith GW (1997) Physiological comparison of bacterial communities from various species of scleractinian corals. Proceedings of the 8th International Coral Reef Symposium, Smithsonian Tropical Research Institute, Panama, 1:521–526

Ritchie KB, Smith GW (1998) Type II white-band disease. Rev. Biol. Trop. 46 Supl. 5:199–203

Ritchie KB, Smith GW (2004) Microbial communities of coral surface mucopolysaccharide layers. In: Rosenberg P.E., Loya P.Y. (eds) Coral Health and Disease. Springer Berlin Heidelberg, pp 259–264

Roder C, Arif C, Bayer T, Aranda M, Daniels C, Shibl A, Chavanich S, Voolstra CR (2014) Bacterial profiling of white plague disease in a comparative coral species framework. ISME J. 8:31–39

Rogers CS (1983) Sublethal and lethal effects of sediments applied to common Caribbean reef corals in the field. Mar. Pollut. Bull. 14:378–382

Rogers CS (1990) Responses of coral reefs and reef organisms to sedimentation. Mar. Ecol. Prog. Ser. 62:185–202

Rogers CS (2010) Words matter: Recommendations for clarifying coral disease nomenclature and terminology. Dis. Aquat. Organ. 91:167–175

Rohwer F, Breitbart M, Jara J, Azam F, Knowlton N (2001) Diversity of bacteria associated with the Caribbean coral *Montastraea franksi*. Coral Reefs 20:85–91

Rohwer F, Seguritan V, Azam F, Knowlton N (2002) Diversity and distribution of coral-associated bacteria. Mar. Ecol. Prog. Ser. 243:1–10

Ronaghi M (2001) Pyrosequencing sheds light on DNA sequencing. Genome Res. 11:3–11

Ronaghi M, Karamohamed S, Pettersson B, Uhlén M, Nyrén P (1996) Real-time DNA sequencing using detection of pyrophosphate release. Anal. Biochem. 242:84–89

Rosenberg E, Ben-Haim Y (2002) Microbial diseases of corals and global warming. Environ. Microbiol. 4:318–326

Rosenberg E, Kellogg CA, Rohwer F (2007a) Coral microbiology. Oceanography 20:146–154

Rosenberg E, Koren O, Reshef L, Efrony R, Zilber-Rosenberg I (2007b) The role of microorganisms in coral health, disease and evolution. Nat. Rev. Microbiol. 5:355–362

Rosenberg E, Kushmaro A (2011) Microbial diseases of corals: Pathology and ecology. In: Dubinsky Z., Stambler N. (eds) Coral Reefs: An Ecosystem in Transition. Springer Netherlands, pp 451–464

Rosenberg E, Loya Y (2004) Coral Health and Disease. Springer, Berlin, Heidelberg, Germany

Rothberg J, Merriman B, Higgs G (2012) Bioinformatics. Introduction. Yale J. Biol. Med. 85:305–308

Rothberg JM, Hinz W, Rearick TM, Schultz J, Mileski W, Davey M, Leamon JH, Johnson K, Milgrew MJ, Edwards M, Hoon J, Simons JF, Marran D, Myers JW, Davidson JF, Branting A, Nobile JR, Puc BP, Light D, Clark TA, Huber M, Branciforte JT, Stoner IB, Cawley SE, Lyons M, Fu Y, Homer N, Sedova M, Miao X, Reed B, Sabina J, Feierstein E, Schorn M, Alanjary M, Dimalanta E,

Dressman D, Kasinskas R, Sokolsky T, Fidanza JA, Namsaraev E, McKernan KJ, Williams A, Roth GT, Bustillo J (2011) An integrated semiconductor device enabling non-optical genome sequencing. Nature 475:348–352

Rowan R (1998) Review—Diversity and ecology of zooxanthellae on coral reefs. J. Phycol. 34:407–417

Ryan KE, Walsh JP, Corbett DR, Winter A (2008) A record of recent change in terrestrial sedimentation in a coral-reef environment, La Parguera, Puerto Rico: a response to coastal development? Mar. Pollut. Bull. 56:1177–1183

Santavy DL (1995) The diversity of microorganisms associated with marine invertebrates and their roles in the maintenance of ecosystems. In: Allsopp D., Colwell R.R., Hawksworth D.L. (eds) Microbial Diversity and Ecosystem Function. CAB International in association with United Nations Environment Programme, Oxon, UK, pp 211–229

Santavy DL, Peters EC (1997) Microbial pests: Coral diseases in the western Atlantic. Proceedings of the 8th International Coral Reef Symposium, Smithsonian Tropical Research Institute, Panama, 1:55-68

Santavy DL, Peters EC, Kozlowski J, Wilkinson SS (1995) Characterization of the bacterium suspected in the incidence of white band disease. Annual Meeting of the American Society for Microbiology, Washington, DC

Segata N, Izard J, Waldron L, Gevers D, Miropolsky L, Garrett WS, Huttenhower C (2011) Metagenomic biomarker discovery and explanation. Genome Biol. 12:R60

Sekar R, Kaczmarsky LT, Richardson LL (2008) Microbial community composition of black band disease on the coral host *Siderastrea siderea* from three regions of the wider Caribbean. Mar Ecol Prog Ser 362:85–98

Sekar R, Mills DK, Remily ER, Voss JD, Richardson LL (2006) Microbial communities in the surface mucopolysaccharide layer and the black band microbial mat of black band-diseased *Siderastrea siderea*. Appl. Environ. Microbiol. 72:5963–5973

Sharp KH, Ritchie KB, Schupp PJ, Ritson-Williams R, Paul VJ (2010) Bacterial acquisition in juveniles of several broadcast spawning coral species. PLoS ONE 5:e10898

Shashar N, Cohen Y, Loya Y, Sar N (1994) Nitrogen fixation (acetylene reduction) in stony corals: Evidence for coral-bacteria interactions. Mar. Ecol.-Prog. Ser. 111:259–264

Shinn EA (1976) Coral reef recovery in Florida and the Persian Gulf. Environ. Geol. 1:241–254

Shokralla S, Spall JL, Gibson JF, Hajibabaei M (2012) Next-generation sequencing technologies for environmental DNA research. Mol. Ecol. 21:1794–1805

Sikaroodi M, Gillevet PM (2012) Quality control in multi-tag pyrosequencing of microbial communities. BioTechniques 53:381–383

Smith A (2013) Tissue Loss Syndromes in Acropora cervicornis off Broward County, Florida: Transmissibility, Rates of Skeletal Extension and Tissue Loss. Nova Southeastern University, Ft. Lauderdale, FL

Sogin ML, Morrison HG, Huber JA, Welch DM, Huse SM, Neal PR, Arrieta JM, Herndl GJ (2006) Microbial diversity in the deep sea and the underexplored "rare biosphere." Proc. Natl. Acad. Sci. 103:12115–12120

Sorokin YI (1973) Trophical role of bacteria in the ecosystem of the coral reef. Nature 242:415–417

Spalding MD, Green EP, Ravilious C (2001) World Atlas of Coral Reefs. University of California Press, Berkeley

Spor A, Koren O, Ley R (2011) Unravelling the effects of the environment and host genotype on the gut microbiome. Nat. Rev. Microbiol. 9:279–290

Stillman JH, Armstrong E (2015) Genomics are transforming our understanding of responses to climate change. BioScience biu219

Storlazzi C., Ogston A., Bothner M., Field M., Presto M. (2004) Wave- and tidally-driven flow and sediment flux across a fringing coral reef: Southern Molokai, Hawaii. Cont. Shelf Res. 24:1397–1419

Sunagawa S, DeSantis TZ, Piceno YM, Brodie EL, DeSalvo MK, Voolstra CR, Weil E, Andersen GL, Medina M (2009) Bacterial diversity and white plague disease-associated community changes in the Caribbean coral *Montastraea faveolata*. ISME J 3:512–521

Sunagawa S, Woodley CM, Medina M (2010) Threatened corals provide underexplored microbial habitats. PLoS ONE 5:e9554

Sutherland KP, Porter JW, Torres C (2004) Disease and immunity in Caribbean and Indo-Pacific zooxanthellate corals. Mar. Ecol. Prog. Ser. 266:273–302

Sutherland KP, Porter JW, Turner JW, Thomas BJ, Looney EE, Luna TP, Meyers MK, Futch JC, Lipp EK (2010) Human sewage identified as likely source of white pox

disease of the threatened Caribbean elkhorn coral, *Acropora palmata*. Environmental Microbiology 12:1122–1131

Sutherland KP, Shaban S, Joyner JL, Porter JW, Lipp EK (2011) Human pathogen shown to cause disease in the threatened eklhorn coral *Acropora palmata*. PLoS ONE 6:e23468

Suzuki MT, Rappé MS, Haimberger ZW, Winfield H, Adair N, Ströbel J, Giovannoni SJ (1997) Bacterial diversity among small-subunit rRNA gene clones and cellular isolates from the same seawater sample. Appl. Environ. Microbiol. 63:983–989

Suzuki null, Rappe null, Giovannoni null (1998) Kinetic bias in estimates of coastal picoplankton community structure obtained by measurements of small-subunit rRNA gene PCR amplicon length heterogeneity. Appl. Environ. Microbiol. 64:4522–4529

Sweet M, Bythell J (2012) Ciliate and bacterial communities associated with white syndrome and brown band disease in reef-building corals. Environ. Microbiol. 14:2184–2199

Sweet MJ, Croquer A, Bythell JC (2011) Bacterial assemblages differ between compartments within the coral holobiont. Coral Reefs 30:39–52

Sweet MJ, Croquer A, Bythell JC (2014) Experimental antibiotic treatment identifies potential pathogens of white band disease in the endangered Caribbean coral Acropora cervicornis. Proc. R. Soc. Lond. B Biol. Sci. 281:20140094

Sweet M, Jones R, Bythell J (2012) Coral diseases in aquaria and in nature. J. Mar. Biol. Assoc. U. K. 92:791–801

Szmant AM (1986) Reproductive ecology of Caribbean reef corals. Coral Reefs 5:43–53

Thompson FL, Barash Y, Sawabe T, Sharon G, Swings J, Rosenberg E (2006) *Thalassomonas loyana* sp. nov., a causative agent of the white plague-like disease of corals on the Eilat coral reef. Int. J. Syst. Evol. Microbiol. 56:365–368

Tunnicliffe V (1981) Breakage and propagation of the stony coral *Acropora cervicornis*. Proceedings of the National Academy of Sciences of the United States of America 78:2427–2431

Vargas-Ángel B, Peters EC, Kramarsky-Winter E, Gilliam DS, Dodge RE (2007) Cellular reactions to sedimentation and temperature stress in the Caribbean coral *Montastraea cavernosa*. Journal of Invertebrate Pathology 95:140–145

Vargas-Ángel B, Thomas JD, Hoke SM (2003) High-latitude *Acropora cervicornis* thickets off Fort Lauderdale, Florida, USA. Coral Reefs 22:465–473

Vega Thurber R, Willner-Hall D, Rodriguez-Mueller B, Desnues C, Edwards RA, Angly F, Dinsdale E, Kelly L, Rohwer F (2009) Metagenomic analysis of stressed coral holobionts. Environ. Microbiol. 11:2148–2163

Vollmer SV, Kline DI (2008) Natural disease resistance in threatened staghorn corals. PLoS ONE 3:e3718

Voss JD, Mills DK, Myers JL, Remily ER, Richardson LL (2007) Black band disease microbial community variation on corals in three regions of the wider Caribbean. Microb. Ecol. 54:730–739

Waddell J, Clarke A (2008) The state of coral reef ecosystems of the United States and Pacific freely associated states: 2008. 574

Weber M, Beer D de, Lott C, Polerecky L, Kohls K, Abed RMM, Ferdelman TG, Fabricius KE (2012) Mechanisms of damage to corals exposed to sedimentation. Proc. Natl. Acad. Sci. 109:E1558–E1567

Weber M, Lott C, Fabricius KE (2006) Sedimentation stress in a scleractinian coral exposed to terrestrial and marine sediments with contrasting physical, organic and geochemical properties. J. Exp. Mar. Biol. Ecol. 336:18–32

Wegley L, Yu Y, Breitbart M, Casas V, Kline DI, Rohwer F (2004) Coral-associated Archaea. Mar. Ecol. Prog. Ser. 273:89–96

Weil E (2004) Coral reef diseases in the wider Caribbean. In: Rosenberg P.E., Loya P.Y. (eds) Coral Health and Disease. Springer, Berlin, Heidelberg, Germany, pp 35–68

Weil E (2006) Diversity and relative abundance of corals, octocorals and sponges at Jaragua National Park, Dominican Republic (in Spanish). Rev. Biol. Trop. 54:423–443

Whitman WB, Coleman DC, Wiebe WJ (1998) Prokaryotes: The unseen majority. Proc. Natl. Acad. Sci. 95:6578–6583

Wilcoxon F (1945) Individual Comparisons by Ranking Methods. Biom. Bull. 1:80–83

Wilkinson CR (2002) Status of Coral Reefs of the World: 2002. Global Coral Reef Monitoring Network and Australian Institute of Marine Science, Townsville, Australia

Wilkinson CR (2004) Status of Coral Reefs of the World: 2004. Global Coral Reef Monitoring Network and Australian Institute of Marine Science, Townsville, Australia

Wilkinson CR (2008) Status of Coral Reefs of the World: 2008. Global Coral Reef Monitoring Network and Reef and Rainforest Research Center, Townsville, Australia

Williams DE, Miller MW (2005) Coral disease outbreak: Pattern, prevalence and transmission in *Acropora cervicornis*. Mar Ecol Prog Ser 301:119–128

Williams WM, Viner AB, Broughton WJ (1987) Nitrogen fixation (acetylene reduction) associated with the living coral *Acropora variabilis*. Mar. Biol. 94:531–535

Wintzingerode FV, Göbel UB, Stackebrandt E (1997) Determination of microbial diversity in environmental samples: Pitfalls of PCR-based rRNA analysis. FEMS Microbiol. Rev. 21:213–229

Wobeser GA (2007) Disease in Wild Animals. Springer Berlin Heidelberg, Berlin, Heidelberg

Work TM, Aeby GS (2006) Systematically describing gross lesions in corals. Dis. Aquat. Organ. 70:155–160

Work TM, Aeby GS (2010) Wound repair in *Montipora capitata*. J. Invertebr. Pathol. 105:116–119

Work TM, Aeby GS (2011) Pathology of tissue loss (white syndrome) in *Acropora* sp. corals from the Central Pacific. J. Invertebr. Pathol. 107:127–131

Work TM, Aeby GS, Coles SL (2008a) Distribution and morphology of growth anomalies in Acropora from the Indo-Pacific. Dis. Aquat. Organ. 78:255–264

Work T, Meteyer C (2014) To understand coral disease, look at coral cells. EcoHealth 11:610–618

Work TM, Richardson LL, Reynolds TL, Willis BL (2008b) Biomedical and veterinary science can increase our understanding of coral disease. J. Exp. Mar. Biol. Ecol. 362:63–70

Work TM, Russell R, Aeby GS (2012) Tissue loss (white syndrome) in the coral *Montipora capitata* is a dynamic disease with multiple host responses and potential causes. Proc. Biol. Sci. 279:4334–4341

Yergeau E, Lawrence JR, Sanschagrin S, Waiser MJ, Korber DR, Greer CW (2012) Next-generation sequencing of microbial communities in the Athabasca River and

its tributaries in relation to oil sands mining activities. Appl Environ Microbiol 78:7626–7637

Yevich PP, Barszcz CA (1983) Preparation of aquatic animals for histopathological examination. Biological field and laboratory methods for measuring the quality of surface waters and effluents. U.S. Environmental Protection Agency, Cincinnati, Ohio

Zhang L, Farrell JJ, Zhou H, Elashoff D, Akin D, Park N-H, Chia D, Wong DT (2010) Salivary transcriptomic biomarkers for detection of resectable pancreatic cancer. Gastroenterology 138:949–957.e7

BIOGRAPHY

Katheryn W. Patterson graduated from Oak Mountain High School, Birmingham, Alabama, in 2002. She received her Bachelor of Science in Biology with a Marine Concentration from Spring Hill College, Mobile, Alabama, in 2006, and received her Master of Science in Environmental Science and Policy from George Mason University, Fairfax, Virginia, in 2010.